MIXED BOUNDARY VALUE PROBLEMS ON WAVE PROPAGATION IN ELASTIC MEDIA

A THESIS SUBMITTED IN FULFILMENT OF THE

REQUIREMENTS

FOR THE DEGREE OF DOCTOR OF PHILOSOPHY
(SCIENCE)

by

UJJAL DHABAL

DEPARTMENT OF MATHEMATICS

JADAVPUR UNIVERSITY, INDIA

2023

Certificate

This is to certify that thesis entitled **"Mixed Boundary Value Problems on Wave Propagation in Elastic Media"** submitted by Ujjal Dhabal who got his name registered on 25/09/2019 (Index No: 109/19/Maths./26) for the award of Ph. D (science) degree of Jadavpur University, is absolutely based upon his own work under the supervision of Prof. Subhas Chandra Mandal, Department of Mathematics, Jadavpur University, Kolkata-700032, and that neither this nor any part of it has been submitted for either any degree/diploma or any other academic award anywhere before.

Date: 05/09/2023
Place: Jadavpur, Kolkata
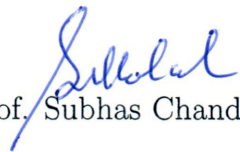
Prof. Subhas Chandra Mandal

Acknowledgements

It gives me immense pleasure to express my sincere gratitude and indebtedness to **Dr. Subhas Chandra Mandal**, *Professor, Department of Mathematics, Jadavpur University, for guiding me throughout the whole tenure of my doctoral program. Without his continuous support, words of motivation and helping hand in all phases it would not have been possible to complete my work.*

I also take this very opportunity to acknowledge the support of the Head of the Department of Mathematics, Jadavpur University and other teachers and staffs for their encouragement. I would also like to thank the Department for providing me all the facilities required to complete my work.

I am grateful to my colleagues Subhadeep Naskar, Somashri Karan and Sourav Kumar Panja at the Department of Mathematics, Jadavpur University and my friends for all their kind assistance and co-operation and sharing of knowledge that helped me to continue my work.

I feel emotional to express my sincere gratitude to my parents. Without their encouragement, inspiration and ceaseless help, it was not possible for me to accomplish my work.

Date: 05/09/2023

Place: *Jadavpur, Kolkata*

Ujjal Dhabal
05/09/2023

Ujjal Dhabal

This thesis is dedicated to my parents,
Himansu Dhabal
&
Meghla Dhabal
for their love, endless support and
encouragement.

Contents

Chapter-1
Introduction

Chapter 1

Introduction

∎ Historical Overview

A deformed body is one in which the relative positions of the molecules of the body are altered under the effect of an external force. Elasticity is the ability of a substance to deform when the substance experiences an external force and then recover its original shape when the force causing deformations has been withdrawn. The elastic limit of a body is the maximum amount of deformation before it no longer retains its original shape, beyond this point, the material may fracture or deform permanently.

The field of mathematical theory of elasticity is an attempt to address the work involved in calculating stress-strain, or relative movement of constituents of a solid body that is either under the effects of an equilibrium system of forces or experiencing slight internal relative motion. It aims to obtain outcomes that are fundamentally crucial in the domain of structural design and all other valuable fields where engineering materials are used. The classical theory of elasticity is a significant subdivision of continuum mechanics which addresses the stresses and distortions that occur in elastic substances as a result of external forces, variations

in temperature or compression. The classical theory of elasticity provides a great framework for evaluating the mechanical properties of a wide variety of solid materials those are frequently used in the design of civil, mechanical, and aeronautical engineering projects etc. This theory was discovered in the early nineteenth century and the implementation of the classical theory of elasticity are in harmony with investigations carried out of many advanced elastic materials provided the stresses are limited. Although, in many dynamic problems characterized by the combination of high frequency and short wavelength significant discrepancies between experimental observations and the classical theory of elasticity are often noticeable.

Actually Galileo was the pioneer mathematician who analysed the resistance of solids to rupture by considering them as objects having nonelastic properties. His investigations established the foundation of a field that was subsequently explored by numerous researchers. Two significant breakthroughs in the history of the elasticity were made after Galileo's observations, one is the discovery of Hooke's Law in 1660 by Robert Hooke and the other is the formulation of the general equations of elasticity by French mathematician Navier in 1821. Hooke's law has dominated the scientific thoughts for long period of time and its outcomes agreed with experiments quite well. As per Hooke's law (1678), there exist a specific correlation between applied forces and distortions that characterizes the behaviour of elastic bodies and later that correlation was expressed in terms of strain and stress of the deformable bodies. In 1680, Edme Mariotte introduced a similar type law for analyzing the stability of cantilever beams. He showed that cantilever beam resists torques induced by a transverse loading by modifying extensional and compressional deformations respectively, in the material fibres. Though, Mariottes assumptions regarding the force distribution in material fibres was appropriate, but his study didn't focus on the beams axis. By studying the bending of a beam under an applied load, Jacob Bernoulli (1705) modified this idea. He came up with an equation which is known

as Bernoulli equation that describes how the axis of the beam curves during deformation and the correlation between the curvature and the bending moment of the beam at every point is narrated by this equation.

In 1821, Navier published an article in which he derived the fundamental equations of elasticity when the applied forces are in equilibrium state. These equations illustrate the relationship between stress, strain, and displacement in a deformable solid body. He formulated three partial differential equations for the determination of stress components of a deformable elastic material using a description of molecular interaction in which forces act along particles movement. The great mathematician Cauchy (1823) recognized that the stresses within a elastic solid could not be expressed by a single quantity, but instead needed a mathematical formulation involving several components and then introduced the idea of a stress tensor, which is a second-order tensor containing the normal and shear stress components act on the three mutually perpendicular planes. Cauchy introduced the principle of virtual work done and the linear theory of elasticity for homogeneous elastic material. He exhibited that the work done by applied forces on an elastic system is identical with the work done by internal stresses in response to deformations formed by those applied forces. That work was a pioneer step in the development of the calculus of variations.

The study of the theory of elasticity was not prioritized by mathematicians and physicists in the early 1800s. Nonetheless, the area gained more recognition later on because of its relevance to geophysics, acoustics, defence sector etc. Specifically, the analysis of wave propagation and vibration phenomenon are crucial in comprehending earthquakes and developing new materials and therefore it becomes an important field of several scientists. After Galileo's findings, numerous researchers including Poission, Ostrogradsky, Lame, Stokes, and Christoffel (1824 - 1887) were made a details study on wave propagation field. It was shown that the equations

of the general theory of elasticity could predict the existence of two distinct types of elastic waves caused by the deformation that are capable of propagating through isotropic elastic solid. One of those waves is commonly referred to dilatational wave where direction of wave propagation and particle's vibration are parallel and the other wave is known as transverse wave where the particles vibrate perpendicular to the direction of wave propagation.

Later in 1885, it was shown by Lord Rayleigh that a wave propagates across the surfaces of a body and the associated motion of that waves diminishes exponentially when the depth of the material from the surface increases. This type of surface wave, known as Rayleigh wave, travels at a speed slightly greater than 90 percent of that of the shear wave and it is characterized by particle motion that occurs in planes parallel to the surface's normal and the direction of wave propagation. Love founded another kind of surface wave that moves transversely, parallel to the surface and perpendicular to wave's path of propagation. This kind of surface wave is noticeable in solids where a surface of the material overlies a bulk solid that is elastically stiffer. The analysis of the reflection and diffraction of elastic waves has evolved into a valuable engineering technique for non-destructive assessment of materials. This technique is employed for the detection of potentially hazardous defects like cracks or flaws.

■ Stress

Let Fig.1.1 represents an elastic body in equilibrium state. When the external forces F_1, F_2, F_3, ...F_n act upon a body, internal forces will be generated between its various constituent parts. In order to analyze the strength of these applied forces at any specific point O, we consider that the body is divided into two parts M and N by means of a cross section $pqrs$ through this point. Considering the portion M,

it can be stated that it is in a state of equilibrium under the influence of external forces F_1, F_2, F_3, ...F_n as well as the inner forces distributed across the cross section $pqrs$. It is considered that these forces are distributed continuously across the cross sectional area $pqrs$. The intensities of these forces are typically determined by the amount of force exerted per unit area of the surface where they act. When referring to internal forces, that intensity is called stress. Hence the stress can be calculated by dividing the total tension force by the cross section. In Fig.1.1 the stress was uniformly distributed across the cross section.
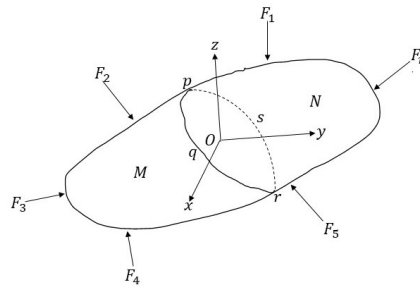
Fig.1.1 An elastic body in equilibrium.

To determine the magnitude of stress generated on a small area ∂M, that is extracted from the cross section $pqrs$ at any point O, we consider that the forces acting across ∂M as a result of the interaction of part N on part M can be reduced to a resultant ∂P. If we now continuously reduce the size of the small elemental area ∂M, the limiting value $\lim_{\partial M \to 0} \frac{\partial P}{\partial M}$ will be the amount of stress loading on the section $pqrs$ at the point O and the limiting direction of the resultant force represents the direction of the stress. In the general case the direction of stress can be resolved into two components, the stress components perpendicular to the surface is known as normal stress and the stress parallel to the surface is known as shear stress.

Let us consider an orthogonal and rectilinear system of axes to analyze the dependence of stress on the orientation of the plane where it acts. To compute the

stresses on a plane containing the point, regardless of its orientation, it is enough to know the stresses acting on three planes that intersect at that point and are mutually perpendicular. We use the symbol σ for the normal stress and the symbol τ for shear stress and subscripts are used with these symbols, to designate the plane's direction on which the stress acts. If we take a very small cubic shape element at a point O (Fig.1.2), whose sides are parallel to the coordinate axes, the stress components acting on the sides of that cubic element and the directions considered as positive are shown in Fig.1.2. The normal stress component acting on the side perpendicular to y-axis is denoted by σ_y, where the subscript y represents that the stress is acting on a plane whose normal is y-axis. The normal stress is considered positive when it results tension and negative when it results compression. The shearing stress is splitted up into two components that's are parallel to the coordinate axes. Two subscript letters are utilized in this case, the first one represents the direction of the normal to the considered plane and the second one represents the direction of the stress component. So for the the side perpendicular to the y-axis, the two components are τ_{yx} and τ_{yz}, where τ_{yx} acts in $x-$direction and τ_{yz} acts in the z-direction.
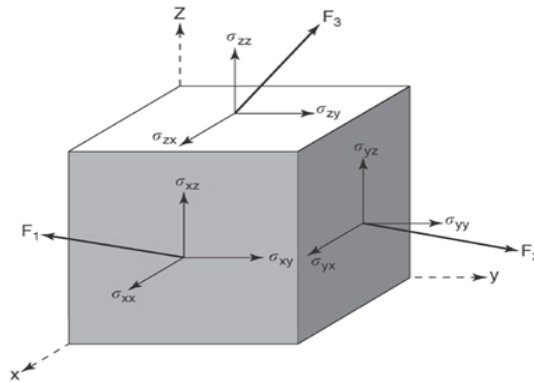
Fig.1.2 Components of stress.

The positive directions of the shear stress components on any given side of the elementary cube are considered as the positive directions of the coordinate axes whether

a tension on the similar side would have the positive direction of the corresponding axis.

We can write those different stress components in a 3×3 matrix as

$$\Sigma = \begin{bmatrix} \sigma_x & \tau_{xy} & \tau_{xz} \\ \tau_{yx} & \sigma_y & \tau_{yz} \\ \tau_{zx} & \tau_{zy} & \sigma_z \end{bmatrix}$$

The equation of equilibrium of an element considering moments of forces about $x-$axis is

$$\tau_{zy} dy \ dz = \tau_{yz} dy \ dz,$$

where $dy \ dz$ (Fig.1.3) represents the dimension of the small elementary area, and the other two equations for $y-$axis and $z-$axis can be drawn in a similar way as above. From those equations we obtain

$$\tau_{xy} = \tau_{yx}, \ \tau_{zx} = \tau_{xz}.$$
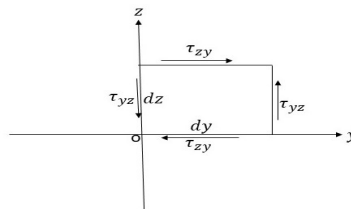
Fig.1.3 Symmetry of stress components.

■ Strain

Just as it is important to comprehend internal forces, it is equally vital to understand the deformations induced by external pressures. Deformations are

defined in terms of strains, or the relative alteration in the body's shape and size. Additionally, a general definition of the strain at a point is given on an infinitesimal cuboid inside a rectangular frame of reference. The sides of the infinitesimal cuboid's lengths vary under various loads. The cube's faces also become deformed. A normal strain is represented by the change of length, while a shearing strain is represented by the distortion of the body. Fig.1.4 exhibits the distortion or strain on the face *ABCD*.
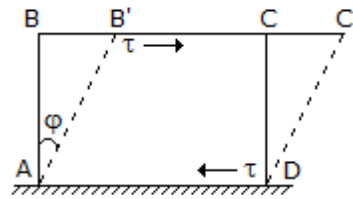
Fig.1.4 Strain

■ **Stress Strain Relation**

Hooke's Law is one of the fundamental principle in mechanical field that demonstrates the co-relation between the distortions (stretching or compression) of an elastic structure and the force that is enforced to it. The law is named after Robert Hooke, an English physicist who pioneered it in the 17Th century. If we stretch an elastic body in the x direction i.e. apply a normal stress σ_{xx}, then we can write mathematically

$$\sigma_{xx} = E\epsilon_{xx},$$

where E denotes the modulus of elasticity related to tensile force.

Also, if a material is loaded by a compressive force within the limit of its elasticity, it will experience a reduction in length that is directly proportional to the magnitude of the applied force

$$\sigma_{yy} = -\nu\epsilon_{yy} \text{ and } \sigma_{zz} = -\nu\epsilon_{zz},$$

where ν is a physical parameter of the material known as Poission's ratio.

For multiple dimensions and directions, the generalised Hooke's Law in tensor form is

$$\sigma_{ij} = C_{ijkl}\epsilon_{kl}, \qquad (i,\ j,\ k,\ l = 1,\ 2,\ 3), \qquad (1.1)$$

where σ_{ij} represents the stress tensor, ϵ_{kl} indicates the strain tensor and the coefficients C_{ijkl} represents the stiffness tensor of fourth order. As the stress tensor and strain tensor are symmetric with respect to indices, the coefficient tensor C_{ijkl} is also symmetric with respect to the first two and last two indices.

We may use the following symbols to avoid the double sum.

$$\sigma_{11} = \sigma_1,\ \sigma_{22} = \sigma_2,\ \sigma_{33} = \sigma_3,\ \sigma_{23} = \sigma_4,\ \sigma_{31} = \sigma_5,\ \sigma_{12} = \sigma_6,$$

$$\epsilon_{11} = \epsilon_1,\ \epsilon_{22} = \epsilon_2,\ \epsilon_{33} = \epsilon_3,\ \epsilon_{23} = \epsilon_4,\ \epsilon_{31} = \epsilon_5,\ \epsilon_{12} = \epsilon_6.$$

Using above symbols equation (1.1) transformed to

$$\sigma_k = C_{kl}\epsilon_l, \qquad (k,\ l = 1,\ 2,\ 3,\ 4,\ 5,\ 6). \qquad (1.2)$$

■ Types of Elastic Body and Planes of Symmetry

Our initial effort is to provide definitions for homogeneous and non-homogeneous elastic bodies. In an elastic solid, if the elastic properties seems to be exactly uniform throughout all of its points, the solid body is named as homogeneous, otherwise the body is said to be non-homogeneous. Within an elastically homogeneous solids, relations of stress-strain become independent with respect to the position, while in non-homogeneous solids, they become functions of positions, i.e. when the medium has non-homogeneous elastic characteristics, the modules of rigidity and Poisson's

ratio are not remain constants and should be anticipated that they change from point to point inside solid material. They might differ either regularly, as in the case of differential functions of spatial coordinates, or discretely, as in the instance of artificial laminated materials.

An isotropic body has characteristic that are consistent in all directions drawn through a particular location, while an anisotropic body often has variable elastic properties for each direction. Material that is orthotropic, their physical characteristics vary along three rotating axes that are mutually orthogonal. They belong to the class of anisotropic solids as their characteristics vary depending on the direction from which measurements are taken. Also an anisotropic material with a special axis of rotational symmetry along which the material properties are fixed is known as a transversely isotropic elastic solid.

The general stress strain relation given by (1.2) contains a highest of 36 independent constants as every one of the six strains is dependent on each of six stresses. Now if we consider the strain energy density function which satisfies

$$W = \frac{1}{2}C_{ij}\epsilon_i\epsilon_j \quad \text{and} \quad \frac{\partial W}{\partial \epsilon_i} = \tau_i \tag{1.3}$$

and then the number of elastic constants concerning a general anisotropic bodies diminishes to 21.

The various types of elastic material can exhibit different types of symmetry, which can be classified as follows:

1. Axis Symmetry (Transversely Isotropy):

A transtropy material such as Cobalt, Cooper, Boron-Epoxy is a material when it admits an axis of symmetry perpendicular to the normal of that axis such that all physical parameters are identical in the perpendicular plane. In this case the

number of independent elastic constants reduced to 5 and the stress-strain relation using matrix notations can be written as

$$
\begin{bmatrix} \sigma_1 \\ \sigma_2 \\ \sigma_3 \\ \sigma_4 \\ \sigma_5 \\ \sigma_6 \end{bmatrix} = \begin{bmatrix} C_{11} & C_{12} & C_{13} & 0 & 0 & 0 \\ C_{12} & C_{11} & C_{13} & 0 & 0 & 0 \\ C_{13} & C_{13} & C_{33} & 0 & 0 & 0 \\ 0 & 0 & 0 & C_{44} & 0 & 0 \\ 0 & 0 & 0 & 0 & C_{44} & 0 \\ 0 & 0 & 0 & 0 & 0 & C_{11} - C_{12} \end{bmatrix} \begin{bmatrix} \epsilon_1 \\ \epsilon_2 \\ \epsilon_3 \\ \epsilon_4 \\ \epsilon_5 \\ \epsilon_6 \end{bmatrix}
$$

Considering z-axis perpendicular to the plane $z = 0$, the explicit form of stress and strain in term of the five dimensionless elastic constants C_{ij} are prescribed as follows

$$
\epsilon_{xx} = C_{11}\sigma_{xx} + C_{12}\sigma_{yy} + C_{13}\sigma_{zz},
$$

$$
\epsilon_{yy} = C_{12}\sigma_{xx} + C_{11}\sigma_{yy} + C_{13}\sigma_{zz},
$$

$$
\epsilon_{zz} = C_{13}(\sigma_{xx} + \sigma_{yy}) + C_{33}\sigma_{zz},
$$

$$
\epsilon_{xy} = 2(C_{11} - C_{12})\sigma_{xy},
$$

$$
\epsilon_{yz} = C_{44}\sigma_{yz},
$$

$$
\epsilon_{zx} = C_{44}\sigma_{zx}
$$

and the expressions of C_{ij} in terms of Young's Modulus and Poisson's ratio defined by Lekhnitskii (1963) are as follows

$$
C_{11} = \frac{E_1}{\Delta \mu_{13}} \left(1 - \frac{E_1}{E_3} \nu_{13}^2 \right),
$$

$$
C_{33} = \frac{E_3}{\Delta \mu_{13}} \left(1 - \nu_{12}^2 \right),
$$

$$C_{12} = \frac{E_1}{\Delta \mu_{13}} \left(\nu_{12} + \frac{E_1}{E_3} \nu_{31}^2 \right),$$

$$C_{13} = \frac{E_1}{\Delta \mu_{13}} \nu_{31} \left(1 + \nu_{12} \right),$$

where $\Delta = 1 + \nu_{12}^2 - 2\frac{E_1}{E_3}\nu_{31}^2(1 + \nu_{12})$.

2. Three Planes Symmetry (Orthotropy):

An orthotropic solid such as Graphite-Epoxy, Carbon-Fibre, Glass-Epoxy has three planes of symmetry that are mutually perpendicular and its material characteristics differ across each of these three orthogonal planes and it has a coefficient matrix of order 6×6 with 9 non zero entries that relates the six independent components of strain to the six independent components of stress.

The general form of stress-strain relation for an orthotropic solid can be written as

$$
\begin{bmatrix} \sigma_1 \\ \sigma_2 \\ \sigma_3 \\ \sigma_4 \\ \sigma_5 \\ \sigma_6 \end{bmatrix}
=
\begin{bmatrix}
C_{11} & C_{12} & C_{13} & 0 & 0 & 0 \\
C_{12} & C_{22} & C_{23} & 0 & 0 & 0 \\
C_{13} & C_{23} & C_{33} & 0 & 0 & 0 \\
0 & 0 & 0 & C_{44} & 0 & 0 \\
0 & 0 & 0 & 0 & C_{55} & 0 \\
0 & 0 & 0 & 0 & 0 & C_{66}
\end{bmatrix}
\begin{bmatrix} \epsilon_1 \\ \epsilon_2 \\ \epsilon_3 \\ \epsilon_4 \\ \epsilon_5 \\ \epsilon_6 \end{bmatrix}
$$

Considering the generalized plane stress, the explicit form of stress and strain in term of the dimensionless elastic constants C_{ij} for orthotropic body are stated as follows

$$\frac{\sigma_{xx}}{\mu_{12}} = C_{11}\epsilon_{xx} + C_{12}\epsilon_{xy},$$

$$\frac{\sigma_{yy}}{\mu_{12}} = C_{12}\epsilon_{xy} + C_{22}\epsilon_{yy},$$

$$\frac{\sigma_{xy}}{\mu_{12}} = \epsilon_{xy},$$

and the constants C_{ij} are given by

$$C_{11} = \frac{E_1}{\triangle}(1 - \nu_{23}\nu_{32}),$$

$$C_{22} = \frac{E_2}{\triangle}(1 - \nu_{13}\nu_{31}),$$

$$C_{12} = \frac{E_1}{\triangle}\left(\nu_{21} + \nu_{13}\nu_{32}\frac{E_2}{E_1}\right)$$

$$= \frac{E_2}{\triangle}\left(\nu_{12} + \nu_{23}\nu_{31}\frac{E_1}{E_2}\right)\triangle,$$

$$\triangle = 1 - \nu_{12}\nu_{21} - \nu_{23}\nu_{32} - \nu_{31}\nu_{13} - \nu_{12}\nu_{23}\nu_{31} - \nu_{13}\nu_{21}\nu_{32},$$

where the subscripts 1, 2, and 3 correspond to the material orthotropy in x, y, and z directions respectively.

Additionally, the elastic constants E_i and ν_{ij} comply with the following Maxwell's relation

$$\frac{\nu_{ij}}{E_i} = \frac{\nu ji}{E_j}.$$

3. Isotropy:

In isotropic materials like Aluminium, Brass, Nickel, Steel, elastic properties remain same irrespective of directions. Here we have only two independent constants and the stress-strain relation in matrix form becomes

$$
\begin{bmatrix} \sigma_1 \\ \sigma_2 \\ \sigma_3 \\ \sigma_4 \\ \sigma_5 \\ \sigma_6 \end{bmatrix} = \begin{bmatrix} C_{11} & C_{12} & C_{12} & 0 & 0 & 0 \\ C_{12} & C_{11} & C_{12} & 0 & 0 & 0 \\ C_{12} & C_{12} & C_{11} & 0 & 0 & 0 \\ 0 & 0 & 0 & C_{11}-C_{12} & 0 & 0 \\ 0 & 0 & 0 & 0 & C_{11}-C_{12} & 0 \\ 0 & 0 & 0 & 0 & 0 & C_{11}-C_{12} \end{bmatrix} \begin{bmatrix} \epsilon_1 \\ \epsilon_2 \\ \epsilon_3 \\ \epsilon_4 \\ \epsilon_5 \\ \epsilon_6 \end{bmatrix}
$$

The substitutions $C_{12} = \lambda$ and $\frac{C_{11}-C_{12}}{2} = \mu$ transform the stress-strain relation to

$$
\sigma_{ij} = \lambda \delta_{ij} \epsilon_{kk} + 2\mu \epsilon_{ij}, \qquad (i, \ j, \ k = 1, \ 2, \ 3). \tag{1.4}
$$

Here the constants λ and μ are familiar as Lame's constants. Also two important elastic constants E (Young's modulus) and ν (Poisson's ratio) are defined as

$$
E = \frac{\mu(3\lambda+2\mu)}{\lambda+\mu}, \qquad \nu = \frac{\lambda}{2(\lambda+\mu)}.
$$

The expression of strain in terms of the elastic constants E and ν can be written as

$$
\epsilon_{ij} = \frac{1+\nu}{E}\sigma_{ij} - \frac{\nu}{E}\delta_{ij}\sigma_{kk}, \qquad (i, \ j, \ k = 1, \ 2, \ 3). \tag{1.5}
$$

■ Equation of Equilibrium

The equation of equilibrium in an isotropic medium is determined by the balance of forces acting on an infinitesimal element of the medium.

The equation of equilibrium for an isotropic media has the following general form

$$
\sigma_{ij,j} + F_i = 0, \tag{1.6}
$$

where $\sigma_{ij,k} = \frac{\partial \sigma_{ij}}{\partial x_k}$ and $F_i's$ are the components of the body force acting on the material.

The strain components in terms of displacements components can be written as

$$\epsilon_{ij} = \frac{1}{2}\left(\frac{\partial u_i}{\partial x_j} + \frac{\partial u_j}{\partial x_i}\right) \quad \text{and} \quad \epsilon_{ii} = \frac{\partial u_i}{\partial x_i}, \tag{1.7}$$

where u_1, u_2, and u_3 are the displacement components in the direction of ox_1, ox_2, ox_3.

Using (1.7), stress components for an isotropic medium can be obtained as

$$\sigma_{ij} = \lambda \delta_{ij} \frac{\partial u_k}{\partial x_k} + \mu\left(\frac{\partial u_i}{\partial x_j} + \frac{\partial u_j}{\partial x_i}\right). \tag{1.8}$$

Using (1.8) and after some algebraic calculations, equation (1.6) can be found as

$$\mu \nabla^2 u_i + (\lambda + \mu)\frac{\partial}{\partial x_i}\left(\frac{\partial u_k}{\partial x_k}\right) + F_i = 0. \tag{1.9}$$

The above equation is known as Navier's equation.

■ Types of Problems

In the context of elastodynamic problems, the Nevier's equations (1.9) are modified by adding the term $\rho\frac{\partial^2 u_i}{\partial t^2}$ to the right-hand side, where ρ represents the density of the material. In general, boundary value problems are linked to the wave propagation and diffraction phenomena.

The boundary value problems are classified into three major categories, which are described as follows:

Type 1: In this kind of boundary value problems, stress components of the elastic body are specified on the boundary surface i.e. the problem is to be solved whenever the body forces and surface forces acting on the surface of the body are provided.

The mathematical formulation of this kind of problem is

$$\mu \nabla^2 u_i + (\lambda + \mu) \frac{\partial}{\partial x_i} \left(\frac{\partial u_k}{\partial x_k} \right) + F_i = \rho \frac{\partial^2 u_i}{\partial t^2} \tag{1.10}$$

The equation (1.10) is to be solved subjected the initial conditions

$$u_i = u_{0i}(x_1, \ x_2, \ x_3) \ \text{ and } \ \frac{\partial u_i}{\partial t} = U_{0i}(x_1, \ x_2, \ x_3) \quad \text{ at } \ t = t_0, \tag{1.11}$$

and the boundary conditions

$$\bar{\sigma}_i(x_1, \ x_2, \ x_3, \ t) = g_i(x_1, \ x_2, \ x_3, \ t) \quad \text{ for } \quad t \geq t_0, \tag{1.12}$$

where $\bar{\sigma}_i$ are given tractions on the surface, ρ is the density of the material, and $(u_1(x_1, \ x_2, \ x_3, \ t), \ u_2(x_1, \ x_2, \ x_3, \ t), \ u_1(x_1, \ x_2, \ x_3, \ t))$ are the displacement components in the directions $ox_1, \ ox_2, \ ox_3$.

Type 2: In this case the body is in equilibrium under the influence of body force and displacements on the surface i.e. in this problem displacement components are given on some parts of the boundary of a solid.

For this displacement prescribed boundary conditions, the equation (1.10) is to solved subjected to the initial conditions (1.11) and the boundary conditions

$$u_i = U_i(x_1, \ x_2, \ x_3, \ t) \quad \text{ for } \quad t \geq t_0, \tag{1.13}$$

where $(U_1, \ U_2, \ U_3)$ are the given displacement components.

Type 3: A mixed boundary value problem in elastic solid is an another kind of boundary value problem that involves specifying both the displacement and the traction on several parts of the boundary of a solid or a region of a solid.

On a part of the boundary, the boundary condition may be given in terms of displacement, i.e.,

$$u_i = U_i(x_1, \ x_2, \ x_3, \ t) \quad \text{for} \quad t \geq t_0, \tag{1.14}$$

where $(U_1, \ U_2, \ U_3)$ are the given displacement components.

On another part of the boundary, the boundary condition may be given in terms of stress, i.e.,

$$\bar{\sigma}_i(x_1, \ x_2, \ x_3, \ t) = g_i(x_1, \ x_2, \ x_3, \ t) \quad \text{for} \quad t \geq t_0, \tag{1.15}$$

where $\bar{\sigma}_i$ are given traction on the surface
and $(u_1(x_1, \ x_2, \ x_3, \ t), \ u_2(x_1, \ x_2, \ x_3, \ t), \ u_1(x_1, \ x_2, \ x_3, \ t))$ are the displacement components in the directions $ox_1, \ ox_2, \ ox_3$.

■ **Magnetoelasticity**

In recent years, the interaction of electromagnetic fields with elastic media is a significant area of interest for many researchers because of the possibilities of their extensive practical applications in diverse fields such as acoustics, geophysics, optics and so on for both theoretical and exploratory investigations. The theory of the coupling effect of magnetic interaction and elasticity is the study of mechanical deformations of a solid structure subjected to an externally applied magnetic field. The total deformation of the solid body and the changes in governing laws are influenced by both magnetic and elastic fields. Maxwell's equations along with the modified Ohm's laws dictate the behavior of the electromagnetic field, whereas the

modified Hooke's law determines the characteristics of the elastic field. Also, due to superposition of electromagnetic field on elastic field, elastic-stress relation and field equations get modified by addition of a new body force known as Lorentz's force.

In 1864, James Clerk Maxwell derived four differential equations to describe electric vector field $\vec{\mathbf{E}}$, the magnetic field density $\vec{\mathbf{B}}$, and the nature of electromagnetic waves. These equations in differential form are as follows

$$\vec{\nabla} \cdot \vec{\mathbf{E}} = \frac{\rho}{\epsilon_0},$$

$$\vec{\nabla} \times \vec{\mathbf{E}} = -\frac{\partial \vec{\mathbf{B}}}{\partial t},$$

$$\vec{\nabla} \cdot \vec{\mathbf{B}} = 0,$$

$$\vec{\nabla} \times \vec{\mathbf{B}} = \mu_0 \vec{\mathbf{J}} + \mu_0 \epsilon_0 \frac{\partial \vec{\mathbf{E}}}{\partial t},$$

where ϵ_0 is the permittivity of free space, μ_0 is the permeability of free space, ρ is the density of electric charge, and $\vec{\mathbf{J}}$ is the density of electric current.

Modified Ohm's law is obtained by merging the traditional Ohm's law with the Lorentz force, which explains the movement of charged particles under the influence of a magnetic field and is given by

$$\vec{\mathbf{J}} = \sigma_0 (\vec{V} \times \vec{\mathbf{B}} + \vec{\mathbf{E}}),$$

where $\vec{V}$ and σ_0 are the velocity of charged particle and the conductivity coefficient of electric current.

The generalized Navier's equation in terms of the Lorentz force in a solid structure can be written as

$$\vec{\nabla} \cdot \vec{\Sigma} + \vec{F} + \vec{\mathbf{J}} \times \vec{\mathbf{B}} = \rho \frac{\partial^2 \vec{U}}{\partial t^2},$$

where $\vec{U}$ is the displacement vector, $\vec{\Sigma}$ is the stress tensor, $\vec{F}$ is the external force per unit volume, and $\vec{\mathbf{J}} \times \vec{\mathbf{B}}$ is the Lowrentz force.

Fracture mechanics is a specialized field of study that focuses on analyzing, prevention, and prediction of structural or mechanical malfunctions that arise from flaws or cracks in materials. Cracks can exist in a solid engineering structure due to variety of factors, including manufacturing defects, environmental conditions like exposure to high temperatures, chemicals, or corrosive substances, natural catastrophe, negligence of materials maintenance etc. In many cases, cracks in solid structures may begin small and gradually increases over time due to dynamic or static loading or other factors. Due to some well known catastrophe made either by naturally such as earthquake or by humanly such as World war II in recent history, numerous research has been carried out to comprehend the circumstances that result in failures and to develop the fracture criterion against such failures. Furthermore, fracture mechanics plays a vital role in advancing the development of new materials and manufacturing processes that exhibit greater resistance to failure and better suited for demanding engineering applications.

The discoveries of fracture mechanics can be traced back to the work of Leonardo Da Vinci in the 15Th century, who analyzed the behavior of cracks in stone and masonry. Kolosov (1909) developed the fundamental mathematical tools for studying fractures in his doctoral degree. A few years later, CE (1913) published a research paper in which he solved some basic problem related to crack. During the same year, Hopkinson (1913) proposed that there is a nonlinear phenomenon near about the vicinity of the crack edge. This issue was eventually resolved by Griffith (1920). He considered the principles of surface energy to analyze the crack edge region. Weibull (1939) developed a statistical approach of fracture mechanics motivated by the Griffith's studies with thin glass rods. The approach developed by Griffith was expanded by Orowan (1949) to include all cases of small scale yielding,

taking into account all forms of internal energy loss, particularly surface energy. Two fundamental physical quantities such as stress intensity factor and energy release rate were first proposed by Irwin (1957). These parameters are used to describe the toughness of solid materials. The field of fracture mechanics has also benefited from Barenblatt (1959), he introduced the Barenblatt-Dugdale cohesive zone model from the linearized model of the neighbourhood of the fatigue edge and his concept of cohesion modulus explains the propagation of cracks in solids materials. This model considers the cohesive forces prevailing at the crack tip, which can influence the material's characteristics as the crack advances.

During the latter half of the 20th century, there were remarkable quantitative and qualitative discoveries in the study of fractography and crack analysis. Many mathematicians and physicists made significant contributions to this field, which have greatly impacted fatigue analysis of material. The first person that comes to recognise is Rice (1968), who developed exceptional fracture criterion in almost every domains of fracture and the crack analysis. Starting in the mid-1960s, he introduced a path-independent integral, J-integral concept for the analysis of the nature of cracks, which served as the base for nonlinear fracture mechanics, and more recently he has made contributions to $3D$ dynamic crack problems. A number of research articles had been addressed in this topic by Geubelle and Rice (1995), Cochard and Rice (1997), Morrissey and Rice (1998). Russian scientist Kostrov (1966) found solutions of many challenging problems and developed Kostrov source model which was effective for the analysis of dynamics of earthquake rupture as well as propagation of dynamic crack. He was also the 1st seismologist to find a solution to the non constant crack expansion model. Material scientist Freund (1972) published a research articles on crack propagation in solid structure under constant velocity along with other physical issues, like stress wave interaction with cracks, that helps to anticipate the conditions under which cracks will advance in materials

and can be utilized to design more resilient materials. Also, some fundamental works and basic concepts dealing with fatigue of materials have been described in the books by Sih and Chen (2012), Freund (1998), Anderson (2017), and Love (1927).

Dynamic fracture mechanics deals with the mechanics of static or dynamic moving cracks in solid materials, where the influences of material inertia and stress wave interaction play a vital role. Therefore, the profound understanding of fracture mechanics is crucial in developing effective strategies for designing new structures that can withstand dynamic loads and prevent catastrophic failure of the material. In general, dynamic fracture problems can be classified as follows

- Solids with stationary cracks under dynamic loading.

- Solids with dynamic and moving crack subject to quasi-static loading.

- Solids with dynamic and moving crack subject to dynamic loading.

It is commonly accepted that the Earth is encompassed by a magnetic field that emanates from its core. As a result, it is imperative to take into account the impact of the magnetic field when dealing with a fractured elastic medium. The presence of a magnetic field can lead to interaction with any charged particles or currents within the cracked elastic medium, resulting in fascinating and valuable phenomena such as magnetostriction, and electromagnetic induction etc. These phenomena can be applied to control the performance of sensors and actuators made from elastic materials, generate electrical power through the process of electromagnetic induction, develop mechanical motion in elastic media which is exploited in electric motors, store and retrieve information in magnetized memory devices, such as hard drives and magnetic tapes etc. When a wave encounters the crack or flaws in an elastic material subjected to an external magnetic field, some of the energy of the wave is reflected back, while some is passes through the crack. The transmitted energy can

interact with the crack and result it to grow through the crack tip, which can lead to catastrophic failure of the material structure. Therefore when cracks are present in material, understanding the behavior of waves is very crucial for assessing the structure's integrity and anticipating its failure. One practical way to achieve this is formulating a physical problem related to the diffraction of elastic waves. Generally there are two categories of diffraction problems, the first approach involves the wave diffraction by semi-infinite plane that contain cracks in the elastic medium and the second approach includes the diffraction of waves influenced by inclusions such as circular disc, rigid strips, cone, elliptical disc or barrier of several random shape. Problems related to mechanics of solids may be divided into two types with respect to the solution, the first one is precise analytical solutions and the other one is approximate solutions estimated by several numerical techniques. In real situation, it seems tough to find exact analytical solution. For this reason, several techniques have been derived to address the solution regarding the characteristic of solid structures that contain crack. The complex variable technique is one of these numerical method to solve 2D mixed boundary value problems. The other well-known recent technique to solve these physical problem is the integral equation approach where the components of displacements are expressed in terms of potential function to reduce mathematical computations.

Many structural materials contain cracks, which can result from inherent imperfections or manufacturing methods. Many times, the cracks are negligibly tiny, meaning that they have little effect on the material's strength. However, in other cases, the cracks are significant enough or could grow to be large enough to cause fatigue, corrosion etc. Mainly three types of cracks are observed in engineering structure and they are classified as Opening Mode, Sliding Mode and Tearing Mode.

■ Opening Mode

The opening mode of crack takes place when the crack surfaces are pulled apart in reverse directions, perpendicular to the crack's plane. This means that the tension acts perpendicular to the crack surface and the crack advances because of the detachment of the material along the crack's plane. This kind of fracture is often observed in brittle materials like ceramics, glass, and certain types of polymers
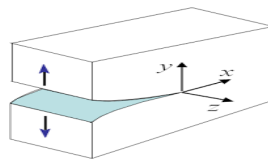
Fig.1.5 Opening Mode

■ Sliding Mode:

The sliding mode of crack refers to a fracture mode where the crack surfaces slide against each other parallel to the crack's plane. In this mode, the tension acts parallel to the crack plane and perpendicular to the direction of crack propagation. This type of fracture is typically observed in materials like metals, as well as certain polymers and composites.
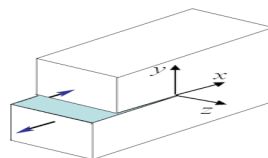
Fig.1.6 Sliding Mode

■ Tearing Mode:

The term tearing mode describes a particular sort of fracture in which the crack surfaces move relative to each other in a direction that is perpendicular to the plane

of the crack. It occurs when the stress acts perpendicular to the crack plane and parallel to the direction of crack propagation. This type of fracture is not common like opening and sliding mode, it can occur in some materials that have complicated geometries, such as thin sheets or laminates.
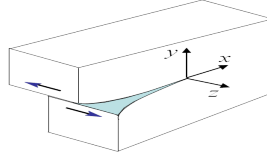
Fig.1.7   Tearing Mode

Such pre-existing cracks in a material lead to stress concentration in the neighbourhood of the tip of the crack, which causes a singularity or a sharp increase in stress levels. The traditional analytical inspection of fracture mechanics entails computing those singular stress and displacement fields near the crack vicinities. These singular stress helps physicist to develop a failure criterion of a continuum model, like the homogeneous isotropic linearly elastic continuum, anisotropic continuum under the influences of body force and surface force. One fundamental failure criterion is to calculate the stress intensity factor, which is generally denoted by K. In fracture mechanics, the stress intensity factor is a key parameter that helps to predict the stress state distribution near the vicinity of the crack caused by an external load or subjected to a body force like Lorentz force. It is a significant method in the domain of damage tolerance for brittle materials and it is a theoretical construct for linear elastic material. This concept can also be extended to materials that display small scale yielding near about the crack tip. The value of stress intensity factor (K) is influenced by various factors, including the geometry and the size of the crack, the distribution of applied loads, materials properties, mode of loadings. According to the linear elastic theory, the stress distributions (σ_{ij}) around the crack vicinity can

be written in terms of polar coordinate (r, θ) as

$$\sigma_{ij}(r, \theta) = \frac{K}{\sqrt{2\pi r}} G(\theta), \tag{1.16}$$

where $G(\theta)$ indicates a dimensionless quantity and its value depends on the loading type and geometry of the cracks.

From the equation (1.16), it concludes that the stress distribution becomes intensely localized and the magnitude of the stress escalates rapidly when the distance (r) from the crack tip diminishes resulting in a square root singularity in the stress distribution.

To describe the stress state around the crack tip, stress intensity factors for three different modes of fracture can be defined by neglecting the square root singularity as

$$K_{(I)} = \sqrt{2\pi} \lim_{r \to 0} \sqrt{r} \ \sigma_{yy}(r, 0),$$
$$K_{(II)} = \sqrt{2\pi} \lim_{r \to 0} \sqrt{r} \ \sigma_{xy}(r, 0),$$
$$K_{(III)} = \sqrt{2\pi} \lim_{r \to 0} \sqrt{r} \ \sigma_{yz}(r, 0),$$

where the suffixes (I), (II), (III) represent the SIF for opening mode, sliding mode and tearing mode.

There are primarily two major categories of fracture mechanics problems that are treated as dynamic problems. The first category includes elastic bodies with cracks that experience rapidly changing loads, while the second category involves bodies that contain cracks which grows so fast. The crack tip surroundings is disturbed by the diffraction or scattering of wave motions in both of these categories. Vibration analysis of the elastic medium and the effect of several loading on the cracks fall into the first category of dynamic problem. In the analysis of these kind of problems,

it is frequently found that at nonhomogeneities in a body, the dynamic stresses is calculated by considering static equilibrium. Numerous engineering structures encounter the issue of rapid crack growth in various forms, such as gas transmission pipelines, nuclear reactor, automobile engine, ship hulls, and aircraft fuselages. The use of elastic waves in seismology and geophysics has become increasingly relevant in recent years, but one major challenge is their diffraction or scattering effect when encountering cracks or other structural irregularities. The investigation of propagation of waves can be done by considering a mixed boundary value problems.

If cracks or inclusions present in a composite medium when the medium is subjected to an externally applied magnetic field, the analysis of singular stress field and the diffraction of waves become more challenging. Numerous researchers have investigated various types of elastodynamic problems for different kind of elastic materials with several geometry regarding to the position of cracks. Mandal and Ghosh (1994) studied the response of a series of coaxial Griffith cracks in an infinite orthotropic plane to time harmonic elastic waves that propagate in the direction normal to the plane.

The dispersion effect of a normally incident shear wave by two symmetrically placed co-planar finite rigid strips in an infinitely long elastic strip that is perpendicular to the lateral surface was investigated by Pramanik et al. (1999). The study also includes the prediction of the dispersion coefficient of the elastic strip. Transient SIF of a cracked elastic structure where the crack is located within a non-homogeneous layer sandwiched by two distinct elastic half-planes have been analyzed by Itou (2001). The study conducted by Matysiak and Pauk (2003) focused on the model that is based on edge cracks in an elastic layer lying on the Winkler foundation. The dynamic behaviour regarding a crack located at the edge of a functionally graded orthotropic strip was examined by Guo et al. (2005). Kadıoğ˘lu (2005) investigated elastodynamic response related to an edge crack located within a hollow cylinder

made of transversely isotropic substance. Munshi and Mandal (2006) addressed the P-wave diffraction problem caused by an edge crack inside an infinitely long elastic strip. The singular stress field of a 3D interfacial crack in different anisotropic materials was analyzed by Nagai et al. (2007).

The model of a flexible elastic plate with a stiff core on the ground (saturated) under the influence of a vertical vibration was examined by Chen et al. (2007). Vibration phenomena due to the cracks inside a generalized anisotropic elastic plane have been discussed by Willis and Movchan (2007). Matbuly (2008) analyzed the propagation behaviour of mode-III crack located at the interface of a functionally graded material and an isotropic material. Eskandari-Ghadi et al. (2011) described rigid circular disc's vibration effect in an infinitely extended transversely isotropic elastic plane and examined that stress singularity exists near the edge of the disc. Ding and Li (2014) considered a series of cracks which are collinear in nature and located within a functionally graded coating-substrate made of orthotropic media and analyzed the singular nature of the stress in the neighbourhood of crack vicinities. Basak and Mandal (2019) developed fracture criterion for a crack (semi-infinite) located at the juncture of two distinguished elastic strips made of isotropic material based on the Wiener-Hopf approach. Singh et al. (2020) calculated the SIF and COD around the rim of a crack (semi-infinite) which propagates in a linear orthotropic strip of finite width implanted between two identical type half-planes. Mandal (2020) derived implicit expressions of SIF and COD near a crack (semi-infinite) moving along the intersection of a strip of finite width and an isotropic half plane to analyzed the scattering phenomena of shear loads. Naskar et al. (2023) solved a physical problem of the dispersion of longitudinal wave caused by the presence of three cracks of finite length under sudden load which acts normally to the crack surfaces.

To generate novel structural designs, advance material characterization, and

optimize their performance, it is crucial to address the influence of torsional waves in order to mitigate damage to solids during earthquakes and other real-world scenarios. Torsion is a type of wave disturbance that generates pressure on crack and disc surfaces, triggering crack propagation and creating stress fields around circular sections within engineering solids. Torsional waves can occur in any type of solid structure like beams, columns, shafts, and plates, etc. Also, in the field of engineering foundations, creating a composite structure under the effect of a magnetic field is a challenging process but the resulting magnetized composite structures exhibit high mechanical performance, such as high-stiffness, lightweight phenomena, flexibility, durability, etc. So the application of magnetic field in the production of composite materials can be crucial in accomplishing the desired material properties and performances. In fracture analysis, the response of layered composites having cracks or inclusions is highly influenced by the anisotropic nature of the materials and the external magnetic field.

Wang et al. (2000) explored the fracture configuration for multi-layers structure containing a circular crack influenced by torsional load. Selvadurai (2002) solved an axisymmetric problem related to the tensile loading on the surface of a penny shaped crack in a homogeneous elastic space. Manna et al. (2003) investigated the physical model of a rigid disc oscillating within an infinite cylinder subjected to an initial torsion. Huang et al. (2005) investigated the stress field and displacement field around a circular shaped crack placed within a heterogeneous elastic media under the effect of torsion. Wu (2006) studied the adhesive characteristics between a circular disc having nano-scale dimension and an infinite elastic surface. Li and Kardomateas (2006) examined the interface crack problem in tearing mode for bi-material engineering structure that have distinct piezo-electro-magneto-elastic properties. An analytic way of describing the stress for a circular crack incorporating with spherical inclusions and(or) voids in an infinite elastic space was discussed by Lee and Tran

(2010). The physical phenomena of torsional vibration of a rigid circular shaped interfacial crack positioned at the juncture of two dissimilar homogeneous elastic media was analyzed by Basu (2014). Hu and Chen (2015) focused on the Mode one crack phenomenon in a magnetoelectroelastic strip that is embedded between two distinct isotropic half-planes and investigated the fracture toughness of the structure under the impact of some mechanical, electric, and magnetic loads.

The axisymmetric mixed boundary value problem regarding the influence of torsional oscillations on a crack of finite radius in a homogeneous elastic layer was solved by Basu and Mandal (2016). Karan et al. (2018) discussed dynamic stress intensity factor due to the presence of penny-shaped crack in a three-component elastic structure consisting of two dissimilar half-spaces and an intermediate layer. Propagation of torsional waves through a perfectly conducting electric medium containing circular crack subjected to a thermal and magnetic load was investigated by Li et al. (2017). Madani and Kebli (2019) analyzed and resolved the issue of axisymmetric torsion in an elastic layer embedded between two semi infinite elastic planes when the layer is weakened by two interfacial penny shaped crack. Panja and Mandal (2021b) discussed the magneto elastic coupling effect on a crack of finite length placed inside a homogeneous strip. The stress–strain state and the crack tip field of a ferromagnetic elastic structure containing a crack under the effect of an external magnetic field was discussed by Baghdasaryan (2023).

Based on the literature survey described above, we will present our thesis in individual chapters as outlined below:

In our research project we have investigated some physical problems having mixed boundary conditions related to the geometry of the location of cracks. In Chapter 2, we present a brief summary of the standard numerical approaches and techniques we employed to address these problems.

Chapter 3 investigates the P-wave diffraction by an asymmetric crack in an isotropic strip under an external impact load. The crack is suddenly loaded by a normal stress such that the crack surfaces displaced in reverse directions. The problem has been transformed into two integral equations and the dual integral equations have been solved with the application of Abel's transform and reduced into a Fredholm integral equation of second kind in the Laplacian domain. The reduced integral equation has been solved numerically by employing Fox and Goodwin's method. Time dependent stress intensity factor has been calculated numerically by Zakian's Laplace inversion approach and displayed graphically for different time interval to demonstrate the influence of impact load over the crack surface.

In the first section of Chapter 4, interaction of shear waves by two collinear finite cracks in an infinite magnetoelastic orthotropic medium has been analyzed. The physical phenomena of wave interaction have been formulated as a mixed boundary value problem (MBVP). The MBVP has been solved with the help of Abel's transform and Hilbert transformation. The analytic expression of stress intensity factors and crack opening displacement have been computed and demonstrated graphically to exhibit the effect of magnetization on elastic media.

In the second section, an analytical solution of the magneto-elastic coupling effect on the dispersion of longitudinal waves in a magnetize isotropic elastic solid containing three co-linear cracks has been investigated. The semi-analytical expressions of crack opening displacement and stress intensity factors have been derived related to low frequency waves. Numerical outcomes of crack opening displacement and stress intensity factors for several crack lengths with the presence of magnetic field have been computed and presented graphically.

In the Chapter 5, we considered the response of torsional impact on a penny shaped crack positioned at the intersection of an isotropic half space and a transversely isotropic magnetoelastic layer of finite thickness. The physical problem has

been converted to a pair of dual integral equation with the use of boundary conditions, Laplace and Hankel transformation approach. A trial solution has been considered to reduce dual integral equations into a Fredholm integral equation in the Laplacian domain. Later, Fox and Goodwin's procedure has been adopted to solve the reduced integral equation numerically. The implicit expression of stress intensity factor around the crack periphery has been calculated utilizing Zakian's inversion formulae and displayed graphically against time for different parameters to demonstrate the influence of torsional impact and the magnetized layer over the crack boundary.

Chapter-2
Methodology

Chapter 2

Methodology

The physical phenomena of wave interaction by single or multiple cracks can be formulated as a mixed boundary value problem (MBVP). Generally, the aim of structural engineer is to resist the propagating crack once it started growing. Determination of singular stress field and displacement field around crack vicinities are crucial to arrest the crack propagation. Most of the fracture mechanics problems involve complex geometries such as irregular shapes or structures with varying thicknesses, multiple cracks, various loading conditions like torsional load, magnetic field, which are difficult to solve using analytical methods. So, evaluation of singular stresses and strains can only be done by employing several numerical approaches also. We have employed following methods in our research work to investigate mixed boundary value problems.

1. Abel's Integral Approach.

2. Dual Integral Equations Method.

3. Hankel Transformation.

4. Numerical Solution of Fredholm Integral Equation of 2nd kind.

5. Numerical Inversion of Laplace Transform using Zakian Algorithm.

2.1 Abel's Integral Approach

Abel's integral equation having singular kernel is utilized to transform the pair of integral equation into a single Fredholm type integral equation.

First kind Abel's integral equation with singular kernel is

$$\alpha(\zeta) = \int_a^\zeta \frac{\beta(x)dx}{\sqrt{\zeta - x}},$$
(2.1.1)

where $\alpha(\zeta)$ is a given function, $\beta(x)$ represents an unknown function which is to be determined, and the kernel $l(\zeta, \ x) = \frac{1}{\sqrt{\zeta - x}} \to \infty$ as $x \to \zeta$ is unbounded.

The unknown function in the equation (2.1.1) is obtained as

$$\beta(\zeta) = \frac{1}{\pi} \frac{d}{d\zeta} \int_a^\zeta \frac{\alpha(x)dx}{\sqrt{\zeta - x}} = \frac{\alpha(a)}{\pi\sqrt{\zeta - a}} + \frac{1}{\pi} \int_a^\zeta \frac{\alpha'(x)dx}{\sqrt{\zeta - x}}.$$
(2.1.2)

The general form of first kind Abel's integral equation is expressed as

$$\alpha(\zeta) = \int_a^\zeta \frac{\beta(x)dx}{(\zeta - x)^m}, \quad 0 < m < 1,$$
(2.1.3)

and the solution of (2.1.3) is

$$\beta(\zeta) = \frac{\sin(\pi m)}{\pi} \frac{d}{d\zeta} \int_a^\zeta \frac{\alpha(x)dx}{(\zeta - x)^{1-m}} = \frac{\sin(\pi m)}{\pi} \left[\frac{\alpha(a)}{(\zeta - a)^{1-m}} + \int_a^\zeta \frac{\alpha'(x)dx}{(\zeta - x)^{1-m}} \right].$$
(2.1.4)

2.2 Dual Integral Equations Method

The method of dual integral equations is a valuable tool for solving mixed boundary value problems. In this method the pair of dual integral equations can be transformed to a single Fredholm integral equation containing some unknown variable with the help of Abel's transform and the implicit form of the unknown function can be derived through straightforward integration technique.

Assume that a mixed boundary value problem has been transformed using some appropriate integral transforms, resulting in a pair of dual integral equations given by

$$\int_0^\infty x^{-1}\Big[1 + K(x)\Big]S(x)J_\nu(rx)dx = f(r), \qquad 0 \leq r < a \qquad (2.2.1)$$

$$\int_0^\infty S(x)J_\nu(rx)dx = g(r), \qquad r > a, \qquad (2.2.2)$$

where $K(x)$, $f(r)$ and $g(r)$ represent known functions. Based on the work of Noble (1963), the following result is derived

$$S(x) = \sqrt{\frac{2x}{\pi}}\left[\int_0^a t^{1/2}\theta(t)J_{\nu-\frac{1}{2}}(xt)dt + \int_a^\infty t^{\nu+\frac{1}{2}}G(t)J_{\nu-\frac{1}{2}}(xt)dt\right], \qquad (2.2.3)$$

where the unknown function $\theta(t)$ satisfies the following Fredholm integral equation

$$\theta(t) + \frac{1}{\pi}\int_0^a M(\tau, t)\theta(\tau)d\tau = t^{-\nu}F(t) - H(t), \quad 0 < t < a \qquad (2.2.4)$$

in which

$$M(\tau, t) = \pi\sqrt{\tau t}\int_0^\infty xK(x)J_{\nu-\frac{1}{2}}(\tau x)J_{\nu-\frac{1}{2}}(tx)dx, \quad \nu > -\frac{1}{2}, \qquad (2.2.5)$$

$$F(t) = \frac{d}{dt}\int_0^t f(r)r^{\nu+1}(t^2 - r^2)^{-1/2}dr, \qquad (2.2.6)$$

$$H(t) = t^{1/2} \int_0^\infty x K(x) J_{\nu-\frac{1}{2}}(xt) dx \int_a^\infty \xi^{\nu+\frac{1}{2}} G(\xi) J_{\nu-\frac{1}{2}}(x\xi) d\xi, \qquad (2.2.7)$$

$$G(\xi) = \int_\xi^\infty g(r) r^{-\nu+1} (r^2 - \xi^2)^{-1/2} dr. \qquad (2.2.8)$$

By solving the integral equation (2.2.4), $\theta(t)$ can be obtained, which in turn lead to the determination of the desired $S(x)$.

2.3 Hankel Transformation

The Hankel transform is a generalization of the Fourier transform and it is often used in solving boundary value problems involving cylindrical or spherical symmetry. This transform is used to convert Laplace's partial differential equation in cylindrical coordinates to an ordinary differential equation. Let $h(s)$ is a function defined for $r \geq 0$. The mth order "Hankel transform" of $h(s)$ can be stated as

$$\mathcal{H}_m(u) = \int_0^\infty sh(s) J_m(su) ds. \qquad (2.3.1)$$

Here $J_m(su)$ represents first kind Bessel function with order m and $s J_m(su)$ represents kernel related to the transformation. If $m > -\frac{1}{2}$, an inversion formula known Hankel inversion is defined by the following integral

$$h(s) = \int_0^\infty u\mathcal{H}_m(u) J_m(su) du. \qquad (2.3.2)$$

Conditions that are sufficient but not essential for the validity of (2.3.1) and (2.3.2) are

1. $h(s) = 0(s^{-\nu})$ for $s \to \infty$ and $\nu > \frac{3}{2}$.

2. The function $h'(s)$ is continuous function on every bounded sub interval of the unbounded interval $[0, \infty)$.

3. The function $|h(s)|$ must be integrable over the range $[0, \infty)$.

2.4   Numerical Solution of Fredholm Integral Equation of 2nd kind

Sometimes it is impossible to solve an integral equation directly. In such cases, an important numerical tool developed by Fox and Goodwin (1953) is employed to solve the problem. This method consists of representing the integral equation as a system of linear equations of desired function, where the known variables are the pivot values of the desired function. Then the values of the desired function can be determined using difference correction approach.

The first and second kind Fredholm-type equations are expressed as follows

$$\int_a^b L(\zeta, \xi)\alpha(\xi)d\xi = \beta(\zeta), \tag{2.4.1}$$

$$\int_a^b L(\zeta, \xi)\alpha(\xi)d\xi = \beta(\zeta) + \alpha(\zeta). \tag{2.4.2}$$

Also, another type of integral equation is given by

$$\lambda \int_a^b L(\zeta, \xi)\alpha(\xi)d\xi = \beta(\zeta). \tag{2.4.3}$$

Here $\alpha(\xi)$ is the desired function which is to be calculated and $L(\zeta, \xi)$, $\beta(\zeta)$ are known either in analytic form or in numeric form. For solving the equation (2.4.3), we need to compute the eigen vectors corresponding to each eigen values λ.

For each cases mentioned above, we will represent the integral as a linear equation in terms of $a_r L(\zeta_s, \xi_r)\alpha(\xi_r)$. To achieve this, we must look at certain formulae regarding numerical integration.

Numerical Integration:

In general, the integral formula involving differences is more preferable over the Lagrangian type formulae. The best finite-difference integration formulae is expressed in the form

$$\frac{1}{h} \int_a^{a+nh} \alpha(\zeta)d\zeta = \frac{1}{2}\alpha_0 + \alpha_1 + ... + \alpha_{n-1} + \frac{1}{2}\alpha_n + \Delta, \qquad (2.4.4)$$

where $\alpha_i = \alpha(a+ih)$, $i = 0, 1, 2, ..., n$ and Δ denotes the difference correction operation related to function $\alpha(\zeta)$.

For $n = 1$, the integral is calculated between two nearby pivotal points a and $a + h$ and using central differences we get the following result

$$\frac{1}{h} \int_a^{a+h} \alpha(\zeta)d\zeta = \frac{1}{2}(\alpha_0 + \alpha_1) - \frac{1}{12}\mu\delta^2\alpha_{\frac{1}{2}} + \frac{11}{720}\mu\delta^4\alpha_{\frac{1}{2}} \qquad (2.4.5)$$

and for generalised case

$$\frac{1}{h} \int_a^{a+nh} \alpha(\zeta)d\zeta = \frac{1}{2}\alpha_0 + \alpha_1 + ... + \alpha_{n-1} + \frac{1}{2}\alpha_n + \Delta, \qquad (2.4.6)$$

where

$$\Delta = \left(-\frac{1}{12}\Delta^1 + \frac{1}{24}\Delta^2 - \frac{19}{720}\Delta^3...\right)(\alpha_n - \alpha_0). \qquad (2.4.7)$$

Each of these formulae use differences that are derived from pivotal points lying outside the integration range. If we consider the pivot point inside the range of integration then equation (2.4.6) can be converted into a formula by rewriting the

difference correction Δ as

$$\Delta = \left(-\frac{1}{12}\nabla^1 + \frac{1}{24}\nabla^2 + \frac{19}{720}\nabla^3...\right)\alpha_n$$
$$+ \left(\frac{1}{12}\Delta^1 - \frac{1}{24}\Delta^2 + \frac{19}{720}\Delta^3...\right)\alpha_0. \tag{2.4.8}$$

This modified difference correction incorporates the Gregory's integration formula. Our main ally in solving Fredholm type integral equations is the Gregory integration formula. We are only interested of its solution at pivotal points under a designated range of the integration.

Solution of Fredholm's Equation of the Second Kind:

We commence by addressing 2nd kind Fredhlom's equation which is represented in equation (2.4.2). Utilizing the value of the integration given by (2.4.4), equation (2.4.2) may be written as follows

$$h\left[\tfrac{1}{2}L(\zeta,0)\alpha_0 + L(\zeta,1)\alpha_1 + ... + L(\zeta,n-1)\alpha_{n-1} + \tfrac{1}{2}L(\zeta,n)\alpha_n + \Delta(\zeta)\right] = \beta(\zeta) + \alpha(\zeta),$$

where $L(\zeta, x)$ gives the value of $L(\zeta, \xi)$ at (ζ, xh). Once all pivotal points are taken into account, the integral equation (2.4.2) can be reduced to a group of $(n+1)$ linear simultaneous equations as

$$h\left[\frac{1}{2}L(r,0)\alpha_0 + L(r,1)\alpha_1 + ... + L(r,n-1)\alpha_{n-1} + \frac{1}{2}L(r,n)\alpha_n + \Delta_r\right]$$
$$= \beta_r + \alpha_r, \tag{2.4.9}$$

where $L(r, x)$ gives the value of $L(\zeta, \xi)$ at (rh, xh), $r = 0$, 1, 2, ...n. By rearranging α_r and Δ_r, equation (2.4.9) can be written as

$$\left[1 - \frac{1}{2}hk(0,0)\right]\alpha_0 - hL(0,1)\alpha_1... - hL(0,n-1)\alpha_{n-1} - \frac{1}{2}hL(0,n)\alpha_n$$
$$= -\beta_0 + h\Delta_0,$$

$$-\frac{1}{2}hL(1,0)\alpha_0 + [1 - hL(1,1)]\,\alpha_1... - hL(1,n-1)\alpha_{n-1} - \frac{1}{2}hL(1,n)\alpha_n$$

$$= -\beta_1 + h\Delta_1,$$

$$\dotfill \qquad (2.4.10)$$

$$-\frac{1}{2}hL(n-1,0)\alpha_0 - hL(n-1,1)\alpha_1... + [1 - hL(n-1,n-1)]\,\alpha_{n-1}$$

$$-\frac{1}{2}hl(n-1,n)\alpha_n = -\beta_{n-1} + h\Delta_{n-1},$$

$$-\frac{1}{2}hL(n,0)\alpha_0 - hL(n,1)\alpha_1... - hL(n,n-1)\alpha_{n-1} + \left[1 - \frac{1}{2}hL(n,n)\right]\alpha_n$$

$$= -\beta_n + h\Delta_n.$$

We will briefly discuss some potential possibilities for solving these equations.

According to Gregory formulae, the difference corrections Δ_r are linear functions of α_r. These linear functions would be known if we know the order of the most significant difference in (2.4.8). Δ_r in (2.4.8) could therefore be moved to the left, leading to a set of linear equations for α_r that would have distinct coefficients.

As an alternative we may select a very tiny interval with the goal of making Δ_r insignificant. This could require solving a large number of linear equations, which can be a time-consuming process and increase the risk of errors due to poor conditioning. So, we could solve the equation by retaining up to the fourth differences in Δ, and then comparing the result by retaining up to the sixth differences.

In iterative method, we obtain an initial approximation to the desired solution by omitting the Δ_r in equation (2.4.10). For each ζ we then compute difference between $L(\zeta,0)\alpha_0$ and $L(\zeta,1)\alpha_1$, using the calculated approximation of α_r. Then all Δ_r can be computed and added in the right-hand side of equations (2.4.10) for correction. Next, necessary corrections to α_r are done trivially and the similar step is iterated until there is no further change.

This method represented symbolically as follows. If M represents the coefficient matrix related to α_r, β is the vector having components as β_r and Δ represents the vector with components Δ_r, we solve the equations sequentially as

$$M\alpha^{(0)} = -\beta,$$

$$M\alpha^{(1)} = h\Delta(\alpha^{(0)}),$$

$$M\alpha^{(2)} = h\Delta(\alpha^{(1)}),$$

$$\dots\dots\dots\dots\dots\dots\dots,$$

and the final solution is

$$\alpha = \alpha^{(0)} + \alpha^{(1)} + \alpha^{(2)} + \dots\dots$$

The methodology is equivalent to that of Fox (1949) when tackling problems that contains differential equations with mixed boundary conditions. The length of interval h can be any value but our aim is to minimize the number of linear equations so that we can get appropriate finite-difference equations, and therefore, the interval should not be too large.

2.5 Numerical Inversion of Laplace Transform using Zakian Algorithm

This numerical approach is one of a class of techniques where the Laplace inverse $l(t)$ of $\mathcal{L}(p)$ is calculated as a sum of a finite series

$$l(t) = \sum_{r=1}^{M} \mathcal{K}_r \mathcal{L}(p_r),$$

where the nodes p_r, weights $\mathcal{K}_r$, and M are computed by a specific technique.

As per Zakian's algorithm (Rice and Duong (1995)), the time function $l(t)$ can be found by computing the value of the sum of the products of weights and exponential functions

$$l(t) = \sum_{r=1}^{M} \mathcal{K}_r e^{x_r t}.$$

The Zakian algorithm is particularly useful for functions having singular or oscillatory behavior, since it can flawlessly capture such configurations having small number of poles. This algorithm gives accurate value for over damped and slightly underdamped configuration, but it is inaccurate for systems that oscillate for a long time.

The Following formula enables us to get the numeric value of $l(t)$ which is the Laplace inversion of $\mathcal{L}(p)$

$$l(t) = \frac{2}{t} \sum_{r=1}^{5} REAL \left(\mathcal{K}_r, \ \mathcal{L}\left(\frac{x_r}{t}\right)\right).$$

The values of the nodes (x_r) and the weights $(\mathcal{K}_r)$ are given by

r	x_r	$\mathcal{K}_r$
I	$12.83767675 + i1.666063445$	$-36902.08210 + i196990.4257$
II	$12.22613209 + i5.012718792$	$61277.02524 - i95408.62551$
III	$10.93430308 + i8.409673116$	$-28916.56288 + i18169.18531$
IV	$8.776434715 + i11.92185389$	$4655.361138 - i1.901528642$
V	$5.22543361 + i15.72952905$	$-118.7414011 - i141.3036911$

The implementation of Zakian's Algorithm is straightforward and yields fast computations. But this algorithm fails to determine the initial phase value $l(0)$ of the function $l(t)$. Also, the numeric values of $l(t)$ becomes incorrect after the second oscillation.

Chapter-3

Impact Response on an Asymmetric Crack

Chapter 3

Impact Response on a Crack at Asymmetric Position in an Elastic Strip

■ Introduction

Mechanics of fracture is a crucial branch of solid mechanics that analyzes the behavior of existing cracks, which arise in a solid engineering structure because of manufacturing obliquity, heavy loadings, negligence in maintenance, and natural catastrophe like earthquake or flood. Whenever a cracked body is experienced an impact load, existing crack may propagates which affects the rigidity and integrity of the material. These flaws create obstruction for the completion of a solid structure. Researchers try to develop new approaches by which the circulation of cracks or flaws can be resisted. One such approach is the determination of stress intensity factor that helps to characterise the singular stress at the vicinity of the crack when the external load is applied. Sih and Chen (1977) calculated singular stress field near the crack vicinity of various crack problem. Nilsson (1972) analyzed dynamic stress intensity factor for the problem of elastic wave diffracted by a crack situated in an elastic strip of finite width. An analysis of normally incident elastic waves by a Griffith crack of finite length located in an isotropic plate was done by Mal

(1970). Srivastava et al. (1981) have discussed the singular stress distribution near the tip of a Griffith crack in an infinitely extended elastic strip. Naskar and Mandal (2018) have investigated the diffraction effects of longitudinal wave by a finite crack whenever an impact load is applied throughout the surface of the crack. With the consideration of a semi infinite cracked elastic strip, Shindo et al. (1986) computed stress intensity factor near the crack tips. Knauss (1966) evaluated asymptotic stress field as a function of crack length and strip width in a cracked infinite strip. The problem of finite edge crack in a semi-infinite elastic strip of finite width caused by the normal impact has been investigated by Das et al. (2008). Wang et al. (2001) proposed a method to calculate the dynamic stress intensity factors in a Laplace transform plane for a crack located in a non uniform elastic media. Mishra et al. (2016) have studied propagation of longitudinal waves in a cracked elastic structure by integral equation method and showed that crack propagation can be arrested. Itou (2004) was made an effort to obtain an analytic expression of stress intensity factor near the crack tips where the crack lies in a non uniform elastic layer which is also bonded by two elastic half spaces. The in-plane problem of diffraction of elastic wave by an edge crack contained in an infinitely extended elastic strip was solved by Munshi and Mandal (2006). Li (2005) investigated the fracture behaviour of an orthotropic elastic strip containing an inter facial crack which is in symmetrical position inside the strip.

The problems analyzed by above mentioned authors deal with cracks located either in an infinite medium or at symmetric position in strip. In some cases, the crack location in the elastic body is not symmetrical with respect to boundary line ant it is difficult to detect the position of such crack as it includes additional boundary conditions. Therefore, the main point of the current approach is to analyzes the effect of impact load applied over the surface of the crack positioned in an asymmetric location in an isotropic strip by determining the stress field around the crack

vicinity. The diffraction effects of P-wave by a finite Griffith crack located in an infinite isotropic strip under the effect of an impact load formulated as an MBVP. In these type of problems, the crack is suddenly loaded by an equal and opposite normal stresses such that the crack surfaces displaced in reverse directions. The MBVP has been transformed into integral equations with the help of Laplace transform, Fourier transform, and boundary conditions. Considering a trial solution, dual integral equations have been solved with the application of Abel's transform and reduced into a Fredholm integral equation of second kind in Laplacian domain. The reduced integral equation has been solved numerically by employing Fox and Goodwin's method. The time dependent expression of stress intensity factor has been derived by Zakian's Laplace inversion approach and displayed graphically for different time interval to show the influence of impact load over the crack surfaces.

■ Problem Construction

Let us assume a Griffith crack located in an infinite elastic strip given by $-b_1 \leq x_1 \leq c_1$ subject to an external impact load and the crack location is $|x_1| \leq a$, $y_1 = 0$, $|z_1| < \infty$. Normalizing all the lengths by a constant 'a' and substituting $\frac{x_1}{a} = x$, $\frac{y_1}{a} = y$, $\frac{z_1}{a} = z$, $\frac{b_1}{a} = b$, $\frac{c_1}{a} = c$, new location of the crack and strip is found to be $|x| \leq 1$, $y = 0$, $|z| < \infty$ and $-b \leq x \leq c$ (Fig.3.1) regarded to the Cartesian frame of reference $(x,\ y,\ z)$.
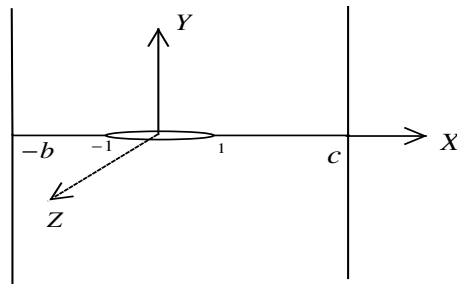
Fig.3.1 Crack Geometry.

Let an external load of magnitude τ_0 acts normally on each crack surface at time $t = 0$. In this problem longitudinal wave propagates in the xy plane, so τ_{yy}, τ_{xx} and τ_{xy} are the non zero stresses and u and v are the non zero displacements only. With the help of Helmholtz decomposition, non-vanishing stress and displacement components can be expressed in terms of wave potentials ϕ and ψ (Panja and Mandal (2021a)) as

$$
\begin{aligned}
u &= \frac{\partial \phi}{\partial x} - \frac{\partial \psi}{\partial y}, \\
v &= \frac{\partial \phi}{\partial y} + \frac{\partial \psi}{\partial x}.
\end{aligned}
\tag{3.1}
$$

The wave equation depending on ϕ and ψ are as follows

$$
\frac{\partial^2 \phi}{\partial x^2} + \frac{\partial^2 \phi}{\partial y^2} = \frac{a^2}{c_1^2} \frac{\partial^2 \phi}{\partial t^2},
\tag{3.2}
$$

$$
\frac{\partial^2 \psi}{\partial x^2} + \frac{\partial^2 \psi}{\partial y^2} = \frac{a^2}{c_2^2} \frac{\partial^2 \psi}{\partial t^2},
\tag{3.3}
$$

where $c_1 = \left(\frac{\lambda + 2\mu}{\rho} \right)^{\frac{1}{2}}$, $c_2 = \left(\frac{\mu}{\rho} \right)^{\frac{1}{2}}$ are the velocities of dilatational and shear wave, μ and λ are the shear moduli, and ρ is the material density.

The boundary conditions are

$$
\tau_{yy}(x, 0, t) = -\tau_0 H(t), \ |x| \leq 1,
\tag{3.4}
$$

$$
\tau_{xy}(x, 0, t) = 0, \ -b \leq x \leq c,
\tag{3.5}
$$

$$
v(x, 0, t) = 0, \ -b \leq x \leq -1, 1 \leq x \leq c,
\tag{3.6}
$$

$$
\tau_{xy}(-b, y, t) = 0, \ -\infty < y < \infty,
\tag{3.7}
$$

$$\tau_{xx}(-b, y, t) = 0, \quad -\infty < y < \infty, \tag{3.8}$$

$$\tau_{xy}(c, y, t) = 0, \quad -\infty < y < \infty, \tag{3.9}$$

$$\tau_{xx}(c, y, t) = 0, \quad -\infty < y < \infty, \tag{3.10}$$

where $H(t)$ is the unit step function.

Variable t can be transformed to a parameter p with the help of Laplace Transform defined as

$$\alpha^*(p) = \int_0^\infty \alpha(t)e^{-pt}dt$$

with inverse

$$\alpha(t) = \frac{1}{2\pi i}\int_{B_r} \alpha^*(p)e^{pt}dp,$$

where B_r indicates Bromwich path of the integration.

Laplace transform converts the equations (3.2) to (3.10) into the following form

$$\frac{\partial^2 \phi^*}{\partial x^2} + \frac{\partial^2 \phi^*}{\partial y^2} = k_1^2 \phi^*, \tag{3.11}$$

$$\frac{\partial^2 \psi^*}{\partial x^2} + \frac{\partial^2 \psi^*}{\partial y^2} = k_2^2 \psi^* \tag{3.12}$$

where

$$k_1^2 = \frac{a^2 p^2}{c_1^2}, \; k_2^2 = \frac{a^2 p^2}{c_2^2}$$

and

$$\tau_{yy}^*(x, 0, p) = -\frac{\tau_0}{p}, \; |x| \leq 1, \tag{3.13}$$

$$\tau_{xy}^*(x, 0, p) = 0, \quad -b \leq x \leq c, \tag{3.14}$$

$$v^*(x, 0, p) = 0, \quad -b \leq x \leq -1, 1 \leq x \leq c, \tag{3.15}$$

$$\tau_{xy}^*(-b, y, p) = 0, \quad -\infty < y < \infty, \tag{3.16}$$

$$\tau_{xx}^*(-b, y, p) = 0, \quad -\infty < y < \infty, \tag{3.17}$$

$$\tau_{xy}^*(c, y, p) = 0, \quad -\infty < y < \infty, \tag{3.18}$$

$$\tau_{xx}^*(c, y, p) = 0, \quad -\infty < y < \infty. \tag{3.19}$$

By separation of variable, the solutions of (3.11) and (3.12) can be written as

$$\phi^*(x, y, p) = \int_{-\infty}^{\infty} A_1(\xi, p) e^{-\gamma_1 y} e^{i\xi x} d\xi$$
$$+ \int_{0}^{\infty} \left[A_3(\zeta, p) e^{\gamma_3 x} + A_4(\zeta, p) e^{-\gamma_3 x} \right] \cos(\zeta y) d\zeta \tag{3.20}$$

and

$$\psi^*(x, y, p) = \int_{-\infty}^{\infty} A_2(\xi, p) e^{-\gamma_2 y} e^{i\xi x} d\xi$$
$$+ \int_{0}^{\infty} \left[A_5(\zeta, p) e^{\gamma_4 x} + A_6(\zeta, p) e^{-\gamma_4 x} \right] \sin(\zeta y) d\zeta. \tag{3.21}$$

where $\gamma_1^2 = \xi^2 + k_1^2$, $\gamma_2^2 = \xi^2 + k_2^2$, $\gamma_3^2 = \zeta^2 + k_1^2$, and $\gamma_4^2 = \zeta^2 + k_2^2$.

Using (3.20) and (3.21) and applying Laplace transformation on (3.1), displacement components u^* and v^* can be found as

$$u^*(x, y, p) = \int_{-\infty}^{\infty} \left[A_1(\xi, p) e^{-\gamma_1 y} i\xi + \gamma_2 A_2(\xi, p) e^{-\gamma_2 y} \right] e^{i\xi x} d\xi$$
$$+ \int_{0}^{\infty} [A_3(\zeta, p) e^{\gamma_3 x} \gamma_3 - A_4(\zeta, p) e^{-\gamma_3 x} \gamma_3$$
$$- \zeta A_5(\zeta, p) e^{\gamma_4 x} - \zeta A_6(\zeta, p) e^{-\gamma_4 x}] \cos(\zeta y) d\zeta \tag{3.22}$$

and

$$v^*(x, y, p) = \int_{-\infty}^{\infty} \left[-A_1(\xi, p)e^{-\gamma_1 y}\gamma_1 + i\xi A_2(\xi, p)e^{-\gamma_2 y} \right] e^{i\xi x} d\xi$$
$$+ \int_0^{\infty} [A_3(\zeta, p)e^{\gamma_3 x}\zeta + A_4(\zeta, p)e^{-\gamma_3 x}\zeta$$
$$+ \gamma_4 A_5(\zeta, p)e^{\gamma_4 x} - \gamma_4 A_6(\zeta, p)e^{-\gamma_4 x}] \sin(\zeta y)d\zeta. \qquad (3.23)$$

Using the boundary condition (3.14) and putting $A_2(\xi, p) = -\frac{2\gamma_1}{2\xi^2 + k_2^2} A(\xi, p)$, $A(\xi, p) = i\xi A_1(\xi, p)$, equations (3.22) and (3.23) become

$$u^*(x, y, p) = \int_{-\infty}^{\infty} \left[e^{-\gamma_1 y}i\xi - \frac{2\gamma_1\gamma_2}{2\xi^2 + k_2^2}e^{-\gamma_2 y} \right] A(\xi, p)e^{i\xi x} d\xi$$
$$+ \int_0^{\infty} [A_3(\zeta, p)e^{\gamma_3 x}\gamma_3 - A_4(\zeta, p)e^{-\gamma_3 x}\gamma_3$$
$$- \zeta A_5(\zeta, p)e^{\gamma_4 x} - \zeta A_6(\zeta, p)e^{-\gamma_4 x}] \cos(\zeta y)d\zeta \qquad (3.24)$$

and

$$v^*(x, y, p) = i \int_{-\infty}^{\infty} \gamma_1 \left[-\frac{2\xi e^{-\gamma_1 y}}{2\xi^2 + k_2^2} + \frac{e^{-\gamma_2 y}}{\xi} \right] A(\xi, p)e^{i\xi x} d\xi$$
$$+ \int_0^{\infty} [A_3(\zeta, p)e^{\gamma_3 x}\zeta + A_4(\zeta, p)e^{-\gamma_3 x}\zeta$$
$$+ \gamma_4 A_5(\zeta, p)e^{\gamma_4 x} - \gamma_4 A_6(\zeta, p)e^{-\gamma_4 x}] \sin(\zeta y)d\zeta. \qquad (3.25)$$

The non vanishing components of stress are given by

$$\tau_{yy}^*(x, y, p) = -i\mu \int_{-\infty}^{\infty} \left[\frac{2\xi^2 + k_2^2}{\xi}e^{-\gamma_1 y} - \frac{4\xi\gamma_1\gamma_2}{2\xi^2 + k_2^2}e^{-\gamma_2 y} \right] A(\xi, p)e^{i\xi x} d\xi$$
$$- \mu \int_0^{\infty} [(2\gamma_3^2 + k_2^2)\{A_3(\zeta, p)e^{\gamma_3 x} + A_4(\zeta, p)e^{-\gamma_3 x}\}$$
$$- 2\zeta\gamma_4 \{A_5(\zeta, p)e^{\gamma_4 x} - A_6(\zeta, p)e^{-\gamma_4 x}\}] \cos(\zeta y)d\zeta, \qquad (3.26)$$

$$\tau_{xx}^*(x,y,p) = i\mu \int_{-\infty}^{\infty} \left[\frac{2\gamma_3^2 + k_2^2}{\xi} e^{-\gamma_1 y} - \frac{4\xi\gamma_1\gamma_2}{2\xi^2 + k_2^2} e^{-\gamma_2 y} \right] A(\xi,p)e^{i\xi x}d\xi$$

$$+\mu \int_0^{\infty} [(2\zeta^2 - k_2^2)\{A_3(\zeta,p)e^{\gamma_3 x} + A_4(\zeta,p)e^{-\gamma_3 x}\}$$

$$-2\zeta\gamma_4 \left\{ A_5(\zeta,p)e^{\gamma_4 x} - A_6(\zeta,p)e^{-\gamma_4 x} \right\}] \cos(\zeta y)d\zeta \qquad (3.27)$$

and $\tau_{xy}^*(x,y,p) = -2\mu \int_{-\infty}^{\infty} \gamma_1 \left[e^{-\gamma_1 y} - e^{-\gamma_2 y} \right] A(\xi,p)e^{i\xi x}d\xi$

$$-\mu \int_0^{\infty} [2\zeta\gamma_3 \left\{ A_3(\zeta,p)e^{\gamma_3 x} - A_4(\zeta,p)e^{-\gamma_3 x} \right\}$$

$$-(2\zeta^2 - k_2^2) \left\{ A_5(\zeta,p)e^{\gamma_4 x} + A_6(\zeta,p)e^{-\gamma_4 x} \right\}] \sin(\zeta y)d\zeta. \qquad (3.28)$$

■ Formation of Dual Integral Equations

As a result of the boundary conditions (3.13) and (3.15), following dual integral equations have been found

$$\int_{-\infty}^{\infty} B(\xi,p)e^{i\xi x}d\xi = 0, \ 1 \le x \le c, \ -b \le x \le -1. \qquad (3.29)$$

$$\int_{-\infty}^{\infty} [\xi + H(\xi,p)]B(\xi,p)e^{i\xi x}d\xi = p_0(x), -1 \le x \le 1, \qquad (3.30)$$

$$\text{where} \qquad B(\xi,p) = \frac{i\gamma_1 k_2^2}{\xi(2\xi^2 + k_2^2)} A(\xi,p), \qquad (3.31)$$

$$H(\xi,p) = \frac{(2\xi^2 + k_2^2)^2 - 4\xi^2\gamma_3\gamma_4}{\gamma_1 k_2^2} - \xi \quad \to 0 \quad as \quad \xi \to \infty, \qquad (3.32)$$

and $p_0(x) = \dfrac{\tau_0}{\mu p} - \displaystyle\int_0^{\infty} [(2\gamma_3^2 + k_2^2)\{A_3(\zeta,p)e^{\gamma_3 x} + A_4(\zeta,p)e^{-\gamma_3 x}\}$

$$+2\zeta\gamma_4\{A_5(\zeta,p)e^{\gamma_4 x} - A_6(\zeta,p)e^{-\gamma_4 x}\}]d\zeta. \qquad (3.33)$$

Employing Fourier inverse transform approach and utilizing boundary conditions (3.16), (3.17), (3.18), and (3.19), following system of equations of the unknowns $A_3(\zeta, p)$, $A_4(\zeta, p)$, $A_5(\zeta, p)$ and $A_6(\zeta, p)$ are obtained

$$-2\zeta\gamma_3\{A_3(\zeta, p)e^{-\gamma_3 c} - A_4(\zeta, p)e^{\gamma_3 c}\} + (2\zeta^2 - k_2^2)\{A_5(\zeta, p)e^{-\gamma_4 c}$$
$$+ A_6(\zeta, p)\}e^{\gamma_4 c} = \int_{-\infty}^{\infty} S_1(\zeta, \xi)B(\xi, p)d\xi, \quad (3.34)$$

$$(2\zeta^2 - k_2^2)\{A_3(\zeta, p)e^{-\gamma_3 c} + A_4(\zeta, p)e^{\gamma_3 c}\} - 2\zeta\gamma_4\{A_5(\zeta, p)e^{-\gamma_4 c}$$
$$- A_6(\zeta, p)\}e^{\gamma_4 c} = \int_{-\infty}^{\infty} S_2(\zeta, \xi)B(\xi, p)d\xi, \quad (3.35)$$

$$(2\zeta^2 - k_2^2)\{A_3(\zeta, p)e^{\gamma_3 b} - A_4(\zeta, p)e^{-\gamma_3 b}\} + 2\zeta\gamma_4\{A_5(\zeta, p)e^{\gamma_4 b}$$
$$+ A_6(\zeta, p)\}e^{-\gamma_4 b} = \int_{-\infty}^{\infty} S_3(\zeta, \xi)B(\xi, p)d\xi, \quad (3.36)$$

and

$$-2\zeta\gamma_3\{A_3(\zeta, p)e^{\gamma_3 b} - A_4(\zeta, p)e^{-\gamma_3 b}\} + (2\zeta^2 - k_2^2)\{A_5(\zeta, p)e^{\gamma_4 b}$$
$$+ A_6(\zeta, p)\}e^{-\gamma_4 b} = \int_{-\infty}^{\infty} S_4(\zeta, \xi)B(\xi, p)d\xi, \quad (3.37)$$

where

$$S_1(\zeta, \xi) = -\frac{4i}{\pi}\left[\frac{1}{\zeta^2 + \gamma_1^2} - \frac{1}{\zeta^2 + \gamma_2^2}\right]\frac{\zeta\xi(2\xi^2 + k_2^2)}{k_2^2}e^{-i\xi c},$$

$$S_2(\zeta, \xi) = -\frac{2}{\pi}\left[\frac{2\gamma_3^2 + k_2^2}{\zeta^2 + \gamma_1^2} - \frac{4\xi\gamma_2^2}{(2\xi^2 + k_2^2)(\zeta^2 + \gamma_2^2)}\right]\frac{\xi(2\xi^2 + k_2^2)}{k_2^2}e^{-i\xi c},$$

$$S_3(\zeta, \xi) = -\frac{2}{\pi}\left[\frac{2\gamma_3^2 + k_2^2}{\zeta^2 + \gamma_1^2} - \frac{4\xi\gamma_2^2}{(2\xi^2 + k_2^2)(\zeta^2 + \gamma_2^2)}\right]\frac{\xi(2\xi^2 + k_2^2)}{k_2^2}e^{i\xi b},$$

$$S_4(\zeta, \xi) = -\frac{4i}{\pi} \left[\frac{1}{\zeta^2 + \gamma_1^2} - \frac{1}{\zeta^2 + \gamma_2^2} \right] \frac{\zeta \xi (2\xi^2 + k_2^2)}{k_2^2} e^{i\xi b}.$$

By Cramer's rule, expressions of $A_i's$ are calculated as follows

$$A_i(\zeta, p) = \sum_{j=1}^{4} \delta_{ij}(\zeta, p) \int_{-\infty}^{\infty} S_j(\zeta, \xi) B(\xi, p) d\xi, \quad i = 3, 4, 5, 6, \qquad (3.38)$$

where $\delta_{31}(\zeta, p) = \frac{H_{31}(\zeta, p)}{\Delta(\zeta, p)}$, $\delta_{32}(\zeta, p) = \frac{H_{32}(\zeta, p)}{\Delta(\zeta, p)}$, $\delta_{33}(\zeta, p) = \frac{H_{33}(\zeta, p)}{\Delta(\zeta, p)}$, $\delta_{34}(\zeta, p) = \frac{H_{34}(\zeta, p)}{\Delta(\zeta, p)}$,

$$\delta_{41}(\zeta, p) = \frac{H_{41}(\zeta, p)}{\Delta(\zeta, p)}, \ \delta_{42}(\zeta, p) = \frac{H_{42}(\zeta, p)}{\Delta(\zeta, p)}, \ \delta_{43}(\zeta, p) = \frac{H_{43}(\zeta, p)}{\Delta(\zeta, p)}, \ \delta_{44}(\zeta, p) = \frac{H_{44}(\zeta, p)}{\Delta(\zeta, p)},$$

$$\delta_{51}(\zeta, p) = \frac{H_{51}(\zeta, p)}{\Delta(\zeta, p)}, \ \delta_{52}(\zeta, p) = \frac{H_{52}(\zeta, p)}{\Delta(\zeta, p)}, \ \delta_{53}(\zeta, p) = \frac{H_{53}(\zeta, p)}{\Delta(\zeta, p)}, \ \delta_{54}(\zeta, p) = \frac{H_{54}(\zeta, p)}{\Delta(\zeta, p)},$$

$$\delta_{61}(\zeta, p) = \frac{H_{61}(\zeta, p)}{\Delta(\zeta, p)}, \ \delta_{62}(\zeta, p) = \frac{H_{62}(\zeta, p)}{\Delta(\zeta, p)}, \ \delta_{63}(\zeta, p) = \frac{H_{63}(\zeta, p)}{\Delta(\zeta, p)}, \ \delta_{64}(\zeta, p) = \frac{H_{64}(\zeta, p)}{\Delta(\zeta, p)},$$

and
$$H_{31}(\zeta, p) = -4\zeta \gamma_4 e^{\gamma_3 c} (2\zeta^2 - k_2^2)^2 + 2\zeta \gamma_4 (2\zeta^2$$
$$-k_2^2) e^{-\gamma_3 b} \cosh\{\gamma_4(b + c)\} - 8\zeta^3 \gamma_3 \gamma_4 e^{-\gamma_3 b} \sinh\{\gamma_4(b + c)\},$$

$$H_{32}(\zeta, p) = -4\zeta^2 \gamma_3 \gamma_4 e^{-\gamma_3 b} (2\zeta^2 - k_2^2) \cosh\{\gamma_4(b + c)\}$$
$$+8\zeta^2 \gamma_3 \gamma_4 (2\zeta^2 - k_2^2) e^{\gamma_3 c} - (2\zeta^2 - k_2^2)^3 e^{-\gamma_3 b} \sinh\{\gamma_4(b + c)\},$$

$$H_{33}(\zeta, p) = -4\zeta^2 \gamma_3 \gamma_4 e^{\gamma_3 c} (2\zeta^2 - k_2^2) \cosh\{\gamma_4(b + c)\}$$
$$+8\zeta^2 \gamma_3 \gamma_4 (2\zeta^2 - k_2^2) e^{-\gamma_3 b} + (2\zeta^2 - k_2^2)^3 e^{\gamma_3 c} \sinh\{\gamma_4(b + c)\},$$

$$H_{34}(\zeta, p) = 2\zeta \gamma_4 e^{\gamma_3 c} (2\zeta^2 - k_2^2) \cosh\{\gamma_4(b + c)\}$$
$$-4\zeta \gamma_4 (2\zeta^2 - k_2^2) e^{-\gamma_3 b} - 8\zeta^3 \gamma_3 \gamma_4^2 e^{\gamma_3 c} \sinh\{\gamma_4(b + c)\},$$

$$H_{41}(\zeta, p) = -2\zeta\gamma_4 e^{\gamma_3 b}(2\zeta^2 - k_2^2)^2 \cosh\{\gamma_4(b+c)\}$$
$$-4\zeta\gamma_4(2\zeta^2 - k_2^2)^2 e^{-\gamma_3 c} - 8\zeta^3\gamma_3\gamma_4^2 e^{\gamma_3 b} \sinh\{\gamma_4(b+c)\},$$

$$H_{42}(\zeta, p) = -2\zeta^2\gamma_3\gamma_4 e^{\gamma_3 b}(2\zeta^2 - k_2^2) \cosh\{\gamma_4(b+c)\}$$
$$+4\zeta^2\gamma_3\gamma_4(2\zeta^2 - k_2^2)e^{-\gamma_3 c} + (2\zeta^2 - k_2^2)^3 e^{\gamma_3 b} \sinh\{\gamma_4(b+c)\},$$

$$H_{43}(\zeta, p) = -4\zeta^2\gamma_3\gamma_4 e^{-\gamma_3 c}(2\zeta^2 - k_2^2) \cosh\{\gamma_4(b+c)\}$$
$$-8\zeta^2\gamma_3\gamma_4(2\zeta^2 - k_2^2)e^{\gamma_3 b} - (2\zeta^2 - k_2^2)^3 e^{-\gamma_3 c} \sinh\{\gamma_4(b+c)\},$$

$$H_{44}(\zeta, p) = -2\zeta\gamma_4 e^{-\gamma_3 c}(2\zeta^2 - k_2^2) \cosh\{\gamma_4(b+c)\}$$
$$-2\zeta\gamma_4(2\zeta^2 - k_2^2)e^{-\gamma_3 c} - 8\zeta^3\gamma_3\gamma_4^2 e^{-\gamma_3 c} \sinh\{\gamma_4(b+c)\},$$

$$H_{51}(\zeta, p) = -4\zeta^2\gamma_3\gamma_4 e^{-\gamma_4 b}(2\zeta^2 - k_2^2) \cosh\{\gamma_3(b+c)\}$$
$$+8\zeta^2\gamma_3\gamma_4(2\zeta^2 - k_2^2)e^{\gamma_4 c} - (2\zeta^2 - k_2^2)^3 e^{-\gamma_4 b} \sinh\{\gamma_3(b+c)\},$$

$$H_{52}(\zeta, p) = 2\zeta\gamma_3 e^{-\gamma_4 b}(2\zeta^2 - k_2^2)^2 \cosh\{\gamma_3(b+c)\}$$
$$-4\zeta\gamma_3(2\zeta^2 - k_2^2)^2 e^{\gamma_4 c} + 8\zeta^3\gamma_3^2\gamma_4 e^{-\gamma_4 b} \sinh\{\gamma_3(b+c)\},$$

$$H_{53}(\zeta, p) = 2\zeta\gamma_3 e^{\gamma_4 c}(2\zeta^2 - k_2^2)^2 \cosh\{\gamma_3(b+c)\}$$
$$-4\zeta\gamma_3(2\zeta^2 - k_2^2)^2 e^{-\gamma_4 b} - 8\zeta^3\gamma_3^2\gamma_4 e^{-\gamma_4 b} \sinh\{\gamma_3(b+c)\},$$

$$H_{54}(\zeta, p) = -e^{\gamma_4 c}(2\zeta^2 - k_2^2)^3 \sinh\{\gamma_3(b+c)\} + 8\zeta^2 \gamma_3 \gamma_4 (2\zeta^2$$
$$-k_2^2)e^{-\gamma_4 b} - 4\zeta^2 \gamma_3 \gamma_4 (2\zeta^2 - k_2^2)e^{\gamma_4 c} \cosh\{\gamma_3(b+c)\},$$

$$H_{61}(\zeta, p) = -4\zeta^2 \gamma_3 \gamma_4 e^{\gamma_4 b}(2\zeta^2 - k_2^2) \cosh\{\gamma_3(b+c)\}$$
$$+8\zeta^2 \gamma_3 \gamma_4 (2\zeta^2 - k_2^2)e^{-\gamma_4 c} + (2\zeta^2 - k_2^2)^3 e^{\gamma_4 b} \sinh\{\gamma_3(b+c)\},$$

$$H_{62}(\zeta, p) = -2\zeta\gamma - 3e^{\gamma_4 b}(2\zeta^2 - k_2^2)^2 \cosh\{\gamma_3(b+c)\}$$
$$+4\zeta\gamma_3(2\zeta^2 - k_2^2)^2 e^{-\gamma_4 c} + 8\zeta^3 \gamma_3^2 \gamma_4 e^{\gamma_4 b} \sinh\{\gamma_3(b+c)\},$$

$$H_{63}(\zeta, p) = -2\zeta\gamma_3 e^{-\gamma_4 c}(2\zeta^2 - k_2^2) \cosh\{\gamma_3(b+c)\}$$
$$+4\zeta\gamma_3(2\zeta^2 - k_2^2)^2 e^{\gamma_4 b} - 8\zeta^3 \gamma_3^2 \gamma_4 e^{-\gamma_4 c} \sinh\{\gamma_3(b+c)\},$$

$$H_{64}(\zeta, p) = -4\zeta^2 \gamma_3 \gamma_4 e^{-\gamma_4 c}(2\zeta^2 - k_2^2) \cosh\{\gamma_3(b+c)\}$$
$$+8\zeta^2 \gamma_3 \gamma_4 (2\zeta^2 - k_2^2)e^{\gamma_4 b} - (2\zeta^2 - k_2^2)^3 e^{-\gamma_4 c} \sinh\{\gamma_3(b+c)\},$$

$$\Delta(\zeta, p) =$$
$$-2\zeta\gamma_3 \left\{ e^{-\gamma_3 c} M_1(\zeta, p) + e^{\gamma_3 c} M_2(\zeta, p) \right\} + (2\zeta^2 - k_2^2) \left\{ e^{-\gamma_4 c} M_3(\zeta, p) - e^{\gamma_4 c} M_4(\zeta, p) \right\},$$

$$M_1(\zeta, p) = -4\zeta\gamma_4(2\zeta^2 k_2^2)^2 e^{\gamma_3 c} + \left[2\zeta\gamma_4(2\zeta^2 - k_2^2)^2 - \right.$$
$$\left. -8\zeta^3 \gamma_3 \gamma_4^2 \right] e^{-\gamma_3 b - \gamma_4 b - \gamma_4 c} - \left[2\zeta\gamma_4(2\zeta^2 - k_2^2)^2 + 8\zeta^3 \gamma_3 \gamma_4^2 \right] e^{-\gamma_3 b + \gamma_4 b + \gamma_4 c},$$

$$M_2(\zeta, p) = -4\zeta\gamma_4(2\zeta^2 - k_2^2)^2 e^{-\gamma_3 c} + \left[2\zeta\gamma_4(2\zeta^2 - k_2^2)^2 \right.$$
$$\left. +8\zeta^3 \gamma_3 \gamma_4^2 \right] e^{\gamma_3 b - \gamma_4 b - \gamma_4 c} + \left[2\zeta\gamma_4(2\zeta^2 - k_2^2)^2 - 8\zeta^3 \gamma_3 \gamma_4^2 \right] e^{\gamma_3 b + \gamma_4 b + \gamma_4 c},$$

$$M_3(\zeta, p) = -8\zeta^2 \gamma_3 \gamma_4 (2\zeta^2 - k_2^2) e^{\gamma_4 c} + \left[(2\zeta^2 - k_2^2)^3 \right.$$
$$- 4\zeta^2 \gamma_3 \gamma_4 (2\zeta^2 - k_2^2) \big] e^{-\gamma_3 b - \gamma_4 b - \gamma_3 c}$$
$$- \left[(2\zeta^2 - k_2^2)^3 + 4\zeta^2 \gamma_3 \gamma_4 (2\zeta^2 - k_2^2) \right] e^{\gamma_3 b - \gamma_4 b + \gamma_3 c},$$

$$M_4(\zeta, p) = -8\zeta^2 \gamma_3 \gamma_4 (2\zeta^2 - k_2^2) e^{-\gamma_4 c} + \left[(2\zeta^2 - k_2^2)^3 \right.$$
$$+ 4\zeta^2 \gamma_3 \gamma_4 (2\zeta^2 - k_2^2) \big] e^{-\gamma_3 b + \gamma_4 b - \gamma_3 c}$$
$$- \left[(2\zeta^2 - k_2^2)^3 - 4\zeta^2 \gamma_3 \gamma_4 (2\zeta^2 - k_2^2) \right] e^{\gamma_3 b + \gamma_4 b + \gamma_3 c}.$$

■ Solution of the Pair of Integral Equations

For the solution of the integral equations given by (3.29) and (3.30), we assume the following trial solution

$$B(\xi, p) = \frac{\tau_0}{2\mu p} \int_0^1 s g(s, p) J_0(\xi s) ds, \qquad (3.39)$$

where $g(s, p)$ is an unknown function. The integral equation (3.29) is automatically satisfied with the help of the relation from Abramowitz and Stegun (1965)

$$\int_0^\infty \cos(\xi x) J_0(\xi s) d\xi = 0, \qquad |x| > |s|.$$

Equation (3.30) can be expressed as

$$g(s, p) + \int_0^1 u g(u, p) du \int_0^\infty H(\xi, p) J_0(\xi s) J_0(\xi u) d\xi = \frac{\mu p}{\pi \tau_0} \int_0^s \frac{p_0(x)}{\sqrt{s^2 - x^2}} dx. \quad (3.40)$$

Using (3.39), (3.38) can be expressed as

$$A_i(\zeta, p) = \frac{\tau_0}{\mu p} \int_0^1 s g(s, p) G_i(\zeta, s) ds, \qquad (3.41)$$

where $G_i(\zeta, s) = \sum_{j=1}^{4} \delta_{ij} Q_i(\zeta, s)$, $i = 3, 4, 5, 6$ and

$$Q_3(\zeta, s) = D_1(\zeta, p)e^{-\gamma_3 b} I_0(\gamma_3 s) - D_2(\zeta, p)e^{-\gamma_4 b} I_0(\gamma_4 s),$$

$$Q_4(\zeta, s) = D_3(\zeta, p)e^{-\gamma_3 b} I_0(\gamma_3 s) - D_4(\zeta, p)e^{-\gamma_4 b} I_0(\gamma_4 s),$$

$$Q_5(\zeta, s) = D_1(\zeta, p)e^{-\gamma_3 c} I_0(\gamma_3 s) - D_2(\zeta, p)e^{-\gamma_4 c} I_0(\gamma_4 s),$$

$$Q_4(\zeta, s) = D_3(\zeta, p)e^{-\gamma_3 c} I_0(\gamma_3 s) - D_4(\zeta, p)e^{-\gamma_4 c} I_0(\gamma_4 s),$$

$$D_1(\zeta, p) = \tfrac{\zeta}{k_2^2}(2\gamma_4^2 - k_2^2), \ D_2(\zeta, p) = \tfrac{\zeta}{k_2^2}(2\gamma_3^2 - k_1^2),$$

$$D_3(\zeta, p) = \tfrac{1}{\gamma_3 k_2^2}(2\gamma_4^2 - k_2^2)(2\gamma_3^2 - k_2^2), \ D_4(\zeta, p) = \tfrac{\zeta^2 \gamma_3}{k_2^2}.$$

Using (3.33), (3.38) and (3.39) the term $\frac{\mu p}{\pi \tau_0} \int_0^s \frac{p_0(x)}{\sqrt{s^2 - x^2}} dx$ can be expressed as

$$\frac{\mu p}{\pi \tau_0} \int_0^s \frac{p_0(x)}{\sqrt{s^2 - x^2}} dx = 1 - \frac{\mu p}{\tau_0} \int_0^\infty \Big[(2\gamma_3^2 + k_2^2)\{R_1(\zeta.s)A_3(\zeta, p)$$

$$+ R_2(\zeta, s)A_4(\zeta, p)\} - 2\zeta\gamma_4\{R_3(\zeta, s)A_5(\zeta, p) - R_4(\zeta, s)A_6(\zeta, p)\}\Big]d\zeta, \tag{3.42}$$

where

$$R_1(\zeta, s) = I_0(\gamma_3 s) + L_0(\gamma_3 s), \ R_2(\zeta, s) = I_0(\gamma_3 s) - L_0(\gamma_3 s),$$

$$R_3(\zeta, s) = I_0(\gamma_4 s) + L_0(\gamma_4 s), \ R_4(\zeta, s) = I_0(\gamma_4 s) - L_0(\gamma_4 s).$$

Using (3.41) and (3.42), from (3.40) we get

$$g(s, p) + \int_0^1 u g(u, p) L(u, s) du = 1, \tag{3.43}$$

where

$$L(u, s) = L_1(u, s) + L_2(u, s), \tag{3.44}$$

$$L_1(u, s) = \int_0^\infty H(\xi, p) J_0(\xi s) J_0(\xi u) d\xi, \tag{3.45}$$

$$L_2(u, s) = \int_0^\infty [(2\gamma_3^2 + k_2^2)\{R_1(\zeta, s)G_3(\xi, p) + R_2(\zeta, s)G_4(\xi, p)\}$$

$$- 2\zeta\gamma_4\{R_3(\zeta, s)G_5(\xi, p) - R_4(\zeta, s)G_6(\xi, p)\}]d\xi. \tag{3.46}$$

The improper integral given by equation (3.45) can be transformed into a proper integral by employing Contour integration (Mal (1970)) as

$$L_1(u,s) = -\int_0^{k_2} \frac{(-2\xi^2 + k_2^2)^2 - 4\xi^2\alpha_1\alpha_2}{\alpha_1 k_2^2} J_0(i\xi u) H_0^{(1)}(i\xi s) d\xi$$
$$-i\int_{k_2}^{k_1} \frac{(-2\xi^2 + k_2^2)^2}{\alpha_1 k_2^2} J_0(i\xi u) H_0^{(1)}(i\xi s) d\xi, \qquad (3.47)$$

where $\alpha_1 = \sqrt{k_1^2 - \xi^2}$ and $\alpha_2 = \sqrt{k_2^2 - \xi^2}$.

■ Singular Stress Field

The normal stress τ_{yy}^* in the neighbourhood of the crack can be calculated by the following equation

$$\tau_{yy}^*(x,0,p) = -i\mu \int_{-\infty}^{\infty} \left[\frac{2\xi^2 + k_2^2}{\xi} - \frac{4\xi\gamma_1\gamma_2}{2\xi^2 + k_2^2}\right] A(\xi,p) e^{i\xi x} d\xi$$
$$-\mu \int_0^{\infty} [(2\gamma_3^2 + k_2^2)\{A_3(\zeta,p)e^{\gamma_3 x} + A_4(\zeta,p)e^{-\gamma_3 x}\}$$
$$-2\zeta\gamma_4 \{A_5(\zeta,p)e^{\gamma_4 x} - A_6(\zeta,p)e^{-\gamma_4 x}\}] d\zeta. \quad (3.48)$$

Substituting the values of $A_i's$ from (3.38) and using (3.39), the expression of the stress on the Laplace transform plane can be found as

$$\tau_{yy}^*(x,0,p) = \frac{x\tau_0 g(1,p)}{p\sqrt{x^2 - 1}} + O(1). \qquad (3.49)$$

The stress intensity factor at the the crack vicinity is defined as

$$K_1^*(p) = \lim_{x\to 1^+} \sqrt{x-1}\,\tau_{yy}^*(x,0,p) = \frac{\tau_0}{\sqrt{2}}\frac{g(1,p)}{p}. \qquad (3.50)$$

With the aid of Laplace inverse, the stress intensity factor $K_1(t)$ in terms of t is calculated as

$$K_1(t) = \frac{\tau_0}{2\sqrt{2}\pi i} \int_{B_r} \frac{e^{pt} g(1, p)}{p} dp, \tag{3.51}$$

where B_r denotes the Bromwich path of integration.

■ Numerical and Graphical Demonstration

The integration given by (3.46) was calculated with the help of Gauess quadrature formula. A numerical solution for the Fredholm integral equation (3.43) has been obtained by using the Fox and Goodwin (1953) method. The integral equation (3.43) has been converted to set of simultaneous linear equations of the desired function $g(s, p)$ as unknowns. First-order approximations of the pivotal values of $g(s, p)$ are obtained by solving the linear algebraic equations and the derived solution was modified by difference correction approach. After getting the numeric values of $g(1, p)$, stress intensity factor $K_1(p)$ is obtained. Using a numerical Laplace inversion scheme by Zakian algorithm Rice and Duong (1995), the stress intensity factor $K_1(t)$ has been obtained in terms of time and displayed graphically for the following elastic materials.

Type-1 Material (Aluminum):

$$\rho = 2700 \ kgm^{-3}, \lambda = 51.08 GPa \ , \mu = 26.32 \ GPa.$$

Type-2 Material (Steel):

$$\rho = 7800 \ kgm^{-3}, \lambda = 112.40 \ GPa, \mu = 162.79 \ GPa.$$
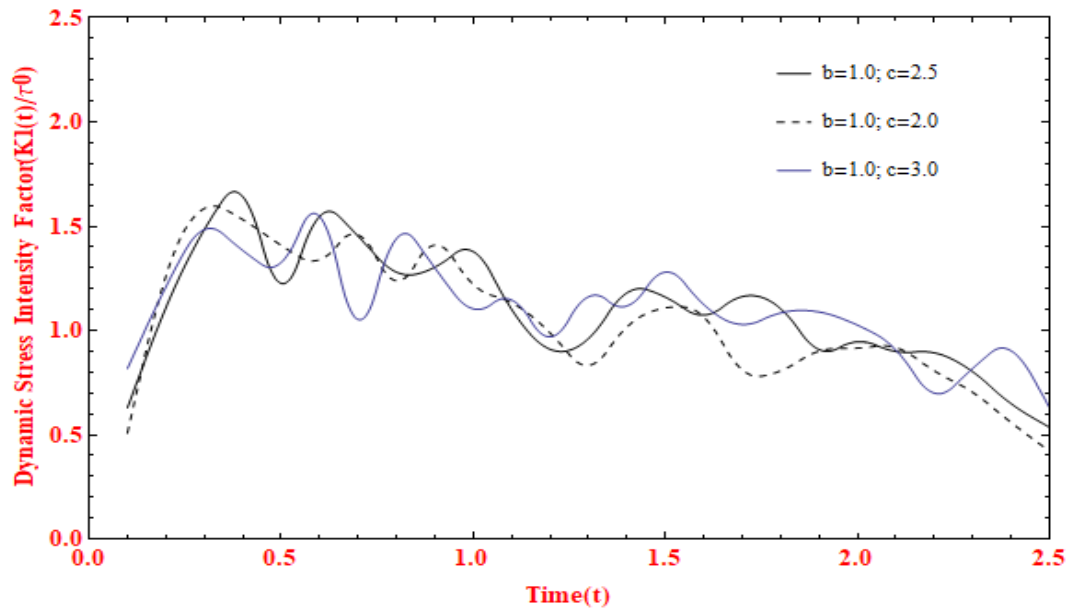
Fig.3.2 SIF vs Time for Type-1 Material.
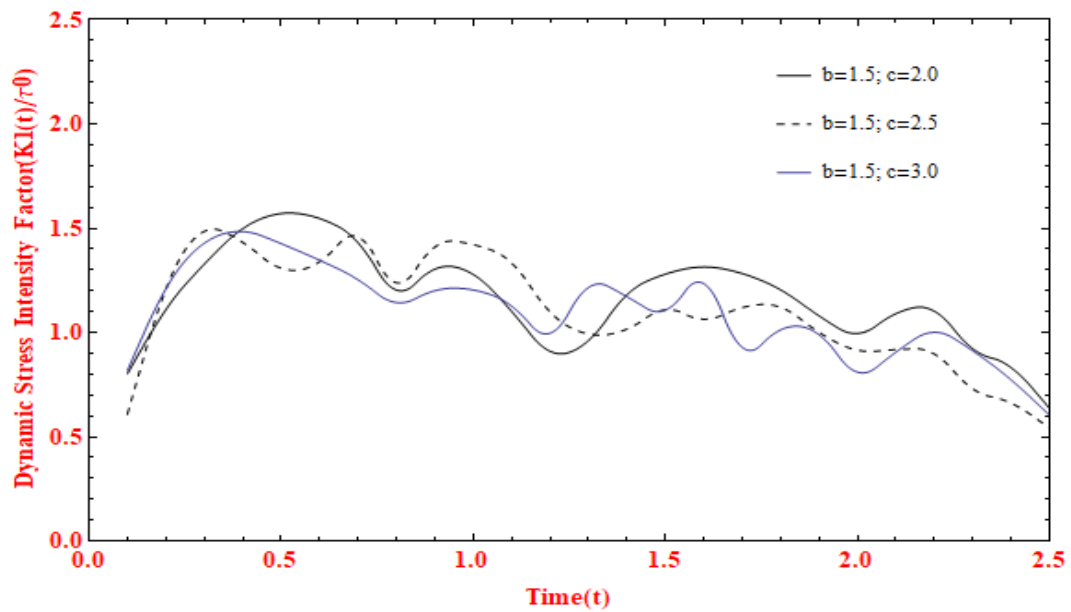
Fig.3.3 SIF vs Time for Type-1 Material.
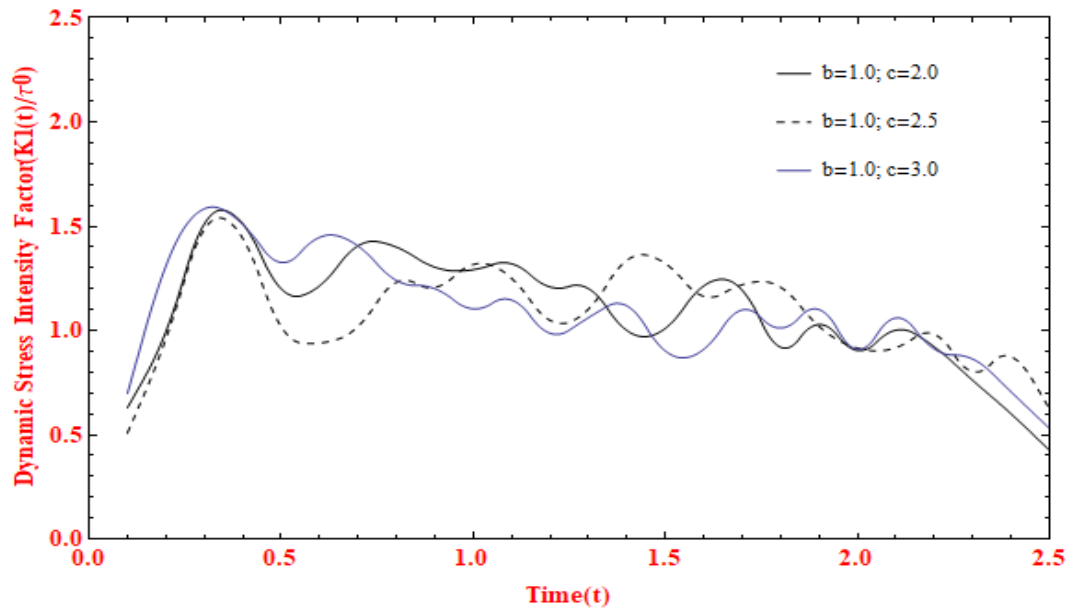
Fig.3.4 SIF vs Time for Type-2 Material.
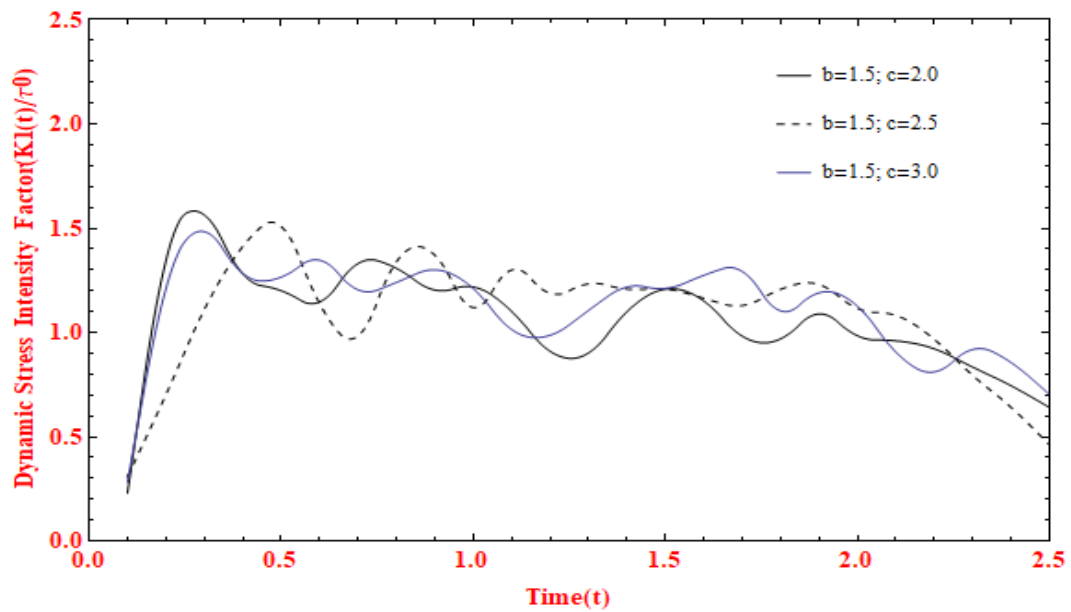
Fig.3.5 SIF vs Time for Type-2 Material.

To show the effects of sudden load on cracked elastic strip, normalized stress intensity factor $\frac{K_1(t)}{\tau_0}$ has been plotted graphically against time for different values of the strip lengths (b and c) for two different isotropic materials.

In Fig.3.2 and Fig.3.4, $\frac{K_1(t)}{\tau_0}$ has been plotted against time t for Type 1 and Type 2 materials for $b = 1.0$, $c = 2.0$, $c = 2.5$, $c = 3.0$. Fig.3.3 and Fig.3.5 represent the same for $b = 1.5$, $c = 2.0$, $c = 2.5$, $c = 3.0$.

From the Fig.3.2 - Fig.3.5, it is clear that the normalized SIF increases first and reaches to a maximum value then follows wave like nature with dumped oscillations after that it decreases with the increasing value of time and ultimately tends to zero for both the materials. The maximum value of the stress intensity factors for each of the cases is different. Therefore, it can be concluded that the utmost values of the SIFs and their position depend on the physical parameters of the materials, strip length and crack position.

■ Conclusions

The analysis of diffraction phenomenon of P-wave over the surface of a crack situated asymmetrically in an isotropic strip under the effect of impact load is the main concern of the present work. Stress intensity factor near the crack vicinity has been obtained and displayed graphically with respect to time. The amount of stress is high near the crack tip with disruptive nature. The graphs of stress intensity factor indicate that SIF increases first and reaches to a higher value then it started decreasing with the nature of damped oscillation for both the materials. As stress intensity factors tend to zero whenever time increases, therefore it has been concluded that the crack propagation is affected by impact load and singular stress can be controlled by maintaining the load capacity within certain limits of time. Also it has been shown that the strip width, material properties play vital role to resist the growth of crack propagation. The present approach can be used to consolidate a material and to create new materials by considering suitable elastic parameters.

Chapter-4

Coupling Effects of Magnetic Field and Elastic Media on Cracked Elastic Medium

Chapter 4

Coupling Effects of Magnetic Field and Elastic Media on Cracked Elastic Medium

4.1 Shear Wave Interaction of two Collinear Finite Cracks in an Infinite Magnetoelastic Orthotropic Media

■ Introduction

In solid structures, the distraught effect such as cracks or voids exist in elastic material which may be caused by material processing, manufacturing irregularities, uncertainties in loadings etc. The presence of such defects may significantly affect the stiffness and integrity of the material. To understand the failure mechanism of materials, analysis of stress and displacement field around the crack vicinities is necessary. The stress field helps to predict the expected crack growth rate, failure

assessment, and fracture behavior of materials and the displacement field measures the fracture toughness of the material. Many elastic materials frequently exhibit strong orthotropy, so the study of wave propagation by cracks in an orthotropic medium is of great importance for fracture analysis of the material. Researcher Sneddon (1961) discussed various crack problems in his technical report mathematical theory of elasticity. Robertson (1967) and Mal (1970) analyzed the diffraction of elastic waves by a circular crack in an infinitely extended elastic medium. Jain and Kanwal (1972) derived singular stress for the problem of the dispersion of elastic waves by two Griffith cracks in an infinite isotropic medium. Interaction of antiplane transverse waves by the influence of two collinear finite cracks in an infinite medium has been investigated by Itou (1980). Itou (1989) also solved the problem of two co-planar finite cracks in an orthotropic layer sandwich between two elastic half planes. Problems of the interaction of longitudinal waves by Griffith cracks in an orthotropic plate have been made by Mandal and Ghosh (1994), Sarkar et al. (1995). Mechanics of magneto-elastic solids have gained significant interest in recent years due to the extensive application of magnetic reinforced materials in aerospace engineering, automotive industries, acoustics, optimal design, signal processing, etc. The coupled properties of magnetic field and elastic media offer great opportunities for engineers to create flawless constructions and devices that are capable of answering to internal and(or) external changes. Therefore, the study of magnetoelastic interaction is the focus of many research scholars in the field of fracture mechanics. The basic equations of magnetoelastic deformation theory have been derived by Dunkin and Eringen (1963). The theory of magnetoelasticity was developed by Knopoff (1955) and Chadwick (1957) which was later extended by Kaliski and Petykiewicz (1959). Verma (1986) has investigated magneto-elastic transverse waves in a self reinforced elastic body. Chattopadhyay and Maugin (1985) analyzed the magnetoelastic response of rigid strips in an infinite plate. The propagation of magnetoelastic

transverse waves in an infinite self-reinforced lamina has been investigated by Chattopadhyay and Choudhury (1995). Marin (1997a,b) investigated the influence of the thermoelastic effect on the body with voids. Acharya et al. (2009) analyzed the dispersion of interface waves by the impact of magnetic field and initial tension in a transversely isotropic plate. The problems of the interaction of magneto-elastic shear waves by a Griffith crack have been solved by Panja and Mandal (2021b,c).

Earth is believed to be surrounded by its own magnetic field dispersing from its center. Therefore, it is very much crucial to consider the effect of magnetic field in a cracked elastic media. To the best of the authors knowledge, no attempt has been made till now to analyse the stress field of an orthotropic elastic material containing two cracks by the impact of magnetic field. Therefore the goal of this paper is to illustrate the shear wave interaction by two collinear finite cracks in an infinite orthotropic plate under the influence of magnetic field. The physical phenomena of wave interaction are formulated as an MBVP. The MBVP has been transformed into a pair of integral equations by introducing Abel's transform, which has further been simplified by using the perturbation method for low frequency. The solution of the simplified integral equations has been derived by Hilbert transformation Srivastava and Lowengrub (1970). The analytic expansions of SIFs and COD have been computed and demonstrated graphically.

■ **Problem Synthesis**

Let us consider two Griffith cracks situated at $b \leq |X| \leq a$, $-\infty < Y < \infty$, $Z = 0$ referred to the rectangular frame of reference (X, Y, Z) in a magnetized orthotropic medium. Normalizing all the lengths with respect to a and putting $\frac{X}{a} = x$, $\frac{Y}{a} = y$, $\frac{Z}{a} = z$ and $\frac{b}{a} = h$, the new crack location becomes $h \leq |x| \leq 1$, $-\infty < y < \infty$, $z = 0$ (Fig.4.1.1). Let us assume that there is a time harmonic anti-plane shear wave $h_0 e^{-i\omega t}$ in the positive direction of the z-axis, where h_o is the

antiplane shear traction acting on the crack periphery in the positive direction of the z-axis. The periodic term $e^{-i\omega t}$ is present in all field variables which is being omitted throughout the analysis.
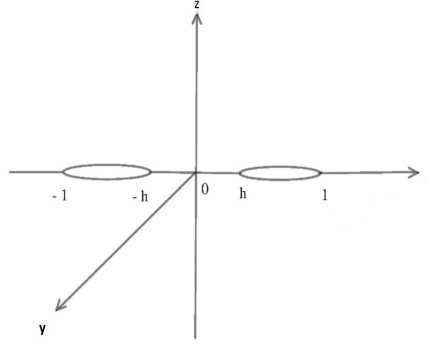
Fig.4.1.1 Geometry of the problem.

Since shear waves propagate in the z direction, so the displacement field can be taken as $(0,\ U_y(x,z),\ 0)$. Field equation (Chattopadhyay and Singh (2014)) for perfectly conducting orthotropic elastic media is

$$\frac{\partial \sigma_{xy}}{\partial x} + \frac{\partial \sigma_{yz}}{\partial z} + (\vec{\mathcal{J}} \times \vec{\mathcal{B}})_y + k^2 U_y = 0, \qquad (4.1.1)$$

where $k^2 = \rho \omega^2$ and $(\vec{\mathcal{J}} \times \vec{\mathcal{B}})_y$ is the y-component of the Lorentz force ($\vec{\mathcal{J}}$ and $\vec{\mathcal{B}}$ are the electric current density and the magnetic flux density vector).

The non vanishing stresses are given by

$$\begin{aligned} \sigma_{xy} &= 2C_{66}\mathcal{E}_{xy} = C_{66}\frac{\partial U_y}{\partial x} \\ \text{and } \sigma_{yz} &= 2C_{44}\mathcal{E}_{yz} = C_{44}\frac{\partial U_y}{\partial z}, \end{aligned} \qquad (4.1.2)$$

where C_{66} and C_{44} are orthotropic elastic constants.

The well known Maxwell's equations (Chattopadhyay and Singh (2014), Panja and

Mandal (2021c)) for the governing electromagnetic field are

$$\operatorname{div} \vec{\mathcal{B}} = 0, \ \operatorname{curl} \vec{E} = -\frac{\partial \vec{\mathcal{B}}}{\partial t}, \ \vec{\mathcal{B}} = \mu_e \vec{\mathcal{H}},$$

$$\vec{\mathcal{J}} = \sigma \left(\vec{E} + \frac{\partial \vec{U}}{\partial t} \times \vec{\mathcal{B}} \right) \ \text{and} \ \operatorname{curl} \vec{\mathcal{H}} = \vec{\mathcal{J}}, \tag{4.1.3}$$

where $\vec{E}$ is the strength of the electric field, $\vec{\mathcal{H}}$ is the intensity of the magnetic field, μ_e is the induced permeability and σ is the conductivity coefficient of electric current.

The expression of Maxwell's stress tensor $\left(\sigma_{ij}^0 \right)^{M_x}$ is given by

$$\left(\sigma_{ij}^0 \right)^{M_x} = \mu_e (\mathcal{H}^{(1i)} \beta_j + \mathcal{H}^{(1j)} \beta_i - \mathcal{H}^{(1k)} \beta_k \delta_{ij}),$$

where $\vec{\mathcal{H}} = \left(\mathcal{H}^{(1x)}, \ \mathcal{H}^{(1y)}, \ \mathcal{H}^{(1z)} \right)$ and $\vec{\beta} = (\beta_x, \ \beta_y, \ \beta_z)$, $\ \beta_x, \ \beta_y$ and β_z are the disturbances in the induced magnetic field.

Ignoring the displacement current vector, from equations (4.1.3) we derive

$$\nabla^2 \vec{\mathcal{H}} = \mu_e \sigma \left[\frac{\partial \vec{\mathcal{H}}}{\partial t} - \vec{\nabla} \times \left(\frac{\partial \vec{U}}{\partial t} \times \vec{\mathcal{H}} \right) \right]. \tag{4.1.4}$$

From the vector equation (4.1.4), we get

$$\frac{\partial \mathcal{H}^{(1x)}}{\partial t} = \frac{1}{\mu_e \sigma} \nabla^2 \mathcal{H}^{(1x)},$$

$$\frac{\partial \mathcal{H}^{(1z)}}{\partial t} = \frac{1}{\mu_e \sigma} \nabla^2 \mathcal{H}^{(1z)}, \tag{4.1.5}$$

$$\frac{\partial \mathcal{H}^{(1y)}}{\partial t} = \frac{1}{\mu_e \sigma} \nabla^2 \mathcal{H}^{(1y)} + \frac{\partial \left(\mathcal{H}^{(1x)} \frac{\partial U_y}{\partial t} \right)}{\partial x} + \frac{\partial \left(\mathcal{H}^{(1z)} \frac{\partial U_y}{\partial t} \right)}{\partial z}.$$

For perfectly electric conductivity ($\sigma \to \infty$), equations (4.1.5) reduce to

$$\frac{\partial \mathcal{H}^{(1x)}}{\partial t} = 0 = \frac{\partial \mathcal{H}^{(1z)}}{\partial t} \tag{4.1.6}$$

and

$$\frac{\partial \mathcal{H}^{(1y)}}{\partial t} = \frac{\partial \left(\mathcal{H}^{(1x)} \frac{\partial U_y}{\partial t} \right)}{\partial x} + \frac{\partial \left(\mathcal{H}^{(1z)} \frac{\partial U_y}{\partial t} \right)}{\partial z}. \tag{4.1.7}$$

According to the equation (4.1.6), we can conclude that there is no magnetic perturbation in the x-component and z-component of $\vec{\mathcal{H}}$, nevertheless the equation (4.1.7) shows that there may exist magnetic perturbation in the y-component of $\vec{\mathcal{H}}$. Therefore we may consider the magnetic field as $\left(\mathcal{H}^{(0x)}, \ \mathcal{H}^{(0y)} + \beta_0, \ \mathcal{H}^{(0z)} \right)$, where β_0 is the small amount of magnetic perturbation in $\mathcal{H}^{(1y)}$ and $\left(\mathcal{H}^{(0x)}, \ \mathcal{H}^{(0y)}, \ \mathcal{H}^{(0z)} \right)$ are three components of magnetic field $\vec{\mathcal{H}}^0$ in the initial state.

Let ψ be the angle at which the wave crosses the magnetic field and let $\mathcal{H}^{(0)} = | \vec{\mathcal{H}}^0 |$, therefore the initial state of magnetic field can be expressed as $\vec{\mathcal{H}}^0 = (\mathcal{H}^{(0)} \cos \psi, \ 0, \ \mathcal{H}^{(0)} \sin \psi)$ and finally we have

$$\vec{\mathcal{H}} = \left(\mathcal{H}^{(0)} \cos \psi, \ \beta_0, \ \mathcal{H}^{(0)} \sin \psi \right). \tag{4.1.8}$$

Putting the value of $\vec{\mathcal{H}}$ in (4.1.7), we derive

$$\frac{\partial \beta_0}{\partial t} = \frac{\partial \left(\mathcal{H}^{(0)} \cos \psi \frac{\partial U_y}{\partial t} \right)}{\partial x} + \frac{\partial \left(\mathcal{H}^{(0)} \sin \psi \frac{\partial U_y}{\partial t} \right)}{\partial z}. \tag{4.1.9}$$

Integrating (4.1.9) with respect to t, we get

$$\beta_0 = \mathcal{H}^{(0)} \cos \psi \frac{\partial U_y}{\partial x} + \mathcal{H}^{(0)} \sin \psi \frac{\partial U_y}{\partial z}. \tag{4.1.10}$$

With the help of $\vec{\nabla}(\frac{\mathcal{H}^2}{2}) = (\vec{\mathcal{H}} . \vec{\nabla})\vec{\mathcal{H}} - (\text{curl } \vec{\mathcal{H}}) \times \vec{\mathcal{H}}$, we obtain

$$(\vec{\mathcal{J}} \times \vec{\mathcal{B}})_y = \mu_e \left[\left(\mathcal{H}^{(0)} \right)^2 \cos^2 \psi \frac{\partial^2 U_y}{\partial x^2} + \left(\mathcal{H}^{(0)} \right)^2 \sin 2\psi \frac{\partial^2 U_y}{\partial x \partial z} + \right.$$
$$\left. \left(\mathcal{H}^{(0)} \right)^2 \sin^2 \psi \frac{\partial^2 U_y}{\partial z^2} \right]. \tag{4.1.11}$$

Utilizing (4.1.2) and (4.1.11), the equation (4.1.1) reduces to

$$A\frac{\partial^2 U_y}{\partial x^2} + B\frac{\partial^2 U_y}{\partial z^2} + C\frac{\partial^2 U_y}{\partial x \partial z} + k^2 U_y = 0, \tag{4.1.12}$$

where

$$A = C_{66} + \mu_e \left(\mathcal{H}^{(0)}\right)^2 \cos^2 \psi,$$
$$B = C_{44} + \mu_e \left(\mathcal{H}^{(0)}\right)^2 \sin^2 \psi, \tag{4.1.13}$$
$$C = \mu_e \left(\mathcal{H}^{(0)}\right)^2 \sin 2\psi.$$

Since the crack geometry is symmetric, we will consider the upper half plane $(z \geq 0)$ only. The equation (4.1.12) is to be solved subject to the following mixed boundary conditions

$$\sigma_{yz}(x, 0) = -h_0, \ h \leq \mid x \mid \leq 1 \tag{4.1.14}$$

and

$$U_y(x, 0) = 0, \ \mid x \mid > 1, \mid x \mid < h. \tag{4.1.15}$$

The general solution of the field equation (4.1.12) can be considered as

$$U_y(x, z) = \int_{-\infty}^{\infty} \mathcal{F}(\zeta) e^{-mz} e^{i\zeta x} d\zeta, \ z > 0, \tag{4.1.16}$$

where $m = \frac{i\zeta C}{2B} + \zeta\sqrt{\frac{1}{B}\left(A - \frac{k^2}{\zeta^2}\right) - \left(\frac{C}{2B}\right)^2}$ and $\mathcal{F}(\zeta)$ is an unknown function. The non vanishing stress component is found as

$$\sigma_{yz}(x, z) = -C_{44} \int_{-\infty}^{\infty} m\mathcal{F}(\zeta) e^{-mz} e^{i\zeta x} d\zeta. \tag{4.1.17}$$

The expression of $\mathcal{F}(\zeta)$ is to be calculated utilizing the boundary conditions.

∎ **Derivation and Solution of Integral Equations**

Using the boundary conditions (4.1.14) and (4.1.15), we derive the following integral equations

$$\int_{-\infty}^{\infty} m\mathcal{F}(\zeta)e^{i\zeta x}d\zeta = \frac{h_0}{C_{44}}, \ h \leq |x| \leq 1 \tag{4.1.18}$$

and

$$\int_{-\infty}^{\infty} \mathcal{F}(\zeta)e^{i\zeta x}d\zeta = 0, \ |x| > 1, \ |x| < h. \tag{4.1.19}$$

Equation (4.1.18) can be expressed as

$$\int_{-\infty}^{\infty} \zeta \left[1 + R_1(\zeta)\right] \mathcal{F}(\zeta)e^{i\zeta x}d\zeta = \frac{h_0}{\vartheta C_{44}}, \ h \leq |x| \leq 1, \tag{4.1.20}$$

where

$$R_1(\zeta) = \frac{R(\zeta)}{\vartheta} - 1, \ R(\zeta) = \frac{iC + \sqrt{4B\left(A - \frac{k^2}{\zeta^2}\right) - C^2}}{2B},$$

$$\vartheta = \frac{iC + \sqrt{4AB - C^2}}{2B} \text{ and } R_1(\zeta) \to 0 \text{ as } \zeta \to \infty. \tag{4.1.21}$$

For the solution of (4.1.18) and (4.1.19), we consider the following trial solution

$$\mathcal{F}(\zeta) = \frac{1}{\zeta} \int_h^1 \phi(q^2)\sin(\zeta q)dq, \tag{4.1.22}$$

where $\phi(q^2)$ is an unknown function which is to be computed with the help of integral transforms.

Using (4.1.22) and $\int_0^{\infty} \frac{\sin \zeta q \cos \zeta x}{\zeta} d\zeta = \begin{cases} \frac{\pi}{2}, & q > x \\ 0, & q < x \end{cases}$ in the equation (4.1.19), it is found that $\phi(q^2)$ satisfy the equation

$$\int_h^1 \phi(q^2)dq = 0. \tag{4.1.23}$$

Again using the result $\displaystyle\int_0^\infty \frac{\sin \zeta q \sin \zeta x}{\zeta} d\zeta = \frac{1}{2}\log\left|\frac{q+x}{q-x}\right|$ from Abramowitz and Stegun (1965) and the expression of $\mathcal{F}(\zeta)$ given by the equation (4.1.22), from the equation (4.1.20) we get

$$\frac{d}{dx}\int_h^1 \phi(q^2)\log\left|\frac{q+x}{q-x}\right|dq = 2\left[\frac{h_0}{\vartheta C_{44}} - \frac{d}{dx}\int_h^1 \phi(q^2)dq \int_0^\infty \zeta R_1(\zeta)\frac{\sin \zeta q \sin \zeta x}{\zeta^2}d\zeta\right]. \quad (4.1.24)$$

Utilizing the result $\displaystyle\frac{\sin \zeta q \sin \zeta x}{\zeta^2} = \int_0^x \int_0^q \frac{mn J_0(\zeta m)J_0(\zeta n)}{\sqrt{x^2-m^2}\sqrt{q^2-n^2}}dm dn$, the equation (4.1.24) becomes

$$\int_h^1 \frac{q\phi(q^2)}{q^2-x^2}dq = \frac{h_0}{\vartheta C_{44}} - $$
$$\frac{d}{dx}\int_h^1 \phi(q^2)dq \int_0^x \int_0^q \frac{mn\, dm\, dn}{\sqrt{x^2-m^2}\sqrt{q^2-n^2}}\int_0^\infty \zeta R_1(\zeta) J_0(\zeta m)J_0(\zeta n)d\zeta$$
$$= \frac{h_0}{\vartheta C_{44}} - \frac{d}{dx}\int_h^1 \phi(q^2)dq \int_0^x \int_0^q \frac{mn\kappa(n,m)\, dm\, dn}{\sqrt{x^2-m^2}\sqrt{q^2-n^2}}, \quad (4.1.25)$$

where

$$\kappa(n,m) = \int_0^\infty \zeta R_1(\zeta)J_0(\zeta m)J_0(\zeta n)d\zeta. \quad (4.1.26)$$

The integrand of the integration (4.1.26) has a branch point at $\zeta = \frac{k}{\sqrt{A}}$. Employing the contour integration technique (Mal (1970)), the improper integral (4.1.26) has therefore been converted to the following finite integral

$$\kappa(n,m) = -\frac{\iota k^2}{2}\int_0^{\frac{1}{\sqrt{A}}} \zeta \frac{\sqrt{4B\left(\frac{1}{\zeta^2}-A\right)+C^2}}{B\vartheta} J_0(k\zeta m)H_0^{(1)}(k\zeta n)d\zeta, n > m. \quad (4.1.27)$$

With the help of the asymptotic series expansion of J_0 and $H_0^{(1)}$, $J_0(k\zeta m)H_0^{(1)}(k\zeta n)$ can be written as

$$J_0(k\zeta m)H_0^{(1)}(k\zeta n) = \frac{2\iota}{\pi}\log k + \left[1 + \frac{2\iota}{\pi}\left(m + \log\left(\frac{\zeta n}{2}\right)\right)\right]. \tag{4.1.28}$$

Using (4.1.28), (4.1.27) becomes

$$\kappa(n,m) = \frac{1}{\pi}k^2 G \log k + \mathcal{O}(k^2), \tag{4.1.29}$$

where

$$G = \int_0^{\frac{1}{\sqrt{A}}} \frac{\zeta}{B\vartheta}\sqrt{4B\left(\frac{1}{\zeta^2} - A\right) + C^2}\,d\zeta. \tag{4.1.30}$$

Let us take the iterative form of $\phi(q^2)$ as follows

$$\phi(q^2) = \phi_0(q^2) + k^2 \log k \phi_1(q^2) + \mathcal{O}(k^2). \tag{4.1.31}$$

Using the above expression of $\phi(q^2)$ and the expression of $\kappa(n,m)$ given by the equation (4.1.29) in (4.1.25) and equating the coefficients of similar powers of k from both sides of the reduced equation, we derive

$$\int_h^1 \frac{q\phi_0(q^2)}{q^2 - x^2}dq = \frac{h_0}{\vartheta C_{44}},\ h \leq |x| \leq 1 \tag{4.1.32}$$

and

$$\int_h^1 \frac{q\phi_1(q^2)}{q^2 - x^2}dq = -\frac{G}{\pi}\int_h^1 q\phi_0(q^2)dq,\ h \leq |x| \leq 1. \tag{4.1.33}$$

Applying Hilbert transformation, from (4.1.32) we get

$$\phi_0(q^2) = \frac{2h_0}{\pi\vartheta C_{44}}\sqrt{\frac{q^2 - h^2}{1 - q^2}} + \frac{\alpha_1}{\sqrt{(q^2 - h^2)(1 - q^2)}} \tag{4.1.34}$$

and from (4.1.33) using (4.1.34) we have

$$\phi_1(q^2) = -G\left(\frac{h_0(1-h^2)}{\pi^2\vartheta C_{44}} + \frac{\alpha_1}{\pi}\right)\sqrt{\frac{q^2-h^2}{1-q^2}} + \frac{\alpha_2}{\sqrt{(q^2-h^2)(1-q^2)}}, \qquad (4.1.35)$$

where α_1 and α_2 are constants to be computed with the help of the following conditions

$$\int_h^1 \phi_0(q^2)dq = 0 \qquad (4.1.36)$$

and

$$\int_h^1 \phi_1(q^2)dq = 0. \qquad (4.1.37)$$

Using (4.1.36) and (4.1.37) we found the values of α_1 and α_2 as follows

$$\alpha_1 = \frac{2h_0}{\pi\vartheta C_{44}}\frac{h^2F_1 - E_1}{F_1} \qquad (4.1.38)$$

and

$$\alpha_2 = \frac{Gh_0}{\pi^2\vartheta C_{44}}\frac{(h^2F_1 - 2E_1 + F_1)(E_1 - h^2F_1)}{F_1^2}, \qquad (4.1.39)$$

where $E_1 = E\left(\frac{\pi}{2}, \sqrt{1-h^2}\right)$ and $F_1 = F\left(\frac{\pi}{2}, \sqrt{1-h^2}\right)$.

Putting the values of the constants α_1 and α_2 given by the expressions (4.1.38) and (4.1.39) in (4.1.34) and (4.1.35), we obtain

$$\phi_0(q^2) = \frac{2h_0}{\pi\vartheta C_{44}}\frac{q^2F_1 - E_1}{F_1\sqrt{(q^2-h^2)(1-q^2)}} \qquad (4.1.40)$$

and

$$\phi_1(q^2) = \frac{Gh_0}{\pi^2\vartheta C_{44}}\frac{(h^2F_1 - 2E_1 + F_1)(E_1 - h^2F_1)}{F_1^2\sqrt{(q^2-h^2)(1-q^2)}}. \qquad (4.1.41)$$

■ Physical Parameters

Stress Intensity Factors:

The non vanishing shear stress outside the crack can be calculated as

$$
\sigma_{yz}(x,0) = \begin{cases} -h_0\left[1 - \frac{G}{2\pi}k^2\log(k)\left(1 - \frac{2E_1}{F_1} + h^2\right)\right]\left[1 - \frac{x^2 - \frac{E_1}{F_1}}{\sqrt{(1-x^2)(h^2-x^2)}}\right], & 0 \le x \le h \\[3mm] -h_0\left[1 - \frac{G}{2\pi}k^2\log(k)\left(1 - \frac{2E_1}{F_1} + h^2\right)\right]\left[1 + \frac{x^2 - \frac{E_1}{F_1}}{\sqrt{(x^2-1)(x^2-h^2)}}\right], & x > 1. \end{cases}
$$

$$(4.1.42)$$

The SIFs K_h and K_1 at the crack vicinities $(x = h$ and $x = 1)$ are computed as

$$
K_h = \mathrm{Lt}_{x \to h^-} \frac{(h-x)^{\frac{1}{2}}\sigma_{yz}(x,0)}{h_0}
$$
$$
= \frac{h^2 - \frac{E_1}{F_1}}{\sqrt{2h(1-h^2)}}\left[1 - \frac{G}{2\pi}k^2\log k\left(1 - \frac{2E_1}{F_1} + h^2\right)\right] + \mathcal{O}(k^2) \qquad (4.1.43)
$$

and

$$
K_1 = \mathrm{Lt}_{x \to 1^+} \frac{(x-1)^{\frac{1}{2}}\sigma_{yz}(x,0)}{h_0}
$$
$$
= \frac{\frac{E_1}{F_1} - 1}{\sqrt{2(1-h^2)}}\left[1 - \frac{G}{2\pi}k^2\log k\left(1 - \frac{2E_1}{F_1} + h^2\right)\right] + \mathcal{O}(k^2). \qquad (4.1.44)
$$

Crack Opening Displacement:

Another physical quantity COD (Magnitude of the distance between two faces of the crack) is given by

$$
\delta W(x) = \mid U_y(x,0^+) - U_y(x,0^-) \mid = 2\int_x^1 \phi(q^2)dq
$$
$$
= \frac{4h_0}{\pi\vartheta C_{44}}\left[1 - \frac{G}{\pi}k^2\log k\left(1 - \frac{2E_1}{F_1} + h^2\right)\right]\left[E_2 - \frac{E_1 F_2}{F_1}\right], \quad (4.1.45)
$$

where $E_2 = E\left(\sin^{-1}\sqrt{\frac{1-x^2}{1-h^2}}, \sqrt{1-h^2}\right)$, $F_2 = F\left(\sin^{-1}\sqrt{\frac{1-x^2}{1-h^2}}, \sqrt{1-h^2}\right)$.

■ Numerical and Graphical Demonstration

From the expansions of SIFs and COD given by (4.1.43), (4.1.44), and (4.1.45), it is obvious that these physical parameters depend on the values of material parameters and magnetic field. For orthotropic elastic medium, we take the following data (Panja and Mandal (2022))

$$\rho = 2.7 \ g/m^3, \ C_{44} = 5.3Gpa, \ C_{66} = 6.47GPa \text{ and } \psi = 10.$$

To display the impact of magnetic field, we plot the graphs of SIF vs frequency and COD vs crack width in the presence and absence of magnetic field. For the presence of magnetic field we consider

$$\epsilon_1 = \frac{\mu_e(\mathcal{H}^{(0)})^2}{C_{66}} = 0.30 \text{ and } \epsilon_2 = \frac{\mu_e(\mathcal{H}^{(0)})^2}{C_{44}} = 0.37$$

and the corresponding graph is represented by dash line. In the absence of magnetic field, we assume

$$\epsilon_1 = 0 \text{ and } \epsilon_2 = 0$$

and the graph is represented by solid line.

Firstly the variations of SIF K_h at the inner vicinity of the crack with $h = 0.5$, 0.6, 0.7 are shown in Fig.4.1,2, secondly the variations of SIF at the outer vicinity of the crack are shown in Fig.4.1.3. From both the graphs it is obvious that SIF has a slower decreasing rate up to a certain value of frequency and then the rate of decreasing become high and finally tends to zero. Comparing both the Fig.4.1.2

and Fig.4.1.3 it is identified that SIF at the outer tip has a higher rate of decreasing as compared to the SIF at the inner tip and SIFs decrease with the increase of the values of h. It has also been observed that the variations of SIFs are not significant in both the cases for the presence and absence of the magnetic field.
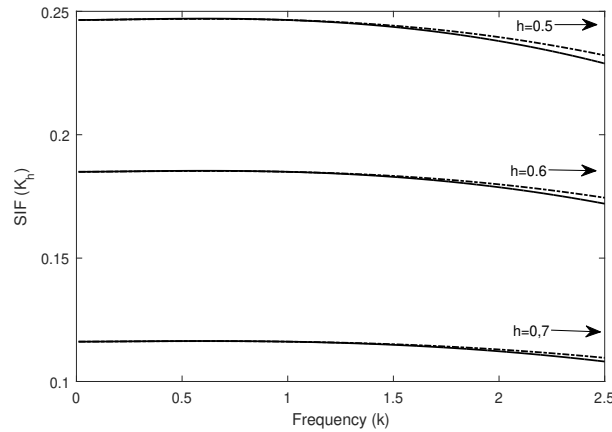
Fig.4.1.2 SIF K_h with respect to frequency (k).
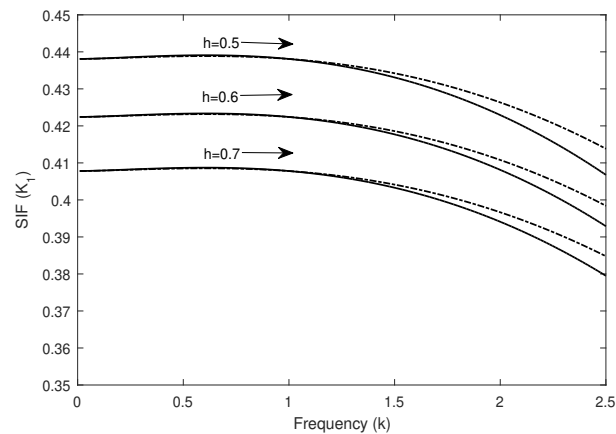
Fig.4.1.3 SIF K_1 with respect to frequency (k).

The nature of the Fig.4.1.2 and Fig.4.1.3 is quite same as the work discussed by Sarkar et al. (1995) in the absence of magnetic field. Fig.4.1.4 represents the graph of COD vs crack width due to the presence and absence of magnetic field. It is notable that the COD achieves its highest value at the point $x = 0.6$ and reaches

zero at the tips of the cracks, so the fracture toughness is high at the point $x = 0.6$. Also, COD increases slightly in the presence of magnetic field as compared to the absence of magnetic field for low frequency k.
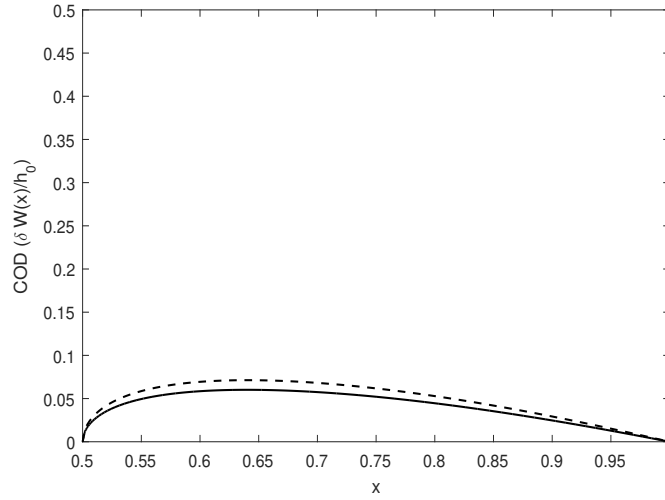
Fig.4.1.4 COD $\frac{\delta W(x)}{h_0}$ against the crack width x.

■ **Comparison of Results**

If we take $h = 0$, then two cracks coincide with a single crack and Fig.4.1.5 represents the graph of SIF for the case of the single crack. If we take $C_{44} = C_{66} \to \mu$, then the medium will tend to be isotropic medium and we have the following expressions

$$A \to \mu + \mu_e (\mathcal{H}^{(0)})^2 \cos^2 \psi,$$
$$B \to \mu + \mu_e (\mathcal{H}^{(0)})^2 \sin^2 \psi,$$
$$C = \mu_e (\mathcal{H}^{(0)})^2 \sin 2\psi.$$

We obtain SIF in the following form

$$K_1 = \frac{\frac{E_1}{F_1} - 1}{\sqrt{2}} \left[1 - \frac{G}{2\pi} k^2 \log k \left(1 - \frac{2E_1}{F_1} \right) \right]. \tag{4.1.46}$$

After some numerical manipulation, the approximate expression for SIF given by (4.1.46) has been derived from the expression of SIF given by Panja and Mandal (2021c) et al. This comparison ensures the validation of the result obtained in this problem.
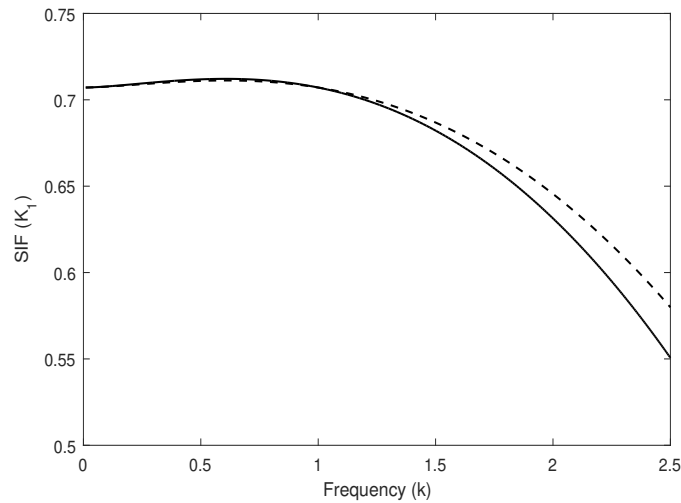
Fig.4.1.5 SIF with respect to frequency (k).

■ Conclusion

In the present study, the analytic expressions for SIFs and COD subjected to the magnetic field in an infinite elastic medium have been obtained. The main advantage of the analytical method is that we can plot physical parameters accurately while in the numerical procedure discrete data is used to plot the parameters. The variations of the mechanical parameters SIFs and COD due to the presence and absence of magnetic field have been represented graphically. Graphical results indicate that the

propagation of the crack in the magneto-elastic medium is more pronounced compare to the non magneto-elastic medium for small frequency. Around the vicinity of the crack, state of stress is disruptive in nature and loses its toughness far away from the crack. From the figures it is seen that the SIFs and COD decrease as frequency and crack width increases which are physically persistent with the problem. It can be concluded that the material parameters play a major role in the case of fracture. Therefore we can settle the rate of crack growth and fracture toughness by considering a particular range of frequency and manipulating the magneto-elastic parameters. The analysis of the stress field in the proposed model may help to find the significant applications for the assessment of the toughness of structures containing multiple cracks. Furthermore, the proposed analysis may significantly give an idea to find the implementations of engineering materials which bring some extraordinary impact on the analysis and the design of sustainable materials used in high rising buildings, constructions of bridges, airplane industries, and many more identical types of reinforced constructions.

4.2 Dispersion of Longitudinal Waves by Three Co-linear Griffith Cracks in a Magnetized Elastic Medium

■ Introduction

Magnetized composite materials have broad implementations, on account of their enumerable number of practical applications in miscellaneous domains such as aerospace engineering, geophysics, optics, cell phone industries, kitchen appliances, acoustics and so on. Due to the interaction of electromagnetic field with cracked elastic media, elastic stress-strain relation gets improved with consideration of Lorentz's force as body force and modifying Ohm's law permeated by an initial magnetic field. The coupled properties of magnetic field and elastic media provide great opportunities for researchers to construct flawless constructions and devices that are able to respond internal and external changes. However, deficiencies or cracks in such materials are usually inevitable which impact the completion and reliability of the products. Adequate failure in structural components may arises due to the presence of such pre-existing cracks or inclusions. To recognize the fracture of materials, it is necessary to know stress field in the neighbourhood of the crack tip which manages the behaviour of the cracks. The impact of this stress field is quantified by means of the so-called stress intensity factor near crack tips. Another fundamental physical parameter COD provides fracture toughness for crack propagation processes. The problem of dispersion of longitudinal waves by cracks of finite length in isotropic medium had been solved by numerous researchers over the years. Some elastodynamic problems of stationary cracks and dynamics aspects of crack propagation had been solved by Sih (1968). Mal (1970) solved the problem of diffraction of normally incident longitudinal and antiplane shear waves by a Griffith crack. Lowengrub and

Srivastava (1968) published a research note on two collinear Griffith cracks in an infinitely extended elastic media. Considering a time-harmonic antiplane shear wave, Itou (1980) inspected the scattering effects of two coplanar Griffith cracks embedded in an infinite elastic medium. Interaction of elastic waves with Griffith crack located in an infinitely long strip was investigated by Srivastava et al. (1981). Jain and Kanwal (1972) had solved the problem of diffraction of elastic waves by two parallel and coplanar Griffith cracks in an infinite homogeneous isotropic elastic medium. A few of researchers solved the elastodynamic problems considering the impact of magnetic field. Wave propagation in an electrifying conducting elastic solid by the influence of an uniform magnetic field was discussed by Knopoff (1955). Chadwick (1957) developed the concept regarding elastic waves propagation in a magnetic field. Linear and nonlinear wave motion in magnetizable distort-able solids was explained by Maugin (1981). Yih-Hsing and Chau-Shioung (1973) presented a linearize theory for soft ferromagnetic elastic solids. Shindo (1977, 1980) also introduced some linear magnetoelastic problem concerning a soft ferromagnetic material consists of a Griffith crack and derived singular stresses at the tip of cracks in a soft ferromagnetic cracked elastic material. Scattering of P-waves by a finite crack under the influence of magnetic field and an applied impact load was analysed by Panja and Mandal (2021a).

Most of the above mentioned researchers had considered the cracked elastic media to analyse normally incident time harmonic waves but not discussed the magneto-elastic coupling effects on the propagation of waves in an isotropic elastic medium. Therefore, this monograph analyses the dispersion of longitudinal waves by three co-linear cracks in an infinite isotropic medium upon magnetization. The dispersion effects of three co-linear Griffith cracks located in an homogeneous infinite isotropic medium due to the influence of magnetic field be formulated as a MBVP. The MBVP have been converted to a set of integral equations with the

help of Abel's transform which have been further simplified by using perturbation method for low frequency by concerning the iterative expansions of Bessel's and Hankel's function. The converted integral equations have been solved by Hilbert transformation and the results of Cooke (1970). The semi-analytical expressions of crack opening displacement and stress intensity factors have been derived for low frequency vibration. Numerical results of crack opening displacement and stress intensity factors for several crack lengths with the presence of magnetic field have been computed and presented graphically to exhibit the influence of magnetization.

■ Formulation of the Problem

Consider three coplanar Griffith cracks embedded in an infinite magnetoelastic medium. The crack faces are loaded by a normally incident wave $\bar{\sigma}_0 e^{-\iota\omega t}$ in the positive direction of $y-$axis, where ω is the frequency of the incident wave and $\bar{\sigma}_0$ is the crack surface traction. Let the cracks are situated at $|x'| \leq m_1$, $m_2 \leq x' \leq m_3$, $-\infty < z' < \infty$, $y' = 0$. For Normalization of all the lengths, we substitute $\frac{x'}{m_3} = x, \frac{y'}{m_3} = y, \frac{z'}{m_3} = z, \frac{m_1}{m_3} = m, \frac{m_2}{m_3} = n$. After normalization, the new location of the cracks are found to be $|x| \leq m$, $n \leq |x| \leq 1$, $-\infty < z < \infty$, $y = 0$, $m < n$ (Fig.4.2.1).
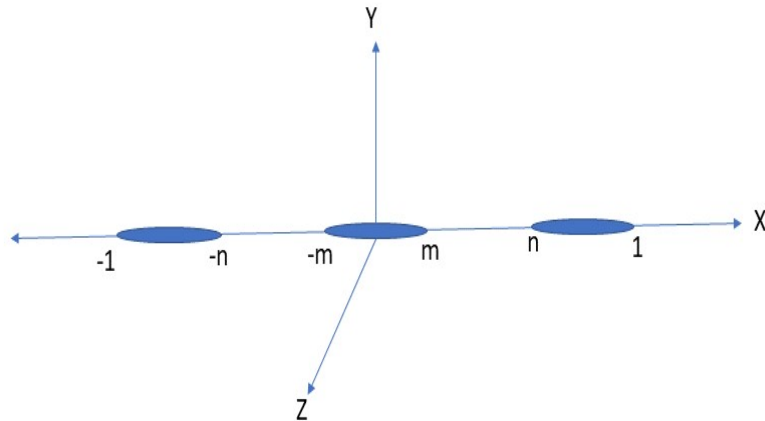
Fig.4.2.1   Geometry of the cracks.

Let $\vec{\mathcal{H}} = (0, 0, \mathcal{H}_{(z)})$ be the magnetic field intensity acting on the crack surface in the direction of z-axis, $\vec{\mathcal{E}}$ is the induced electric field intensity and $\vec{h} = (0, 0, h_{(z)})$ is the induced magnetic field.

The Maxwell's equation for electromagnetic waves are follows

$$\vec{\mathcal{J}} = \vec{\Delta} \times \vec{h} - \epsilon_0 \frac{\partial^2 \vec{\mathcal{E}}}{\partial t^2}, \quad \vec{\Delta} \times \vec{\mathcal{E}} = -\mu_0 \frac{\partial^2 \vec{h}}{\partial t^2},$$
$$\vec{\mathcal{E}} = -\mu_0 \left(\frac{\partial^2 \vec{U}}{\partial t^2} \times \vec{\mathcal{H}} \right), \quad \vec{\Delta} \cdot \vec{h} = 0,$$

(4.2.1)

where μ_0 is the magnetic permeability, $\vec{\mathcal{J}}$ is the electric current density, $\vec{U}$ is the displacement field and ϵ_0 is the electric permittivity.

The displacement equations in terms of Lorentz force and Hooke's law due to the influence of electromagnetic field are

$$\rho \frac{\partial^2 U_i}{\partial t^2} = \tau_{ij,j} + \mu_0 (\vec{\mathcal{J}} \times \vec{\mathcal{H}})_i$$

(4.2.2)

and

$$\tau_{ij} = 2\mu e_{ij} + 2\lambda e \delta_{ij},$$

(4.2.3)

where λ and μ are Lame's constants, e is the dilatation, ρ is the electric current density, δ_{ij} is the Kronecker delta, e_{ij} are the strain components and τ_{ij} are the stress components.

Since P-waves propagate in $z = 0$ plane, so the displacement field can be taken as $\vec{U} = (U_x(x, y, t), \ U_y(x, y, t), \ 0)$.

The strain components e_{ij} and the dialatation e in terms of displacement components

are

$$e_{xy} = \frac{1}{2} \left(\frac{\partial U_x}{\partial y} + \frac{\partial U_y}{\partial x} \right), \ e_{xx} = \frac{\partial U_x}{\partial x}, \ e_{yy} = \frac{\partial U_y}{\partial y},$$
$$e_{xz} = e_{yz} = 0, \ e = \frac{\partial U_x}{\partial x} + \frac{\partial U_y}{\partial y}. \tag{4.2.4}$$

Using the results (4.2.1), (4.2.3) and (4.2.4) in (4.2.2), we derive the displacement equations as

$$\left(\lambda + \mu + \mu_0 \mathcal{H}_{(z)}^2 \right) \left(\frac{\partial^2 U_x}{\partial x^2} + \frac{\partial^2 U_y}{\partial x \partial y} \right) + \mu \left(\frac{\partial^2 U_x}{\partial x^2} + \frac{\partial^2 U_x}{\partial^2 y} \right)$$
$$= \left(\rho + \mu_0^2 \epsilon_0 \mathcal{H}_{(z)}^2 \right) \frac{\partial^2 U_x}{\partial^2 t} \tag{4.2.5}$$

and

$$\left(\lambda + \mu + \mu_0 \mathcal{H}_{(z)}^2 \right) \left(\frac{\partial^2 U_x}{\partial x \partial y} + \frac{\partial^2 U_y}{\partial^2 y} \right) + \mu \left(\frac{\partial^2 U_y}{\partial x^2} + \frac{\partial^2 U_y}{\partial^2 y} \right)$$
$$= \left(\rho + \mu_0^2 \epsilon_0 \mathcal{H}_{(z)}^2 \right) \frac{\partial^2 U_y}{\partial^2 t} \tag{4.2.6}$$

On introduction of wave potential functions $\bar{\phi}_1$ and $\bar{\psi}_1$, displacement components can be written as

$$U_x = \frac{\partial \bar{\phi}_1}{\partial x} - \frac{\partial \bar{\psi}_1}{\partial y}, \ U_y = \frac{\partial \bar{\psi}_1}{\partial x} + \frac{\partial \bar{\phi}_1}{\partial y}. \tag{4.2.7}$$

Using (4.2.7), equations (4.2.5) and (4.2.6) transform into

$$\frac{\partial^2 \bar{\phi}_1}{\partial x^2} + \frac{\partial^2 \bar{\phi}_1}{\partial y^2} = \rho_1^2 \frac{\partial^2 \bar{\phi}_1}{\partial t^2} \tag{4.2.8}$$

and

$$\frac{\partial^2 \bar{\psi}_1}{\partial x^2} + \frac{\partial^2 \bar{\psi}_1}{\partial y^2} = \rho_2^2 \frac{\partial^2 \bar{\phi}_1}{\partial t^2}, \tag{4.2.9}$$

where $\rho_1^2 = \frac{\rho + \mu_0^2 \epsilon_0 \mathcal{H}_{(z)}^2}{\lambda + 2\mu + \mu_0 \mathcal{H}_{(z)}^2}$ and $\rho_2^2 = \frac{\rho + \mu_0^2 \epsilon_0 \mathcal{H}_{(z)}^2}{\mu}$.

The considered problem is symmetric about y-axis, so the problem can be solved subjected to the following boundary conditions

$$\tau_{yy}(x,0,t) = -\bar{\sigma}_0 e^{-i\omega t}, \quad 0 \le x \le m, \ n \le x \le 1 \tag{4.2.10}$$

$$\tau_{xy}(x,0,t) = 0, \qquad\qquad\qquad |x| < \infty \tag{4.2.11}$$

$$U_y(x,0,t) = 0, \qquad m \le x \le n, \ 1 \le x < \infty. \tag{4.2.12}$$

Substituting $\bar{\phi}_1(x,y,t) = \bar{\phi}(x,y)e^{-i\omega t}$ and $\bar{\psi}_1(x,y,t) = \bar{\psi}(x,y)e^{-i\omega t}$ in the equations (4.2.8) and (4.2.9), we have

$$\frac{\partial^2 \bar{\phi}}{\partial x^2} + \frac{\partial^2 \bar{\phi}}{\partial y^2} = k_1^2 \bar{\phi} \tag{4.2.13}$$

$$\frac{\partial^2 \bar{\psi}}{\partial x^2} + \frac{\partial^2 \bar{\psi}}{\partial y^2} = k_2^2 \bar{\psi}, \tag{4.2.14}$$

where $k_1^2 = \omega^2 \rho_1^2$ and $k_2^2 = \omega^2 \rho_2^2$.

The modified boundary conditions are

$$\tau_{yy}(x,0) = -\bar{\sigma}_0, \quad 0 \le x \le m, \ n \le x \le 1 \tag{4.2.15}$$

$$\tau_{xy}(x,0) = 0, \qquad\qquad |x| < \infty \tag{4.2.16}$$

$$U_y(x,0) = 0, \quad m \le x \le n, \ 1 \le x < \infty. \tag{4.2.17}$$

The solutions of (4.2.13) and (4.2.14) can be considered as

$$\bar{\phi}(x,y) = \int_0^\infty \mathcal{A}_1(\zeta) e^{-\beta_1 y} \cos(\zeta x) d\zeta \tag{4.2.18}$$

and

$$\bar{\psi}(x,y) = \int_0^\infty \mathcal{A}_2(\zeta) e^{-\beta_2 y} \cos(\zeta x) d\zeta, \tag{4.2.19}$$

where $\beta_1^2 = \zeta^2 - k_1^2$ and $\beta_2^2 = \zeta^2 - k_2^2$.

Using (4.2.18) and (4.2.19), we have the displacement components as follows

$$U_x(x,y) = -\int_0^\infty \mathcal{A}_1(\zeta)e^{-\beta_1 y}\zeta\sin(\zeta x)d\zeta + \int_0^\infty \mathcal{A}_2(\zeta)e^{-\beta_2 y}\beta_2\sin(\zeta x)d\zeta \quad (4.2.20)$$

and

$$U_y(x,y) = -\int_0^\infty \mathcal{A}_1(\zeta)e^{-\beta_1 y}\beta_1\cos(\zeta x)d\zeta + \int_0^\infty \mathcal{A}_2(\zeta)e^{-\beta_2 y}\zeta\cos(\zeta x)d\zeta. \quad (4.2.21)$$

Applying boundary condition (4.2.16), we obtain

$$\mathcal{A}_2(\zeta) = \alpha_1\mathcal{A}_1(\zeta), \quad (4.2.22)$$

where $\alpha_1 = \frac{2\zeta\beta_1}{2\zeta^2 - k_2^2}$.

Using the boundary conditions (4.2.15) and (4.2.17), we derive the following dual integral equations

$$\int_0^\infty B(\zeta)\cos\zeta x d\zeta = 0, \ m \le x \le n, 1 \le x < \infty \quad (4.2.23)$$

and

$$\int_0^\infty D(\zeta)B(\zeta)\cos\zeta x d\zeta = -\bar{\sigma}_0, \ 0 \le x \le m, n \le x \le 1. \quad (4.2.24)$$

Equation (4.2.24) can be written as

$$\int_0^\infty \zeta[1 + D_1(\zeta)]B(\zeta)\cos\zeta x d\zeta = p_0, \ 0 <\le x \le m, \ n \le x \le 1, \quad (4.2.25)$$

where

$$D_1(\zeta) = \frac{D(\zeta)}{\zeta\nu} - 1, \ p_0 = -\frac{\bar{\sigma}_0}{\nu}, \ D(\zeta) = \frac{2\mu\beta_1^2 + \lambda(\beta_1^2 - \zeta^2) - 2\mu\zeta\beta_2\alpha_1}{\alpha_1\zeta - \beta_1},$$
$$\nu = -\frac{2(\lambda + \mu)k_1^2}{k_2^2} \text{ and } D_1(\zeta) \to 0 \text{ as } \zeta \to \infty. \quad (4.2.26)$$

■ **Derivation of Integral Equation**

Let us take the trial solution of equations (4.2.23) and (4.2.24) in the form

$$B(\zeta) = \frac{1}{\zeta} \int_0^m f_1(r) sin(\zeta r) dr + \frac{1}{\zeta} \int_n^1 f_2(s^2) sin(\zeta s) ds, \qquad (4.2.27)$$

where $f_1(r)$ and $f_2(s^2)$ are the unknown functions to be determined with the help of integral transforms.

Using (4.2.27) and $\int_0^\infty \dfrac{\sin \zeta r \cos \zeta x}{\zeta} d\zeta = \begin{cases} \frac{\pi}{2} & r > x \\ 0 & r < x \end{cases}$ in the equation (4.2.23), it is seen that $f_2(s^2)$ satisfy the equation

$$\int_n^1 f_2(s^2) ds = 0. \qquad (4.2.28)$$

Again using the result $\int_0^\infty \dfrac{\sin \zeta r \sin \zeta x}{\zeta} d\zeta = \dfrac{1}{2} \log \left| \dfrac{r+x}{r-x} \right|$ and $B(\zeta)$ from equation (4.2.27), we get from the equation (4.2.25)

$$\frac{d}{dx} \int_0^m f_1(r) \log \left| \frac{r+x}{r-x} \right| dr + \frac{d}{dx} \int_n^1 f_2(s^2) \log \left| \frac{s+x}{s-x} \right| ds =$$
$$2p_0 - 2\frac{d}{dx} \int_0^m f_1(r) dr \int_0^\infty D_1(\zeta) \frac{\sin \zeta r \sin \zeta x}{\zeta} d\zeta \qquad (4.2.29)$$
$$-2\frac{d}{dx} \int_n^1 f_2(s^2) ds \int_0^\infty D_1(\zeta) \frac{\sin \zeta s \ \sin \zeta x}{\zeta} d\zeta, \ 0 \le x \le m, \ n \le x \le 1.$$

Utilizing the result $\dfrac{\sin \zeta x \sin \zeta r}{\zeta^2} = \int_0^x \int_0^r \dfrac{vw J_0(\zeta v) J_0(\zeta w)}{\sqrt{x^2 - v^2}\sqrt{r^2 - w^2}} dv dw$, the equation (4.2.29) becomes

$$\frac{d}{dx} \int_0^m f_1(r) \log \left| \frac{r+x}{r-x} \right| dr + \frac{d}{dx} \int_n^1 f_2(s^2) \log \left| \frac{s+x}{s-x} \right| ds =$$
$$2p_0 - 2\frac{d}{dx} \int_0^m f_1(r) dr \int_0^x \int_0^r \frac{vw L(v,w)}{\sqrt{x^2 - w^2}\sqrt{r^2 - v^2}} dv dw \qquad (4.2.30)$$
$$-2\frac{d}{dx} \int_n^1 f_2(s^2) ds \int_0^x \int_0^s \frac{vw L(v,w)}{\sqrt{x^2 - w^2}\sqrt{s^2 - v^2}} dv dw,$$

where

$$L(v,w) = \int_0^\infty \zeta D_1(\zeta) J_0(\zeta v) J_0(\zeta w) d\zeta. \tag{4.2.31}$$

The integrand of the equation (4.2.31) is a multi-valued function, has branch points at $\zeta = k_1$ and $\zeta = k_2$. Following contour integration technique, the infinite integral has been transformed into the finite integral as

$$L(v,w) = \frac{ik_2^2}{\nu} \int_0^\epsilon \frac{2\mu(\epsilon^2-\xi^2)-\lambda\epsilon^2+4\mu\xi^2\sqrt{(\epsilon^2-\xi^2)(1-\xi^2)}}{\sqrt{\epsilon^2-\xi^2}} J_0(k_2\xi v) H_0^{(1)}(k_2\xi w) d\xi$$
$$+\frac{4ik_2^2}{\nu} \int_\epsilon^1 \xi^2\sqrt{1-\xi^2} J_0(k_2\xi v) H_0^{(1)}(k_2\xi w) d\xi, \quad w > v, \tag{4.2.32}$$

where $\frac{k_1}{k_2} = \epsilon$. The expression of $L(v,w)$ for $w < v$ is calculated by interchanging v and w in (4.2.32).

Applying the iterative series expansions for the Bessel function and the Hankel function, we have

$$J_0(k_2 v\xi) H_0^{(1)}(k_2 w\xi) = \frac{2\iota}{\pi} \log k_2 + \left[1 + \frac{2\iota}{\pi}\left(v + \log\frac{w\xi}{2}\right)\right] \tag{4.2.33}$$

and (4.2.32) becomes

$$L(v,w) = \frac{2}{\pi} k_2^2 I \log k_2 + \mathcal{O}(k_2^2), \tag{4.2.34}$$

where

$$I = -\frac{1}{\nu} \int_0^\epsilon \frac{2\mu(\epsilon^2 - \xi^2) - \lambda\epsilon^2 + 4\mu\xi^2\sqrt{(\epsilon^2 - \xi^2)(1 - \xi^2)}}{\sqrt{\epsilon^2 - \xi^2}} d\xi$$
$$-\frac{4}{\nu} \int_\epsilon^1 \xi^2\sqrt{1-\xi^2} d\xi. \tag{4.2.35}$$

■ Solution of the Integral Equations

Let us assume the iterative form of $f_1(r)$ and $f_2(s^2)$ as follows

$$f_1(r) = f_{10}(r) + (k_2^2 \log k_2) f_{11}(r) + \mathcal{O}(k_2^2) \tag{4.2.36}$$

and

$$f_2(s^2) = f_{20}(s^2) + (k_2^2 \log k_2) f_{21}(s^2) + \mathcal{O}(k_2^2). \tag{4.2.37}$$

Substituting the expressions of $f_1(r)$ and $f_2(s^2)$ from (4.2.36) and (4.2.37) and the value of $L(v, w)$ given by (4.2.34) in the equations (4.2.28) and (4.2.30) and equating the coefficient of equal power of k_2, we derived the following equations

$$\frac{d}{dx} \int_0^m f_{10}(r) \log \left| \frac{r+x}{r-x} \right| dr + 2 \int_n^1 \frac{s f_{20}(s^2)}{s^2 - x^2} ds = 2p_0, \tag{4.2.38}$$

$$\frac{d}{dx} \int_0^m f_{11}(r) \log \left| \frac{r+x}{r-x} \right| dr + 2 \int_n^1 \frac{s f_{21}(s^2)}{s^2 - x^2} ds$$
$$= -\frac{4I}{\pi} \left[\int_0^m r f_{10}(r) dr + \int_n^1 s f_{20}(s^2) ds \right] \tag{4.2.39}$$

and

$$\int_n^1 f_{20}(s^2) ds = 0, \quad \int_n^1 f_{21}(s^2) ds = 0. \tag{4.2.40}$$

Rewrite the equation (4.2.38) as follows

$$\frac{d}{dx} \int_0^m f_{10}(r) \log \left| \frac{r+x}{r-x} \right| dr = \pi F_1'(x), \tag{4.2.41}$$

where $F_1(x) = -\dfrac{2}{\pi} \displaystyle\int_0^x \left[\dfrac{\bar{\sigma}_0}{\nu} + \displaystyle\int_n^1 \dfrac{s f_{20}(s^2)}{s^2 - \eta^2} ds \right] d\eta.$

Applying Hilbert transform technique, we have the solution of the integral equation (4.2.41) as follows

$$f_{10}(r) = -\frac{2}{\pi} \frac{r}{\sqrt{m^2 - r^2}} \int_0^m \frac{\sqrt{m^2 - x^2}}{x^2 - r^2} F_1'(x) dx + \frac{2}{\pi} \frac{F_1(x)}{r\sqrt{m^2 - r^2}}. \tag{4.2.42}$$

Using Cook's result, the equation (4.2.42) can be expressed as

$$f_{10}(r) = -\frac{2}{\pi}\frac{\bar{\sigma}_0}{\nu}\frac{r}{\sqrt{m^2-r^2}} - \frac{2}{\pi}\frac{r}{\sqrt{m^2-r^2}}\int_n^1 \frac{\sqrt{s^2-m^2}}{s^2-r^2}f_{20}(s^2)ds. \qquad (4.2.43)$$

Substituting the value of $f_{10}(r)$ from (4.2.43) in the equation (4.2.38), the following integral equation has been obtained

$$\int_n^1 \frac{\sqrt{s^2-m^2}}{s^2-x^2}f_{20}(s^2)ds = -\frac{\bar{\sigma}_0}{\nu} \qquad (4.2.44)$$

and the solution of which is

$$f_{20}(s^2) = -\frac{2}{\pi}\frac{\bar{\sigma}_0}{\nu}\sqrt{\frac{s^2(s^2-n^2)}{(s^2-m^2)(1-s^2)}} + \frac{s\delta_1}{\sqrt{(s^2-m^2)(s^2-n^2)(1-s^2)}}, \qquad (4.2.45)$$

where δ_1 is unknown, to be determined with the help of the condition (4.2.40). Now substituting the value of $f_{20}(s^2)$ from (4.2.45) in (4.2.43) and using some integral formulas from Abramowitz et al. (1988), we derived the expression of $f_{10}(r)$ in the following form

$$f_{10}(r) = -\frac{2}{\pi}\frac{\bar{\sigma}_0}{\nu}\frac{r}{\sqrt{m^2-r^2}}\sqrt{\frac{n^2-r^2}{1-r^2}} - \delta_1\frac{r}{\sqrt{m^2-r^2}}\frac{1}{\sqrt{(n^2-r^2)(1-r^2)}}. \qquad (4.2.46)$$

We express the term $\int_0^m rf_{10}(r)dr + \int_n^1 sf_{20}(s^2)ds$ as follows

$$\int_0^m rf_{10}(r)dr + \int_n^1 sf_{20}(s^2)ds = -\frac{2}{\pi}\frac{\bar{\sigma}_0}{\nu}[G_0^m + G_n^1] + \delta_1[T_0^m - T_n^1] = C, \qquad (4.2.47)$$

where $G_i^j = \int_i^j \sqrt{\frac{s^4(s^2-n^2)}{(s^2-m^2)(1-s^2)}}ds$ and $T_i^j = \int_i^j \frac{s^2}{\sqrt{(s^2-m^2)(s^2-n^2)(1-s^2)}}ds.$
Using the value from (4.2.47), equation (4.2.39) can be expressed as

$$\frac{d}{dx}\int_0^m f_{11}(r)\log\left|\frac{r+x}{r-x}\right|dr = \pi F_2'(x), \qquad (4.2.48)$$

where $F_2(x) = \int_0^x \left[-\frac{4IC}{\pi^2} - \frac{2}{\pi} \int_n^1 \frac{s f_{21}(s^2)}{s^2 - \eta^2} ds \right] d\eta.$

By similar procedure as above, we finally obtain

$$f_{21}(s^2) = -\frac{4IC}{\pi^2} \sqrt{\frac{s^2(s^2 - n^2)}{(s^2 - m^2)(1 - s^2)}} + \frac{s\delta_2}{\sqrt{(s^2 - m^2)(s^2 - n^2)(1 - s^2)}} \qquad (4.2.49)$$

and

$$f_{11}(r) = -\frac{4IC}{\pi^2} \frac{r}{\sqrt{m^2 - r^2}} \frac{1}{\sqrt{(n^2 - r^2)(1 - r^2)}}$$
$$-\delta_2 \frac{r}{\sqrt{m^2 - r^2}} \frac{1}{\sqrt{(n^2 - r^2)(1 - r^2)}}, \qquad (4.2.50)$$

where δ_2 is to be determined with the help of the condition (4.2.40). Substituting the values of $f_{20}(s^2)$ and $f_{21}(s^2)$ from (4.2.45) and (4.2.49) in (4.2.40), we attained the values of δ_1 and δ_2 as follows

$$\delta_1 = \frac{2}{\pi} \frac{\bar{\sigma}_0}{\nu} \left[(1 - m^2)\frac{E}{F} + (m^2 - n^2) \right]$$
$$\text{and } \delta_2 = \frac{4IC}{\pi^2} \left[(1 - m^2)\frac{E}{F} + (m^2 - n^2) \right], \qquad (4.2.51)$$

where $E = E\left(\frac{\pi}{2}, \sqrt{\frac{1-n^2}{1-m^2}}\right)$ and $F = F\left(\frac{\pi}{2}, \sqrt{\frac{1-n^2}{1-m^2}}\right).$

Substituting the values of δ_1 and δ_2 given by (4.2.51) in the equations (4.2.45), (4.2.46), (4.2.49) and (4.2.50), we obtain

$$f_{2l}(s^2) = M_l \frac{s \left[s^2 - \frac{E}{F} + m^2 \left(\frac{E}{F} - 1\right) \right]}{\sqrt{(s^2 - m^2)(s^2 - n^2)(1 - s^2)}}, \qquad (4.2.52)$$

$$f_{1l}(r) = M_l \frac{r \left[\frac{E}{F} - r^2 + m^2 \left(1 - \frac{E}{F}\right) \right]}{\sqrt{(m^2 - r^2)(n^2 - r^2)(1 - r^2)}}, \qquad (4.2.53)$$

where $M_0 = -\frac{2\bar{\sigma}_0}{\pi\nu}$ and $M_1 = -\frac{4IC}{\pi^2}, \ l = 0, \ 1.$

■ **Quantity of Physical Interest**

Stress Intensity Factor:

The normal stress $\tau_{yy}(x,0)$ is given by

$$
\begin{aligned}
\tau_{yy}(x,0) = {}& \nu \int_0^m \frac{r f_{10}(r)}{r^2 - x^2} dr + (\nu k_2^2 \log k_2) \int_0^m \frac{r f_{11}(r)}{r^2 - x^2} dr \\
&+ \nu \int_n^1 \frac{s f_{20}(s^2)}{s^2 - x^2} ds + (\nu k_2^2 \log k_2) \int_n^1 \frac{s f_{21}(s^2)}{s^2 - x^2} ds
\end{aligned}
\tag{4.2.54}
$$

Substituting the values of $f_{10}(r)$, $f_{11}(r)$, $f_{20}(s^2)$ and $f_{21}(s^2)$ given by (4.2.52) and (4.2.53) in the equation (4.2.54), the expressions of stress intensity factors κ_m, κ_n and κ_1 at the vicinity of cracks at the points $x = m$, $x = n$ and $x = 1$ respectively are found to be

$$
\begin{aligned}
\kappa_m = {}& Lt_{x \to m^+} \left| \frac{\tau_{yy}(x,0)\sqrt{x-m}}{\bar{\sigma}_0} \right|, \qquad m \le x \le n \\
= {}& \sqrt{\frac{m}{2}} \sqrt{\frac{1-m^2}{n^2-m^2}} \left[1 - N k_2^2 \log k_2 \right] \frac{E}{F} + \mathcal{O}(k_2^2),
\end{aligned}
\tag{4.2.55}
$$

$$
\begin{aligned}
\kappa_n = {}& Lt_{x \to n^-} \left| \frac{\tau_{yy}(x,0)\sqrt{n-x}}{\bar{\sigma}_0} \right|, \qquad m \le x \le n \\
= {}& \sqrt{\frac{n}{2}} \sqrt{\frac{1}{(1-m^2)(1-n^2)}} \left[1 - N k_2^2 \log k_2 \right] \\
& \left[\frac{E}{F} - n^2 - m^2 \left(\frac{E}{F} - 1 \right) \right] + \mathcal{O}(k_2^2)
\end{aligned}
\tag{4.2.56}
$$

and

$$
\begin{aligned}
\kappa_1 = {}& Lt_{x \to 1^+} \left| \frac{\tau_{yy}(x,0)\sqrt{x-1}}{\bar{\sigma}_0} \right|, \qquad x \ge 1 \\
= {}& \sqrt{\frac{1}{2}} \sqrt{\frac{1-m^2}{1-n^2}} \left[1 - N k_2^2 \log k_2 \right] \left[1 - \frac{E}{F} \right] + \mathcal{O}(k_2^2),
\end{aligned}
\tag{4.2.57}
$$

where $N = \frac{4I}{\pi^2} \left[G_0^m + G_n^1 + \left(\frac{E}{F} - n^2 - m^2(\frac{E}{F} - 1) \right) (T_0^m - T_n^1) \right]$.

Crack Opening Displacement:

The crack opening displacement is given by

$$\delta U_y(x, 0) = |U_y(x, 0^+) - U_y(x, 0^-)| = 2 \int_x^m f_1(r)dr, \quad 0 \le x \le m$$
$$= 2 \int_x^1 f_2(s^2)ds, \quad n \le x \le 1. \tag{4.2.58}$$

Putting the values of $f_{10}(r)$, $f_{11}(r)$, $f_{20}(s^2)$ and $f_{21}(s^2)$ given by (4.2.52) and (4.2.53) in the equation (4.2.58), expression (4.2.58) becomes

$$\delta U_y(x, 0) = \frac{4\bar{\sigma}_0}{\pi\nu} \left[1 - Nk_2^2 \log k_2 \right]$$
$$\left[\sqrt{\frac{(1 - x^2)(m^2 - x^2)}{n^2 - x^2}} + \sqrt{1 - m^2}F(\Lambda, \Upsilon) \left(\frac{E}{F} - \frac{E(\Lambda, \Upsilon)}{F(\Lambda, \Upsilon)} \right) \right]$$
$$+ \mathcal{O}(k_2^2), \; 0 \le x \le m \tag{4.2.59}$$

and

$$\delta U_y(x, 0) = \frac{4\bar{\sigma}_0}{\pi\nu} \left[1 - Nk_2^2 \log k_2 \right] \left[\sqrt{1 - m^2}F(\Lambda, \Upsilon) \left(\frac{E}{F} - \frac{E(\Omega, \Upsilon)}{F(\Omega, \Upsilon)} \right) \right]$$
$$+ \mathcal{O}(k_2^2), \quad n \le x \le 1, \tag{4.2.60}$$

where $\sin\Lambda = \sqrt{\frac{m^2 - x^2}{n^2 - x^2}}$, $\sin\Omega = \sqrt{\frac{1 - x^2}{1 - m^2}}$ and $\Upsilon = \sqrt{\frac{1 - n^2}{1 - m^2}}$.

■ Numerical and Graphical Discussions

Semi-analytical expressions for Stress Intensity factors and COD given by the equations (4.2.55) - (4.2.57), (4.2.59) and (4.2.60) have been obtained for low frequency. We notice that material constants and magnetic field parameters are present in the expressions of SIFs and COD. To plot SIFs and COD for the homogeneous isotropic material, we consider the following data (Panja and Mandal (2021a))

$$\lambda = 51.06 GPa,\ \mu = 26.32 GPa \text{ and } \rho = 2700\ kg/m^3.$$

In Fig.4.2.2, Fig.4.2.3 and Fig.4.2.4, keeping the length of the central crack as $m = 0.2$, SIFs at the vicinity of the central crack and the vicinities of the outer cracks have been plotted against frequency for different length of the outer crack ($0.5,\ 0, 3,\ 0.1$).

For the coupling effect of elastic media and magnetic field, we consider the values of magnetoelastic parameters as follows

$$\mathcal{H}_{(z)} = 5\ ,\ \epsilon_0 = 0.3 \text{ and } \mu_0 = 1.7.$$

and the graphs are represented by solid line. If we take $\mathcal{H}_{(z)} = 0$, then the effect of magnetic field is neglected and the corresponding graphs are represented by dash line.
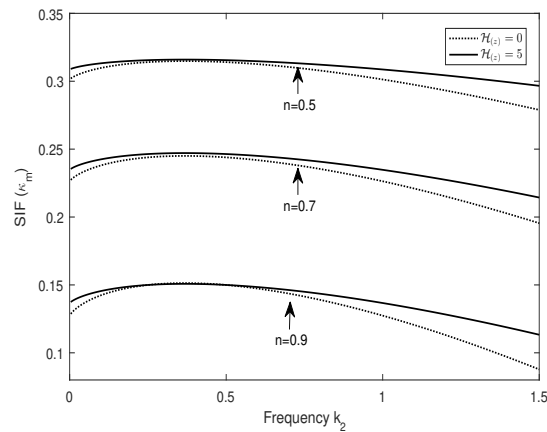
Fig.4.2.2 SIF κ_m **against dimensionless frequency** (k_2).
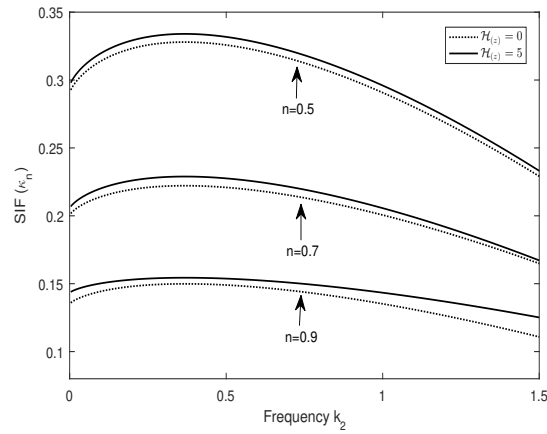
Fig.4.2.3 SIF κ_n against dimensionless frequency (k_2).
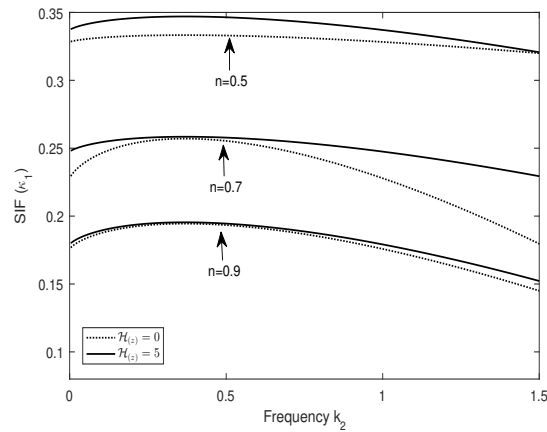
Fig.4.2.4 SIF κ_1 against dimensionless frequency (k_2).

From the figures it is observed that SIFs κ_m, κ_n and κ_1 decreases when frequency and the length of the outer cracks increases due to the presence and absence of magnetic field. Also, SIFs are slightly higher when the isotropic elastic material is influenced by an external magnetic field for normally incidence wave. Therefore the impact of magnetic field in not much functional.
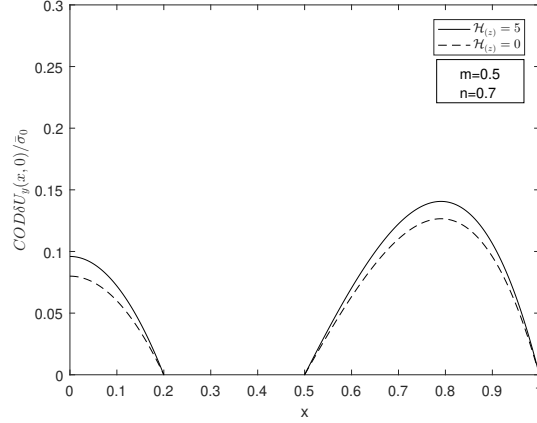
Fig.4.2.5: COD against crack width (x).

In Fig.4.2.5, COD has been plotted against crack width for the presence and absence of magnetic field. It is seen from the graph Fig.4.2.5 that COD at the middle position of the crack is higher and COD at the vicinity of the cracks is zero which means fracture toughness at the middle position of cracks is high.

■ Special Case

When $m \to 0$, then the considered elastodynamics problem converted to a problem containing two cracks occupying the region $n \leq |x| \leq 1$, $y = 0$, $|z| < \infty$ and the corresponding stress intensity factors are found as

$$\kappa_n = \sqrt{\frac{1}{2n}} \sqrt{\frac{1}{1-n^2}} \left[1 - Nk_2^2 \log k_2\right] \left[\frac{E}{F} - n^2\right] + \mathcal{O}(k_2^2) \tag{4.2.61}$$

and

$$\kappa_1 = \sqrt{\frac{1}{2}} \sqrt{\frac{1}{1-n^2}} \left[1 - Nk_2^2 \log k_2\right] \left[\frac{E}{F} - 1\right] + \mathcal{O}(k_2^2), \tag{4.2.62}$$

where $N = \frac{4I}{\pi^2} \left[G_n^1 - \left(\frac{E}{F} - n^2\right) T_n^1\right]$.
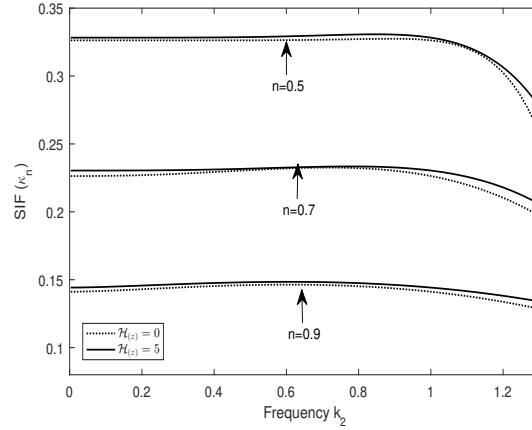
Fig.4.2.6: SIF κ_n against dimensionless frequency (k_2).
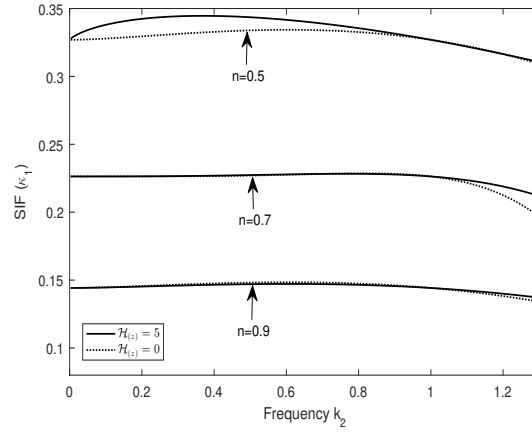
Fig.4.2.7: SIF κ_1 against dimensionless frequency (k_2).

Fig.4.2.6 and Fig.4.2.7 represent the graphs of SIF vs frequency for the problem of two cracks. Further if we neglect the effect of magnetic field by considering $\mathcal{H}_{(z)} = 0$ and take $n \to 0$, then three cracks coincide with one crack occupying $|x| \leq 1$ and the stress intensity factor is

$$\kappa_1 = -\sqrt{\frac{1}{2}} \left[1 - N k_2^2 \log k_2 \right] + \mathcal{O}(k_2^2), \tag{4.2.63}$$

where $N = \frac{2I}{\pi}$. This result is the approximation of SIF obtained by Mal (1970).

■ Conclusion

A semi-analytic viewpoint has been carried out in this monograph to exhibit the coupling effect of magnetic field and isotropic elastic media containing three cracks by determining the crack tip singular field. SIFs at the tip of interior and exterior cracks and COD have been computed using iterative scheme for low frequency distribution and presented graphically. The graphical results indicate that the impact of interaction between interior crack and exterior cracks is a composition of shielding and amplification or simply amplification depending on the length of the cracks, material specifications and induced magnetic field. Based on the graphs it can conclude that SIFs decreases smoothly and tend to zero when frequency and the length of the exterior cracks increases. Also, variations of SIFs due to the presence of magnetic field is slightly higher than those for the absence of magnetic field. So the impact of induced magnetic field in not much functional. Therefore, when the outer crack is smaller, there is a possibility of arrest the crack growth.

The stress-intensity factors and crack opening displacement evaluated herein determine the stress field near the crack tips which is useful in correlating and predicting fatigue crack growth rates and in deciding fracture strength of a cracked magnetize elastic solid.

Chapter-5

Torsional Impact on a Penny-shaped Crack at the Interface of a Semi-infinite Medium and a Magnetoelastic Layer

Chapter 5

Torsional Impact on a Penny-shaped Crack at the Interface of a Semi-infinite Medium and a Magnetoelastic Layer

■ Introduction

Composite materials have accomplished enormous growth since the introduction of the so-called "advanced composites" in recent times. This growth has mainly been the result of a desire to use high-strength, high stiffness and high-modulus but lightweight materials in airplane industry, national defense, automobile industry, and construction field etc. While developing new composite structure many calamities could occurred because of material deficiencies, poor design that lead to failure (for example cracks, inclusions) of the material. Also when an isolated impact load is applied on the crack surface normal to its plane, crack will become unstable and may grow catastrophically causing more fracture. Therefore, in order to overcome those difficulties, researchers provide some mechanical tools to serve engineering demands and to assess the material safety. This can be done by developing fracture criterion by estimating the singular stress field close to the crack tip which optimizes composite materials in terms of physical parameters, crack length etc. The problem of two

semi-infinite cracks occurring at the interface of two dissimilar elastic strips under inplane deformations was done by Wu et al. (2003). Ueda et al. (1984) investigated the influence of torsional shear on a circular-shaped crack situated in a semi infinite layer which is embedded between two different isotropic half spaces. Mal (1970) derived Fredhlom integral equation for the computation of stress intensity factor and displacement for the elastic problem of a circular crack in an isotropic elastic medium. Sih and Loeber (1968) analysed the singular stress field around the crack periphery of a penny shaped crack in an infinite elastic medium under torsional load acting on the crack surfaces. Embley and Sih (1971) analyzed the effect of impact response on a circular crack in an infinite elastic plane. Selvadurai (2002) made a detailed study of an axisymmetric problem of penny shaped crack located at a finite depth of an isotropic elastic half space where a rigid circular disc is affixed to the surface of the half-space. He reduced the physical phenomenon of crack-bonded disc problem to a pair of Fredholm integral equations and solved them numerically. The axially symmetric problem for a circular crack lying in an elastic layer bonded by two isotropic half spaces was investigated by Arin and Erdogan (1971), they developed the results for stress intensity factor in the close neighbourhood of crack tip at low frequencies. Shul and Lee (2001) considered a physical problem of inter-facial crack in a multilayered orthtropic half spaces under anti plane shear impact and solved the problem numerically using Gauss Lagueere and Gauss Legendre approaches. The problem of a penny shaped crack placed in the plane of the intersection of two bonded dissimilar materials under uniform pressure has been studied by Kassir and Bregman (1972) and they showed that the stresses around the crack periphery tend to infinity and have square root singularity.

Many natural and artificial materials such as Zinc, Cadmium, Cobalt having hexagonal symmetry exhibit transversely isotropy and this type of materials used as a coatings or main component to construct layered composite structure. In recent

times, researchers have established that magnetic effect can be used to develop sensor technology for process control, monitoring, safety measurement, security reasons etc. Whenever an external magnetic field is applied to an elastic material then the magnetization effect can change the physical nature of the material and the material can be considered as a magnetoelastic materials. Therefore, it is of need to inquire the propagation nature of torsional waves through such magneto elastic material containing cracks in order to upgrade their mechanical and magnetic performances. A number of eminent researchers have studied crack problems in magnetoelastic materials because of their applications in engineering construction, optics, acoustics, and geophysics. Considering an electrically conducted elastic solid under the influence of an electromagnetic field, De and Sengupta (1972) investigated the dilatational waves subjected to initial stress. A detail review of linear and nonlinear wave propagation in magnetized distorted solid was published by Maugin (1981). Chattopadhyay and Maugin (1985) analysed the diffraction effects of magnetoelastic shear wave by a crack in an infinite medium made of a material of different physical and electromagnetic properties. The coupling effects of magnetic field and transverse isotropy on the elastic waves in a perfectly conducting medium subjected to initial pressure was interpreted by Acharya et al. (2009). Panja and Mandal (2021b) discussed the elastic wave diffraction by a finite crack placed in an semi infinite magnetized elastic strip.

It has been reported that a number of problems have been studied regarding the propagation of elastic waves in a magnetizable elastic media. The problem concerning two dissimilar composite layer structure where one layer is affected by a magnetic field is still undiscovered. Therefore, the present article focuses to discuss the torsional impact on a circular-shaped crack situated at the interface of an isotropic half space and a transversely isotropic magnetoelastic layer. At first, the problem has

been converted to a pair of dual integral equation with the aid of boundary conditions and Hankel transform. A trial solution is considered to transform dual integral equations into a second kind Fredholm integral equation and solve it numerically by Fox and Goodwin (1953) method. Singular stress has been calculated around the crack surface employing Rice and Duong (1995) Laplace inversion formula and presented against time by means of graph for different parameters.

■ Problem Formulation

Assuming the impact response of torsional shear on a circular shaped crack of radius 'a' situated at the interface of a transversely isotropic magnetoelastic layer of thickness 'h' and a semi infinite isotropic half space regarding to the polar frame of reference (r, θ, z) (Fig.5. 1).

Here the load is applied in the tangential direction, so u_θ and $\tau_{\theta z}, \tau_{r\theta}$ are the only non vanishing displacement and stress components.
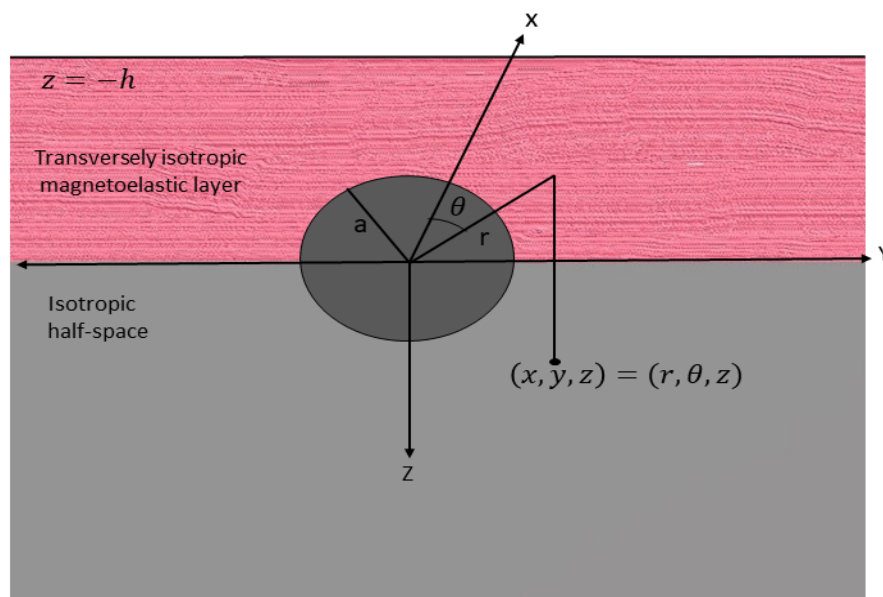
Fig.5.1   Geometry of the Problem.

Governing equation (Kumari et al. (2016)) for the transversely isotropic magnetoelastic layer is

$$\frac{\partial \tau_{r\theta}^I}{\partial r} + \frac{\partial \tau_{\theta z}^I}{\partial z} + 2\frac{\tau_{r\theta}^I}{r} + (J \times B)_\theta = \frac{1}{c_1^2}\frac{\partial^2 u_\theta^I}{\partial t^2}, \tag{5.1}$$

where $c_1^2 = \frac{\mu_1}{\rho_1}$ (μ_1, ρ_1 are the shear modulus and material density) and $(\vec{\mathcal{J}} \times \vec{\mathcal{B}})_\theta$ is the circumferential component of the Lourentz force ($\vec{\mathcal{J}}$ and $\vec{\mathcal{B}}$ represent the density of electric current and the magnetic flux density vector respectively) and the prefix $'I'$ represents the transversely isotropic magnetoelastic layer.

The expressions of stress components are followed by

$$\tau_{r\theta}^I = \frac{C_{11} - C_{12}}{2}\left(\frac{\partial u_\theta^I}{\partial r} - \frac{u_\theta^I}{r}\right) \tag{5.2}$$

and

$$\tau_{\theta z}^I = C_{44}\frac{\partial u_\theta^I}{\partial z}, \tag{5.3}$$

where C_{11}, C_{12}, and C_{44} are elastic moduli.

The Maxwell's equations for the considered electromagnetism are

$$div\ \vec{\mathcal{B}} = 0,\ \vec{\mathcal{J}} = \sigma\left(\vec{E} + \frac{\partial \vec{U}}{\partial t} \times \vec{\mathcal{B}}\right),$$

$$curl\ \vec{E} = -\frac{\partial \vec{\mathcal{B}}}{\partial t},\ curl\ \vec{\mathcal{H}} = \vec{\mathcal{J}},\ \vec{\mathcal{B}} = \mu_e\vec{\mathcal{H}}, \tag{5.4}$$

where $\vec{E}$ represents the strength of the electric field, $\vec{\mathcal{H}}$ represents the magnetic intensity, μ_e is the permeability for the magnetic effect and σ represents the conductivity of electric current. The Maxwell's stress tensor $\left(\tau_{ij}^0\right)^{M_r}$ for electromagnetism is followed by

$$\left(\tau_{ij}^0\right)^{M_r} = \mu_e(\mathcal{H}_{(1i)}\beta_j + \mathcal{H}_{(1j)}\beta_i - \mathcal{H}_{(1k)}\beta_k\delta_{ij}),$$

where $\vec{\mathcal{H}} = (\mathcal{H}_r,\ \mathcal{H}_\theta,\ \mathcal{H}_z)$ and $\vec{\beta} = (\beta_r,\ \beta_\theta,\ \beta_z),\ \beta_r, \beta_\theta$ and β_z indicate the disturbances induced by magnetic field.

Equations (5.4) can be simplified to the following form by neglecting the displacement current

$$\nabla^2 \vec{\mathcal{H}} = \mu_e \sigma \left[\frac{\partial \vec{\mathcal{H}}}{\partial t} - \vec{\nabla} \times \left(\frac{\partial \vec{U}}{\partial t} \times \vec{\mathcal{H}} \right) \right],$$ (5.5)

which can be written component wise as

$$\frac{\partial \mathcal{H}_r}{\partial t} = \frac{1}{\mu_e \sigma} \nabla^2 \mathcal{H}_r,$$

$$\frac{\partial \mathcal{H}_z}{\partial t} = \frac{1}{\mu_e \sigma} \nabla^2 \mathcal{H}_z,$$ (5.6)

$$\text{and} \quad \frac{\partial \mathcal{H}_\theta}{\partial t} = \frac{1}{\mu_e \sigma} \nabla^2 \mathcal{H}_\theta + \frac{\partial \left(\mathcal{H}_r \frac{\partial u_\theta^I}{\partial t} \right)}{\partial r} + \frac{\partial \left(\mathcal{H}_z \frac{\partial u_\theta^I}{\partial t} \right)}{\partial z}.$$

For absolutely electric conductivity ($\sigma \to \infty$), equations (5.6) are transformed to

$$\frac{\partial \mathcal{H}_r}{\partial t} = 0 = \frac{\partial \mathcal{H}_z}{\partial t}$$ (5.7)

and

$$\frac{\partial \mathcal{H}_\theta}{\partial t} = \frac{\partial \left(\mathcal{H}_r \frac{\partial u_\theta^I}{\partial t} \right)}{\partial r} + \frac{\partial \left(\mathcal{H}_z \frac{\partial u_\theta^I}{\partial t} \right)}{\partial z}$$ (5.8)

Equation (5.7) ensures that the magnetic disturbances in r-component and z- component of $\vec{\mathcal{H}}$ are zero, although the equation (5.8) exhibits that there exists magnetic disturbances in θ-component of $\vec{\mathcal{H}}$. Therefore we can consider the magnetic field as $(\mathcal{H}_{0r}, \ \mathcal{H}_{0\theta} + \beta_0, \ \mathcal{H}_{0z})$, where β_0 is the small disturbances of magnetic perturbation in circumferential direction and $\vec{\mathcal{H}}_0 = (\mathcal{H}_{0r}, \ \mathcal{H}_{0\theta}, \ \mathcal{H}_{0z})$ is the initial magnetic field. Let the magnetic field and wave oscillation intersect at an angle ψ and let $\mathcal{H}_0 = | \vec{\mathcal{H}}_0 |$. So, initially magnetic field can be taken as $\vec{\mathcal{H}}_0 = (0, \ 0, \ \mathcal{H}_0 \sin \psi)$ and finally we have

$$\vec{\mathcal{H}} = (0, \ \beta_0, \ \mathcal{H}_0 \sin \psi).$$ (5.9)

Substituting the value of $\vec{\mathcal{H}}$ in (5.8), we derive

$$\frac{\partial \beta_0}{\partial t} = \frac{\partial \left(\mathcal{H}_0 \sin \psi \frac{\partial u_\theta^I}{\partial t} \right)}{\partial z}.$$ (5.10)

Integrating equation (5.10) with respect to the variable t, we derive

$$\beta_0 = \mathcal{H}_0 \sin \psi \frac{\partial u_\theta^I}{\partial z}.$$ (5.11)

Using the relation $\vec{\nabla}(\frac{\mathcal{H}^2}{2}) = (\vec{\mathcal{H}}.\vec{\nabla})\vec{\mathcal{H}} - \text{curl } \vec{\mathcal{H}} \times \vec{\mathcal{H}}$ from vector calculus, we obtain

$$(\vec{J} \times \vec{B})_\theta = \mu_e \left(\mathcal{H}_0 \right)^2 \sin^2 \psi \frac{\partial^2 u_\theta^I}{\partial z^2}.$$ (5.12)

Using (5.2), (5.3), (5.12), equation (5.1) can be rewritten as

$$a_1 \left(\frac{\partial^2 u_\theta^I}{\partial r^2} + \frac{1}{r} \frac{\partial u_\theta^I}{\partial r} - \frac{u_\theta^I}{r^2} \right) + a_2 \frac{\partial^2 u_\theta^I}{\partial z^2} = \frac{1}{c_1^2} \frac{\partial^2 u_\theta^I}{\partial t^2},$$ (5.13)

where $a_1 = \frac{C_{11}-C_{12}}{2}$ and $a_2 = C_{44} + \left(\mathcal{H}_0 \right)^2 \sin^2 \psi$.

Also, the governing equation for the considered isotropic half space is

$$\frac{\partial \tau_{r\theta}^{II}}{\partial r} + \frac{\partial \tau_{\theta z}^{II}}{\partial z} + 2 \frac{\tau_{r\theta}^{II}}{r} = \frac{1}{c_2^2} \frac{\partial^2 u_\theta^{II}}{\partial t^2},$$ (5.14)

where $c_2 = \left(\frac{\mu_2}{\rho_2} \right)^{\frac{1}{2}}$ represents the wave velocity and ρ_2, μ_2 are the density and shear modulus of the material and the prefix $'II'$ represents the isotropic half space.

The non vanishing stress components for the case of isotropic medium are

$$\tau_{r\theta}^{II} = \mu_2 \left(\frac{\partial u_\theta^{II}}{\partial r} - \frac{u_\theta^{II}}{r} \right)$$ (5.15)

and

$$\tau_{\theta z}^{II} = \mu_2 \frac{\partial u_\theta^{II}}{\partial z}.$$ (5.16)

Using (5.15) and (5.16), equation (5.14) reduces to

$$\frac{\partial^2 u_\theta^{II}}{\partial r^2} + \frac{1}{r}\frac{\partial u_\theta^{II}}{\partial r} - \frac{u_\theta^{II}}{r^2} + \frac{\partial^2 u_\theta^{II}}{\partial z^2} = \frac{1}{c_2^2}\frac{\partial^2 u_\theta^{II}}{\partial t^2}. \tag{5.17}$$

The equations (5.13) and (5.17) are to be solved with the help the following boundary conditions

$$\tau_{\theta z}^I(r,0,t) = \tau_{\theta z}^{II}(r,0,t) = \tau_0\left(\frac{r}{a}\right)H(t), \ r \in [0,\ a], \tag{5.18}$$

$$u_\theta^I(r,0,t) = u_\theta^{II}(r,0,t), \ r \in (a,\ \infty), \tag{5.19}$$

$$\tau_{\theta z}^I(r,-h,t) = 0, \tag{5.20}$$

where $H(t)$ represents the Heaviside step function and τ_0 is the loading constant. The time variable will be transformed to a parameter by adopting the Laplace Transform, defined as

$$L^*(p) = \int_0^\infty l(t)e^{-pt}dt$$

and

$$l(t) = \frac{1}{2\pi i}\int_{B_r} L^*(p)e^{pt}dp,$$

where B_r represents the Bromwich curve of integration.

After the application of the Laplace Transform, equations (5.13) and (5.17) become

$$a_1\left(\frac{\partial^2 u_\theta^{*I}}{\partial r^2} + \frac{1}{r}\frac{\partial u_\theta^{*I}}{\partial r} - \frac{u_\theta^{*I}}{r^2}\right) + a_2\frac{\partial^2 u_\theta^{*I}}{\partial z^2} = \frac{p^2}{c_1^2}u_\theta^{*I}, \tag{5.21}$$

$$\frac{\partial^2 u_\theta^{*II}}{\partial r^2} + \frac{1}{r}\frac{\partial u_\theta^{*II}}{\partial r} - \frac{u_\theta^{*II}}{r^2} + \frac{\partial^2 u_\theta^{*II}}{\partial z^2} = \frac{p^2}{c_2^2}u_\theta^{*II} \tag{5.22}$$

and the boundary conditions (5.18) - (5.20) are expressed as

$$\tau_{\theta z}^{*\,I}(r,0,p) = \tau_{\theta z}^{*\,II}(r,0,p) = \frac{\tau_0}{p}\left(\frac{r}{a}\right), \ r \in [0,\ a], \tag{5.23}$$

$$u_\theta^{*I}(r,0,p) = u_\theta^{*II}(r,0,p), \ r \in (a, \ \infty), \tag{5.24}$$

$$\tau_{\theta z}^{*\,I}(r,-h,p) = 0. \tag{5.25}$$

Using Hankel Transform, the solutions of the equation (5.21) and (5.22) are computed as follows

$$u_\theta^{*I}(r,z,p) = \int_0^\infty \left[M_1(s,p)e^{-\gamma_1 z} + M_2(s,p)e^{\gamma_1 z} \right] J_1(sr)ds \tag{5.26}$$

and

$$u_\theta^{*II}(r,z,p) = \int_0^\infty M_3(s,p)e^{-\gamma_2 z} J_1(sr)ds, \tag{5.27}$$

where $\gamma_1^2 = (\frac{a_1}{a_2}s^2 + k_1^2)$, $\gamma_2^2 = (s^2 + k_2^2)$, $k_1^2 = \frac{\rho_1^2 p^2}{a_2}$, and $k_2^2 = \frac{\rho_2^2 p^2}{\mu_2}$.

M_1, M_2 and M_3 in equation (5.26) and (5.27) are unknown functions and we have to evaluate them with the help of boundary conditions and integral transform.

Using equations (5.26) and (5.27), stress components $\tau_{\theta z}^{*\,I}$ and $\tau_{\theta z}^{*\,II}$ are found as

$$\tau_{\theta z}^{*\,I} = -C_{44} \int_0^\infty \left[\gamma_1 M_1(s,p)e^{-\gamma_1 z} - \gamma_1 M_2(s,p)e^{\gamma_1 z} \right] J_1(sr)ds \tag{5.28}$$

and

$$\tau_{\theta z}^{*\,II} = -\mu_2 \int_0^\infty \gamma_2 M_3(s,p)e^{-\gamma_2 z} J_1(sr)ds. \tag{5.29}$$

Using (5.28) and (5.29), the boundary conditions (5.23) and (5.25) yield

$$C_{44} \int_0^\infty \gamma_1[M_1(s,p) - M_2(s,p)]J_1(s,r)ds = \mu_2 \int_0^\infty \gamma_2 M_3(s,p)J_1(s,r)ds \tag{5.30}$$

and

$$\int_0^\infty [M_1(s,p)e^{\gamma_1 h} - M_2(s,p)e^{-\gamma_1 h}]J_1(sr)ds = 0. \tag{5.31}$$

Hankel inversion on (5.30) and (5.31) leads to following two equations

$$\gamma_1[M_1(s,p) - M_2(s,p)] = \frac{\mu_2}{C_{44}}\gamma_2 M_3(s,p), \tag{5.32}$$

$$M_1(s,p)e^{\gamma_1 h} - M_2(s,p)e^{-\gamma_1 h} = 0. \tag{5.33}$$

After solving (5.32) and (5.33), we can express $M_2(s,p)$ and $M_3(s,p)$ in terms of $M_1(s,p)$ as

$$M_2(s,p) = M_1(s,p)e^{2\gamma_1 h} \tag{5.34}$$

and

$$M_3(s,p) = \frac{C_{44}\gamma_1(1 - e^{2\gamma_1 h})}{\mu_2 \gamma_2} M_1(s,p). \tag{5.35}$$

■ Derivation of the Integral Equation

Using $(5.26) - (5.29)$, the boundary conditions (5.23) and (5.24) yield the following dual integral equations

$$\int_0^\infty \alpha^*(s,p)J_1(sr)ds = 0, \qquad r \in (a, \infty), \tag{5.36}$$

$$\int_0^\infty sP^*(s,p)\alpha^*(s,p)J_1(sr)ds = -\frac{\tau_0 r}{p\mu_1 a}, \qquad r \in [0, a], \tag{5.37}$$

with

$$\alpha^*(s,p) = \frac{\mu_2\gamma_2\left(1 + e^{2\gamma_1 h}\right) - C_{44}\gamma_1\left(1 - e^{2\gamma_1 h}\right)}{\mu_2\gamma_2}F_1(s,p) \tag{5.38}$$

and

$$P^*(s,p) = \frac{\mu_2\gamma_1\gamma_2\left(1 - e^{2\gamma_1 h}\right)}{s\left\{\mu_2\gamma_2\left(1 + e^{2\gamma_1 h}\right) - C_{44}\gamma_1\left(1 - e^{2\gamma_1 h}\right)\right\}}. \tag{5.39}$$

∎ **Solution of the Dual Integral Equations**

Dual integral equations (5.36) and (5.37) can be transformed to a Fredholm integral equation by taking the form of $\alpha^*(s, p)$ as

$$\alpha^*(s, p) = \frac{4\tau_0 a^{\frac{5}{2}}}{3C_{44}p\sqrt{2\pi}}\sqrt{s}\int_0^1 \sqrt{\zeta}\Gamma_I^*(\zeta, p)J_{3/2}(sa\zeta)d\zeta, \tag{5.40}$$

where $\Gamma_I^*(\zeta, p)$ is a desired function to be found.

With the aid of the formula

$$J_{3/2}(z_1\zeta) = -\frac{\sqrt{\zeta}}{z_1}\frac{d}{d\zeta}\{\zeta^{-1/2}J_{1/2}(z_1\zeta)\}, \tag{5.41}$$

$\alpha^*(s, p)$ can be rewritten as

$$\alpha^*\left(\frac{z_1}{a}, p\right) = \frac{4\tau_0 a^2}{3C_{44}p\sqrt{2\pi z_1}}\left[\int_0^\infty \Gamma_{II}^*(\zeta, p)J_{1/2}(z_1\zeta)d\zeta - \Gamma_I^*(1, p)J_{1/2}(z_1)\right] \tag{5.42}$$

where, $z_1 = sa$ and

$$\Gamma_{II}^*(\zeta, p) = \frac{1}{\sqrt{\zeta}}\frac{d}{d\zeta}\{\zeta\Gamma_I^*(\zeta, p)\}. \tag{5.43}$$

The expression $P^*(\frac{z_1}{a}, p) \to -\frac{1}{Q_1^*}$ whenever $z_1 \to \infty$, therefore $1 + Q_1^*P^*(\frac{z_1}{a}, p) \to 0$ as $z_1 \to \infty$ where, $\frac{1}{Q_1^*} = \frac{\mu_2\sqrt{a_2} + C_{44}\sqrt{a_1}}{a_1^{\frac{3}{2}}}$.

Now, equation (5.37) can be transformed in terms of dimensionless quantities as follows

$$\int_0^\infty z_1\alpha^*\left(\frac{z_1}{a}, p\right)J_1(\beta z_1)dz_1 = \frac{\tau_0 a^2 Q_1^*\beta}{\rho C_{44}} + \int_0^\infty z_1\left[1 + Q_1^*P^*\left(\frac{z_1}{a}, p\right)\right]$$
$$\alpha^*\left(\frac{z_1}{a}, p\right)J_1(\beta z_1)dz_1 \left(\beta = \frac{r}{a} \text{ and } \beta \in (1, \infty)\right). \tag{5.44}$$

Using equation (5.42) and the result (Abramowitz et al. (1988))

$$\int_0^\infty x^{1/2}J_1(cx)J_{1/2}(dx)dx = 0, \qquad 0 < c < d,$$

$$= \sqrt{\frac{2}{\pi}} \frac{\sqrt{d}}{c\sqrt{d^2 - c^2}}, \quad 0 < d < c,$$

equation (5.44) reduces to

$$\sqrt{\frac{2}{\pi}} \int_0^\beta \frac{\sqrt{\zeta}}{\sqrt{\beta^2 - \zeta^2}} \Gamma_{II}^*(\zeta, p) d\zeta = \frac{3\pi Q_1^* \beta^2}{4} + \frac{\pi}{2}\beta \int_0^1 \sqrt{\zeta} \Gamma_I^*(\zeta, p) d\zeta$$

$$\int_0^\infty z_1^{3/2} N_1\left(\frac{z_1}{a}, p\right) J_1(\beta z_1) J_{3/2}(\zeta z_1) dz_1 = E^*(\beta), \tag{5.45}$$

where, $N_1(\frac{z_1}{a}, p) = 1 + Q_1^* P^*(\frac{z_1}{a}, p)$ and

$$E^*(\beta) = \frac{3\pi Q_1^* \beta^2}{4} + \sqrt{\frac{\pi}{2}}\beta \int_0^1 \sqrt{\zeta} \Gamma_I^*(\zeta, p) d\zeta \int_0^\infty z_1^{3/2}$$

$$N_1\left(\frac{z_1}{a}, p\right) J_1(\beta z_1) J_{3/2}(\zeta z_1) dz_1. \tag{5.46}$$

Employing Abel's integral technique to (5.45), we get

$$\sqrt{\zeta} \Gamma_{II}^*(\zeta, p) = \frac{2}{\pi} \frac{d}{d\zeta} \int_0^\zeta \frac{\beta E^*(\beta)}{\sqrt{\zeta^2 - \beta^2}} d\beta.$$

Now, using equation (5.43), equation (5.45) can be expressed as

$$\zeta \Gamma_{II}^*(\zeta, p) = \frac{2}{\pi} \int_0^\zeta \frac{\beta^2}{\sqrt{\zeta^2 - \beta^2}} \left[\frac{3Q_1^* \pi \beta}{4} + \sqrt{\pi/2} \int_0^1 \sqrt{u} \Gamma_I^*(u, p) du \right.$$

$$\left. \int_0^\infty z_1^{3/2} N_1(\frac{z_1}{a}, p) J_1(\beta z_1) J_{3/2}(u z_1) dz_1 \right] d\beta. \tag{5.47}$$

Using the result Abramowitz et al. (1988)

$$\int_0^1 x^{m+1}(1 - x^2)^n J_l(bx) dx = 2^n \Gamma(n+1) l^{-(n+1)} J_{l+n+1}(b)$$

and Hankel transformation, the equation (5.47) can be converted into a Fredholm type integral equation as follows

$$\Gamma_I^*(\zeta, p) = \int_0^1 \Gamma_I^*(u, p) L^*(\zeta, u, p) du + Q_1^* \zeta^2, \tag{5.48}$$

where

$$L^*(\zeta, u, p) = a^2 \sqrt{\zeta u} \int_0^\infty s \left[1 + Q_1^* P^*(s,p) \right] J_{3/2}(us) J_{3/2}(\zeta s) ds. \tag{5.49}$$

∎ Quantity of Physical Interest

To compute stress intensity factor $K_1(t)$ in terms of t from $K_1^*(p)$, the local coordinates r^1 and θ^1 are used to get the expansion of stress components in the matrix layer for small values of β. The relations between (r^1, θ^1) and (r, θ) are as follows

$$r = a + r^1 \cos\theta^1, \; z = r^1 \sin\theta^1 \tag{5.50}$$

where $\frac{x}{r} = \cos\theta$ and $\frac{y}{r} = \sin\theta$.

From equation (5.28), we get

$$\tau_{\theta z}^{* \, I}(r, 0, p) = -C_{44} \int_0^\infty s P^*(s,p) \alpha^*(s,p) J_1(sr) ds, \qquad r \in (a, \; \infty). \tag{5.51}$$

For very large values of s, $P^*(s,p) \to -1/Q_1^*$ and equation (5.51) transformed to

$$\tau_{\theta z}^{* \, I}(r, 0, p) = \frac{4\tau_0}{3\sqrt{2\pi p} \, Q_1^*} \left[\int_0^1 \frac{\sqrt{\zeta} \Gamma_{II}^*(\zeta, p)}{\beta\sqrt{\beta - \zeta}\sqrt{\beta + \zeta}} d\zeta - \sqrt{\frac{2}{\pi}} \frac{\Gamma_1^*(1,p)}{\beta\sqrt{\beta - 1}\sqrt{\beta + 1}} \right]$$
$$= -\frac{4\tau_0}{3\pi p Q_1^*} \frac{\Gamma_I^*(1,p)}{\beta\sqrt{\beta - 1}\sqrt{\beta + 1}} + O(1), \qquad \beta \in (1, \; \infty). \tag{5.52}$$

Putting $r = a\beta$, equation (5.52) changes in the following form

$$\tau_{\theta z}^{* \, I}(r, 0, p) = -\frac{4a^2 \tau_0}{3\pi p Q_1^*} \frac{\Gamma_I^*(1,p)}{(r\sqrt{r - a}\sqrt{r + a})}, \qquad r \in (a, \; \infty). \tag{5.53}$$

SIF in the Laplacian domain is defined as

$$K_1^*(p) = \lim_{r \to a} \left| \tau_{\theta z}^{* \, I}(r, 0, p) \right| (r - a)^{\frac{1}{2}}. \tag{5.54}$$

With the help of (5.53), equation (5.54) becomes

$$K_1^*(p) = \frac{2\sqrt{2a}\tau_0}{3\pi Q_1^*} \frac{\Gamma_I^*(1,p)}{p}.$$
(5.55)

Applying Laplace inversion approach, the stress intensity factor $K_1(t)$ is computed as

$$K_1(t) = \frac{2\sqrt{2a}\tau_0}{3\pi Q_1^*} \frac{1}{2\pi i} \int_{B_r} \frac{\Gamma_I^*(1,p)}{p} e^{pt} dp$$
(5.56)

where, B_r represents the Bromwich curve.

■ Numerical Outcomes and Discussions

To determine the value of $\Gamma_I^*(1,p)$ from the equation (5.48), the numerical approach by Fox and Goodwin (1953) is adopted. The Zakian's Algorithm (Rice and Duong (1995)) has been utilized for Laplace inversion of equation (5.55) to compute the stress intensity factor $K_1(t)$ in the neighbourhood of the tip of the crack for different composite elastic materials and the considered magnetic field. For the transversely isotropic layer affected by magnetic field we consider the the values of parameters (Sharma et al. (2015)) as

$$\mathcal{H}_0 = 5, \ \psi = 10, \ C_{11} = 18.78 \times 10^{10} Kgm^{-1}s^{-2}, \ C_{44} = 5.06 \times 10^{10} Kgm^{-1}s^{-2},$$
$$C_{12} = 8.76 \times 10^{10} Kgm^{-1}s^{-2}.$$

For the Isotropic elastic half space we consider the values of elastic constants as

$$\rho_2 = 2700 Kgm^{-3}, \ \lambda_2 = 51.08 GPa, \ \mu_2 = 26.32 GPa.$$

For different values of the radius of crack 'a', thickness of the strip 'h' and magnetic intensity $\mathcal{H}_0$, the time dependent SIF $\frac{K_1(t)}{\tau_0}$ has been plotted with respect to t.
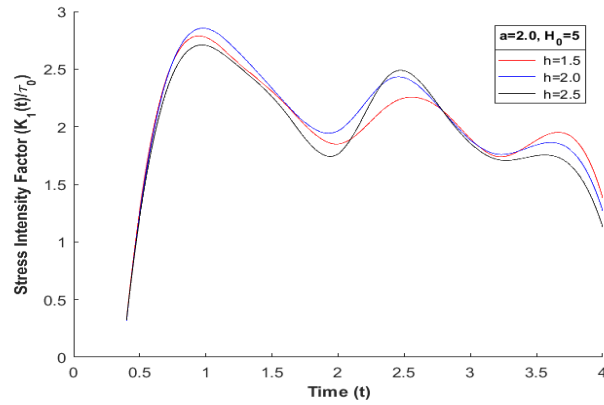
Fig.5.2 **Stress Intensity Factor $\left(\frac{K_1(t)}{\tau_0}\right)$ against time**
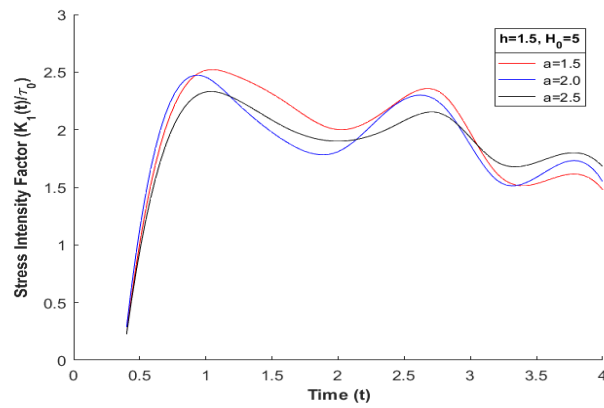
Fig.5.3 **Stress Intensity Factor $\left(\frac{K_1(t)}{\tau_0}\right)$ against time**
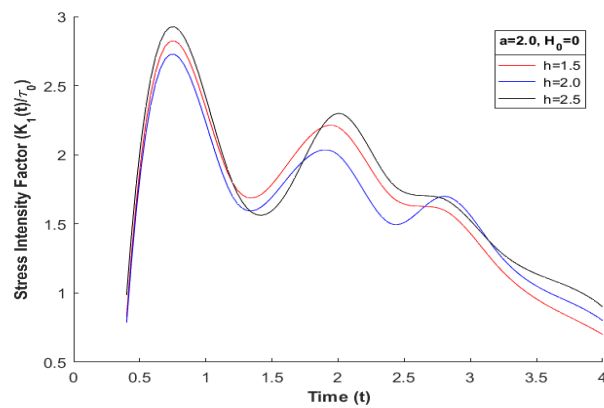
Fig.5.4 **Stress Intensity Factor $\left(\frac{K_1(t)}{\tau_0}\right)$ against time**
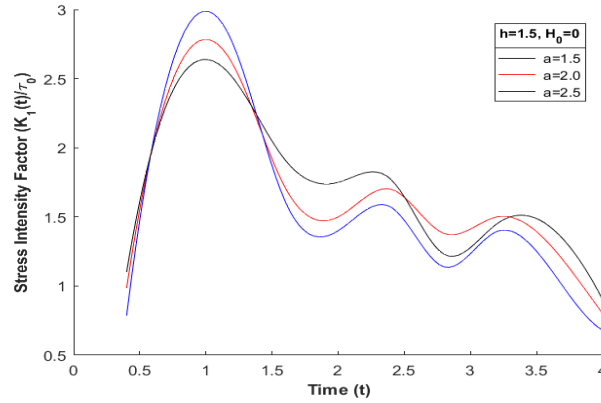
Fig.5.5 **Stress Intensity Factor** $(\frac{K_1(t)}{\tau_0})$ **against time**

In Fig.5.2, SIF is plotted with respect to time for magnetic intensity $\mathcal{H}_0 = 5$, crack radius $a = 2.0$ and three different values of the width of the layer $h = 1.5, \ 2.0, \ 2.5$ and in Fig.5.4, the same has been plotted against time by neglecting the magnetic field ($\mathcal{H}_0 = 0$).

In Fig.5.3, SIF is plotted with respect to time for magnetic intensity $\mathcal{H}_0 = 5$, width of the layer $h = 1.5$ and three different values of the radius $a = 1.5, \ 2.0, \ 2.5$ and in Fig.5.5, the same thing has been plotted against time by neglecting the magnetic field ($\mathcal{H}_0 = 0$).

In all of the figures (Fig.5.2, Fig.5.3, Fig.5.4, Fig.5.5) it can be seen that initially the SIF increases and reaches maximum value near $t = 1$ that means the fracture toughness is high at that point and then follows wave like nature and finally tends to zero. The wave-like nature can result in changes in crack propagation rates and direction, which can affect the overall structural integrity of the material. Therefore, the material may experience increased crack growth rates, resulting in a reduction of its fatigue life.

Fig.5.2 and Fig.5.3 demonstrate that the stress intensity factor (SIF) is elevated when the magnetic field is present, as compared to its absence. Furthermore, it is observed that the SIF takes a longer time to reach zero in the presence of a magnetic

field. Therefore magnetic field generates residual stresses in the material, which increase the stress concentration at the crack tip.

■ Validation and Comparison of Results

If we consider $\frac{C_{11}-C_{12}}{2} = C_{44} = \mu_1$ and $\mathcal{H}_0 = 0$, then the transversely isotropic magnetoelasic layer will be converted to a homogeneous isotropic half space and we have following expressions

$a_1 = a_2 = \mu_1$, $Q_1^* = \frac{\mu_1}{\mu_1+\mu_2}$ and

$$K_1(t) = \frac{2\mu_1\sqrt{2a}\tau_0}{3\pi(\mu_1+\mu_2)} \frac{1}{2\pi i} \int_{B_r} \frac{\Gamma_I^*(1,p)}{p} e^{pt} dp. \tag{5.57}$$

To plot the graph we consider the the values of parameters for two different isotropic mediums as $\mu_1 = 28$, $\rho_1 = 2.7$, $\mu_2 = 39$, $\rho_2 = 8.4$.
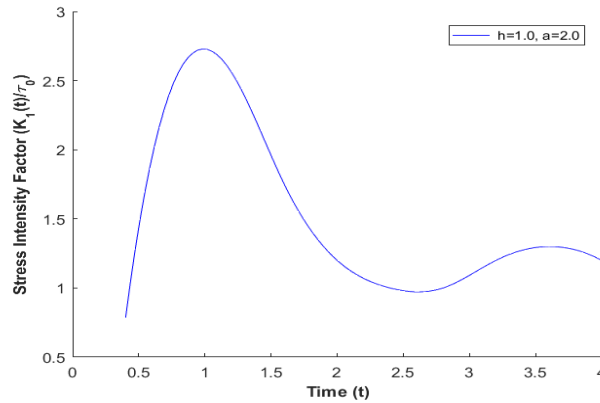
Fig.5.6   Stress Intensity Factor ($\frac{K_1(t)}{\tau_0}$) against time.

Fig.5.6 represents the graph of SIF verses time and the graph is similar in nature with graphs presented by Ueda et al. (1984).

◾ Conclusions

An analytical approach has been conducted to examine the fracture behaviour of a composite structure that contains a crack situated at the interface between a semi infinite isotropic half space and a magnetoelastic layer. The singular stress has been computed near the crack periphery. The figures indicate that the stress intensity factor increases first and reaches its highest value then it decreases and finally tends to zero. Highest value of SIF at $t = 1$ is an indication that the material is under severe stress and is at risk of failure. Also, in the presence of magnetic field SIF is elevated due to the residual stress generated by magnetostriction of the structure that increases the likelihood of crack growth or failure of the material. The elevated SIF indicates that the energy required to propagate a crack is higher in the presence of a magnetic field, which means that the material may be more prone to cracking or failure when subjected to a mechanical load. Therefore, it is important to reduce the stress intensity factor by redesigning the structure or by applying stress-relieving techniques such as heat treatment or shot peening or by magnetic field shielding to improve the material's resistance to cracking.

Bibliography

Bibliography

Abramowitz, M. and Stegun, I. A. (1965). Handbook of mathematical functions with formulas, graphs, and mathematical table. *US Department of Commerce; National Bureau of Standards Applied Mathematics Series*, 55.

Abramowitz, M., Stegun, I. A., and Romer, R. H. (1988). Handbook of mathematical functions with formulas, graphs, and mathematical tables.

Acharya, D., Roy, I., and Sengupta, S. (2009). Effect of magnetic field and initial stress on the propagation of interface waves in transversely isotropic perfectly conducting media. *Acta mechanica*, 202(1):35–45.

Anderson, T. L. (2017). *Fracture mechanics: fundamentals and applications*. CRC press.

Arin, K. and Erdogan, F. (1971). Penny-shaped crack in an elastic layer bonded to dissimilar half spaces. *International Journal of Engineering Science*, 9(2):213–232.

Baghdasaryan, G. Y. (2023). Stress–strain state of a magnetoelastic ferromagnetic plane with a crack under the action of a magnetic field. In *Solid Mechanics, Theory of Elasticity and Creep*, pages 77–92. Springer.

Barenblatt, G. (1959). Concerning equilibrium cracks forming during brittle fracture. the stability of isolated cracks. relationships with energetic theories. *Journal of Applied Mathematics and Mechanics*, 23(5):1273–1282.

Basak, P. and Mandal, S. (2019). Semi-infinite moving crack between two bonded dissimilar isotropic strips. *Meccanica*, 54:855–871.

Basu, S. (2014). Torsional oscillation of rigid disk at the bi-material interface. *A A*, 1:2.

Basu, S. and Mandal, S. (2016). Impact of torsional load on a penny-shaped crack in an elastic layer sandwiched between two elastic half-space. *International Journal of Applied and Computational Mathematics*, 2:533–543.

CE, I. (1913). Stresses in a plate due to the presence of cracks and sharp corners. *Trans Inst Naval Archit*, 55:219–241.

Chadwick, P. (1957). Elastic wave propagation in a magnetic field. In *Proceedings of the 9th international congress of applied mechanics*, volume 7, pages 143–153.

Chattopadhyay, A. and Choudhury, S. (1995). Magnetoelastic shear waves in an infinite self-reinforced plate. *International Journal for Numerical and Analytical Methods in Geomechanics*, 19(4):289–304.

Chattopadhyay, A. and Maugin, G. (1985). Diffraction of magnetoelastic shear waves by a rigid strip. *The Journal of the Acoustical Society of America*, 78(1):217–222.

Chattopadhyay, A. and Singh, A. K. (2014). Propagation of a crack due to magnetoelastic shear waves in a self-reinforced medium. *Journal of Vibration and Control*, 20(3):406–420.

Chen, S. L., Chen, L., and Pan, E. (2007). Vertical vibration of a flexible plate with rigid core on saturated ground. *Journal of engineering mechanics*, 133(3):326–337.

Cochard, A. and Rice, J. R. (1997). A spectral method for numerical elastodynamic fracture analysis without spatial replication of the rupture event. *Journal of the Mechanics and Physics of Solids*, 45(8):1393–1418.

Cooke, J. (1970). The solution of some integral equations and their connection with dual integral equations and series. *Glasgow Mathematical Journal*, 11(1):9–20.

Das, S., Chakraborty, S., Srikanth, N., and Gupta, M. (2008). Symmetric edge cracks in an orthotropic strip under normal loading. *International journal of fracture*, 153(1):77–84.

De, S. and Sengupta, P. (1972). Magneto-elastic waves and disturbances in initially stressed conducting media. *pure and applied geophysics*, 93:41–54.

Dhaliwal, R., Singh, B., Vrbik, J., and Khan, S. (1984). Torsional oscillations by an annular disk on a semi-infinite cylinder embedded in an elastic half-space. *Engineering fracture mechanics*, 20(5-6):719–727.

Ding, S.-H. and Li, X. (2014). The collinear crack problem for an orthotropic functionally graded coating–substrate structure. *Archive of Applied Mechanics*, 84:291–307.

Do, D. D., Maneval, J. E., and Rice, R. G. (2023). *Applied mathematics and modeling for chemical engineers*. John Wiley & Sons.

Dunkin, J. W. and Eringen, A. C. (1963). On the propagation of waves in an electro-magnetic elastic solid. *International Journal of Engineering Science*, 1(4):461–495.

Embley, G. and Sih, G. (1971). Response of a penny-shaped crack to impact waves. In *Proceedings of the 12th Midwestern Mechanics Conference*, volume 6, pages 473–487.

Erdogan, F. (1969). Approximate solutions of systems of singular integral equations. *SIAM Journal on Applied Mathematics*, 17(6):1041–1059.

Eskandari-Ghadi, M., Mirzapour, A., and Ardeshir-Behrestaghi, A. (2011). Rocking vibration of a rigid circular disc in a transversely isotropic full-space. *International*

Journal for Numerical and Analytical Methods in Geomechanics, 35(14):1587–1603.

Fox, L. and Goodwin, E. (1953). The numerical solution of non-singular linear integral equations. *Philosophical Transactions of the Royal Society of London. Series A, Mathematical and Physical Sciences*, 245(902):501–534.

Freund, L. (1972). The motion of a crack in an elastic solid subjected to general loading. In *Proceedings of an international conference on Dynamic Crack Propagation*, pages 553–562. Springer.

Freund, L. B. (1998). *Dynamic fracture mechanics*. Cambridge university press.

Geubelle, P. H. and Rice, J. R. (1995). A spectral method for three-dimensional elastodynamic fracture problems. *Journal of the Mechanics and Physics of Solids*, 43(11):1791–1824.

Graham, M. D. (1995). Applied mathematics and modeling for chemical engineers: By rg rice and dd do. wiley, new york.

Griffith (1920). The phenomena of rupture and flow in solids. *Philosophical transactions of the royal society of london. Series A, containing papers of a mathematical or physical character*.

Guo, L.-C., Wu, L.-Z., and Zeng, T. (2005). The dynamic response of an edge crack in a functionally graded orthotropic strip. *Mechanics Research Communications*, 32(4):385–400.

Hopkinson, B. (1913). Discussion to paper by ce inglis. *Trans. Inst. Nav. Arch*, 55:232–234.

Hu, K. and Chen, Z. (2015). Mode-i crack in a magnetoelectroelastic layer sandwiched by two elastic half-planes. *Engineering Fracture Mechanics*, 134:79–94.

Huang, G. Y., Wang, Y. S., and Yu, S. W. (2005). Stress concentration at a penny-shaped crack in a nonhomogeneous medium under torsion. *Acta mechanica*, 180:107–115.

Irwin, G. R. (1957). Analysis of stresses and strains near the end of a crack traversing a plate.

Itou, S. (1980). Diffraction of an antiplane shear wave by two coplanar griffith cracks in an infinite elastic medium. *International Journal of Solids and Structures*, 16(12):1147–1153.

Itou, S. (1989). Dynamic stress intensity factors around two coplanar griffith cracks in an orthotropic layer sandwiched between two elastic half-planes. *Engineering fracture mechanics*, 34(5-6):1085–1095.

Itou, S. (2001). Stress intensity factors around a crack in a nonhomogeneous interfacial layer between two dissimilar elastic half-planes. *International Journal of Fracture*, 110:123–135.

Itou, S. (2004). Stress intensity factors around a moving griffith crack in a nonhomogeneous layer between two dissimilar elastic half-planes. *Acta mechanica*, 167(3):213–232.

Jain, D. and Kanwal, R. (1972). Diffraction of elastic waves by two coplanar griffith cracks in an infinite elastic medium. *International Journal of Solids and Structures*, 8(7):961–975.

Jian-ke, D., Ya-peng, S., and Bo, G. (2004). Scattering of anti-plane shear waves by a single crack in an unbounded trasversely isotropic electro-magneto-elastic medium. *Applied Mathematics and Mechanics*, 25:1344–1353.

Kadıoğˇlu, F. S. (2005). Axisymmetric crack problem for a hollow cylinder imbedded in a dissimilar medium. *International journal of engineering science*, 43(8-9):617–638.

Kaliski, S. and Petykiewicz, J. (1959). Equation of motion coupled with the field of temperature in a magnetic field involving mechanical and electrical relaxation for anisotropic bodies. In *Proceedings Vibration Problems*, volume 4.

Karan, S., Basu, S., and Mandal, S. (2018). Impact of a torsional load on a penny-shaped crack sandwiched between two elastic layers embedded in an elastic medium. *Acta Mechanica*, 229:1759–1772.

Kassir, M. and Bregman, A. (1972). The stress-intensity factor for a penny-shaped crack between two dissimilar materials. *J. Appl. Mech.*

Knauss, W. G. (1966). Stresses in an infinite strip containing a semi-infinite crack. *J. Appl. Mech.*

Knopoff, L. (1955). The interaction between elastic wave motions and a magnetic field in electrical conductors. *Journal of Geophysical Research*, 60(4):441–456.

Kolosov, G. (1909). On an application of complex function theory to a plane problem of the mathematical theory of elasticity. *Yuriev, Russia*.

Kostrov, B. (1966). Unsteady propagation of longitudinal shear cracks. *Journal of applied Mathematics and Mechanics*, 30(6):1241–1248.

Kumari, P., Modi, C., and Sharma, V. (2016). Torsional waves in a magneto-viscoelastic layer over an inhomogeneous substratum. *The European Physical Journal Plus*, 131:1–11.

Lee, H.-K. and Tran, X. (2010). On stress analysis for a penny-shaped crack interacting with inclusions and voids. *International journal of solids and structures*, 47(5):549–558.

Lekhnitskii (1963). Theory of elasticity of an anisotropic elastic body.

Li, P.-D., Li, X.-Y., Kang, G.-Z., and Müller, R. (2017). Three-dimensional fundamental solution of a penny-shaped crack in an infinite thermo-magneto-electroelastic medium with transverse isotropy. *International Journal of Mechanical Sciences*, 130:203–220.

Li, R. and Kardomateas, G. (2006). The mode iii interface crack in piezo-electro-magneto-elastic dissimilar bimaterials. *J. Appl. Mech.*

Li, X.-F. (2005). Two perfectly-bonded dissimilar orthotropic strips with an interfacial crack normal to the boundaries. *Applied Mathematics and Computation*, 163(2):961–975.

Love, A. E. H. (1927). *A treatise on the mathematical theory of elasticity*. University press.

Lowengrub, M. and Srivastava, K. (1968). On two coplanar griffith cracks in an infinite elastic medium. *International Journal of Engineering Science*, 6(6):359–362.

Madani, F. and Kebli, B. (2019). Axisymmetric torsion of an elastic layer sandwiched between two elastic half-spaces with two interfaced cracks. *Studia Geotechnica et Mechanica*, 41(2):57–66.

Mal, A. K. (1970). Interaction of elastic waves with a griffith crack. *International Journal of Engineering Science*, 8(9):763–776.

Mandal, P. (2020). Moving semi-infinite mode-iii crack inside the semi-infinite elastic media. *Journal of Theoretical and Applied Mechanics*, 58.

Mandal, S. and Ghosh, M. (1994). Interaction of elastic waves with a periodic array of coplanar griffith cracks in an orthotropic elastic medium. *International journal of engineering science*, 32(1):167–178.

Manna, S., Gosh, S., and Mandal, S. (2003). Torsional oscillation of rigid disk in an infinite cylinder. *Journal of Technical Physics*, 44(4):341–347.

Marin, M. (1997a). On the domain of influence in thermoelasticity of bodies with voids. *Archivum Mathematicum*, 33(3):301–308.

Marin, M. (1997b). An uniqueness result for body with voids in linear thermoelasticity. *Rendiconti di Matematica*, 17(7):103–113.

Matbuly, M. (2008). Analysis of mode iii crack perpendicular to the interface between two dissimilar strips. *Acta Mechanica Sinica*, 24:433–438.

Matysiak, S. and Pauk, V. (2003). Edge crack in an elastic layer resting on winkler foundation. *Engineering fracture mechanics*, 70(17):2353–2361.

Maugin, G. A. (1981). Wave motion in magnetizable deformable solids. *International Journal of Engineering Science*, 19(3):321–388.

Mishra, P., Das, S., and Gupta, M. (2016). Interaction between interfacial and sub-interfacial cracks in a composite media–revisited. *ZAMM-Journal of Applied Mathematics and Mechanics/Zeitschrift für Angewandte Mathematik und Mechanik*, 96(9):1129–1136.

Morrissey, J. W. and Rice, J. R. (1998). Crack front waves. *Journal of the Mechanics and Physics of Solids*, 46(3):467–487.

Munshi, N. and Mandal, S. C. (2006). Diffraction of p-waves by edge crack in an infinitely long elastic strip. *JSME International Journal Series A Solid Mechanics and Material Engineering*, 49(1):116–122.

Nagai, M., Ikeda, T., and Miyazaki, N. (2007). Stress intensity factor analysis of a three-dimensional interface crack between dissimilar anisotropic materials. *Engineering Fracture Mechanics*, 74(16):2481–2497.

Naskar, S., Jana, S., and Mandal, S. (2023). P-wave diffraction by three collinear griffith cracks under normal impact. *Waves in Random and Complex Media*, 33(1):62–77.

Naskar, S. and Mandal, S. (2018). P-wave diffraction by a crack under impact load. *International Journal of Applied and Computational Mathematics*, 4(4):1–9.

Nilsson, F. (1972). Dynamic stress-intensity factors for finite strip problems. *International Journal of Fracture Mechanics*, 8(4):403–411.

Noble, B. (1963). The solution of bessel function dual integral equations by a multiplying-factor method. In *Mathematical Proceedings of the Cambridge Philosophical Society*, volume 59, pages 351–362. Cambridge University Press.

Orowan, E. (1949). Fracture and strength of solids. *Reports on progress in physics*, 12(1):185.

Panja, S. K. and Mandal, S. (2021a). Impact response of a finite crack in the presence of magnetic field. *Engineering Fracture Mechanics*, 253:107851.

Panja, S. K. and Mandal, S. (2021b). Interaction of magnetoelastic shear waves with a griffith crack in an infinite strip. *Journal of Engineering Mathematics*, 126:1–11.

Panja, S. K. and Mandal, S. (2022). Propagation of love wave in multilayered viscoelastic orthotropic medium with initial stress. *Waves in Random and Complex Media*, 32(2):1000–1017.

Panja, S. K. and Mandal, S. C. (2021c). Interaction of a finite crack with shear waves in an infinite magnetoelastic medium. *Applied and Computational Mechanics*, 15(1):45–56.

Pramanik, R., Pal, S., and Ghosh, M. (1999). Shear wave interaction with a pair of rigid strips embedded in an infinitely long elastic strip. *Journal of Technical Physics*, 40(1):31–44.

Rice, J. R. (1968). A path independent integral and the approximate analysis of strain concentration by notches and cracks.

Rice, R. G. and Do, D. D. (2012). *Applied mathematics and modeling for chemical engineers*. John Wiley & Sons.

Rice, R. G. and Duong, D. D. (1995). Applied mathematics and modeling for chemical engineers, new york: John willey & sons.

Robertson, I. A. (1967). Diffraction of a plane longitudinal wave by a penny-shaped crack. In *Mathematical Proceedings of the Cambridge Philosophical Society*, volume 63, pages 229–238. Cambridge University Press.

Sarkar, J., Mandal, S., and Ghosh, M. (1994). Interaction of elastic waves with two coplanar griffith cracks in an orthotropic medium. *Engineering fracture mechanics*, 49(3):411–423.

Sarkar, J., Mandal, S., and Ghosh, M. (1995). Diffraction of elastic waves by three coplanar griffith cracks in an orthotropic medium. *International journal of engineering science*, 33(2):163–177.

Selvadurai, A. (2002). Mechanics of a rigid circular disc bonded to a cracked elastic half-space. *International journal of solids and structures*, 39(24):6035–6053.

Sharma, N., Kumar, R., and Lata, P. (2015). Disturbance due to inclined load in transversely isotropic thermoelastic medium with two temperatures and without energy dissipation. *Mater. Phys. Mech*, 22(2):107–117.

Shindo, Y. (1977). The linear magnetoelastic problem for a soft ferromagnetic elastic solid with a finite crack. *J. Appl. Mech.*

Shindo, Y. (1980). Singular stresses in a soft ferromagnetic elastic solid with two coplanar griffith cracks. *International Journal of Solids and Structures*, 16(6):537–543.

Shindo, Y., Nozaki, H., and Higaki, H. (1986). Impact response of a finite crack in an orthotropic strip. *Acta Mechanica*, 62(1):87–104.

Shul, C. W. and Lee, K. Y. (2001). Dynamic response of subsurface interface crack in multi-layered orthotropic half-space under anti-plane shear impact loading. *International journal of solids and structures*, 38(20):3563–3574.

Sih, G. and Chen, E. (1977). Elastodynamic crack problems in mechanics of fracture. *Noordhoff, Leyden.*

Sih, G. and Loeber, J. (1968). Torsional vibration of an elastic solid containing a penny-shaped crack. *The Journal of the Acoustical Society of America*, 44(5):1237–1245.

Sih, G. C. (1968). Some elastodynamic problems of cracks. *International Journal of Fracture Mechanics*, 4(1):51–68.

Sih, G. C. and Chen, E. (2012). *Cracks in composite materials: a compilation of stress solutions for composite systems with cracks*, volume 6. Springer Science & Business Media.

Singh, A., Das, S., and Craciun, E. (2020). Study of semi-infinite crack in a sandwiched orthotropic strip. *Journal of Mechanics*, 36(2):149–158.

Sneddon, I. N. (1961). Crack problems in the mathematical theory of elasticity. Technical report, North carolina state university Raleigh.

Srivastava, K., Gupta, O., and Palaiya, R. (1981). Interaction of elastic waves with a griffith crack situated in an infinitely long strip. *ZAMM-Journal of Applied Mathematics and Mechanics/Zeitschrift für Angewandte Mathematik und Mechanik*, 61(11):583–587.

Srivastava, K. and Lowengrub, M. (1970). Finite hilbert transform technique for triple integral equations with trigonometric kernels. *Proceedings of the Royal Society of Edinburgh Section A: Mathematics*, 68(4):309–321.

Ueda, S., Shindo, Y., and Atsumi, A. (1984). Torsional impact response of a penny-shaped interface crack in a layered composite. *Engineering fracture mechanics*, 19(6):1095–1104.

Verma, P. (1986). Magnetoelastic shear waves in self-reinforced bodies. *International journal of engineering science*, 24(7):1067–1073.

Wang, B., Han, J., and Du, S. (2000). Fracture mechanics for multilayers with penny-shaped cracks subjected to dynamic torsional loading. *International journal of engineering science*, 38(8):893–901.

Wang, C., Rubio-Gonzalez, C., and Mason, J. (2001). The dynamic stress intensity factor for a semi-infinite crack in orthotropic materials with concentrated shear impact loads. *International journal of solids and structures*, 38(8):1265–1280.

Weibull, W. (1939). Astatistical theory ofthe strength of materials. *Proc. Royal 4cademy Engrg Science*, 15.

Willis, J. and Movchan, N. (2007). Crack front waves in an anisotropic medium. *Wave motion*, 44(6):458–471.

Wu, J.-J. (2006). Nanoadhesion between a rigid circular disc and an infinite elastic surface. *International journal of solids and structures*, 43(6):1624–1637.

Wu, X.-F., Dzenis, Y. A., and Fan, T.-Y. (2003). Two semi-infinite interfacial cracks between two bonded dissimilar elastic strips. *International Journal of Engineering Science*, 41(15):1699–1710.

Yih-Hsing, P. and Chau-Shioung, Y. (1973). A linear theory for soft ferromagnetic elastic solids. *International Journal of Engineering Science*, 11(4):415–436.

List of Publications and Communicated Papers

Published Paper

1. "Shear Wave Interaction of Two Collinear Finite Cracks in an Infinite Magnetoelastic Orthotropic Media." International Journal of Applied and Computational Mathematics 8.5 (2022): 243. *https://doi.org/10.1007/s40819-022-01451-w*

List of Communicated Papers

1. Impact Response on a Crack at Asymmetric Position in an Elastic Strip. (Journal of Dynamic Behavior of Materials)

2. Dispersion of Longitudinal Waves by Three Co-linear Griffith Cracks in a Magnetized Elastic Medium. (European Journal of Computational Mechanics)

3. Torsional Impact on a Penny-shaped Crack at the Interface of a Semi-infinite Medium and a Magnetoelastic Layer. (Waves in Random and Complex Media)

ORIGINAL PAPER

Check for
updates

Shear Wave Interaction of Two Collinear Finite Cracks in an Infinite Magnetoelastic Orthotropic Media

Ujjal Dhabal[1] · **S. K. Panja[1]** · **S. C. Mandal[1]**

Abstract

This monograph depicts the interaction of shear waves by two collinear finite cracks in an infinite magnetoelastic orthotropic medium. The physical phenomena of wave interaction have been formulated as a mixed boundary value problem (MBVP). The MBVP has been transformed into a pair of integral equations by introducing Abel's transform. The integral equations have been simplified by the perturbation method for low frequency with the help of the iterative expansion of Bessel's and Hankel's functions. The solution of the simplified integral equations has been derived by Hilbert transformation. The analytic expression of stress intensity factors (SIFs) and crack opening displacement (COD) have been computed and demonstrated graphically to exhibit the effect of magnetization on elastic media.

Keywords Finite crack · Magnetoelasticity · Shear wave · SIF · COD

Introduction

In solid structures, the distraught effect such as cracks or voids exist in elastic material which may be caused by material processing, manufacturing irregularities, uncertainties in loadings etc. The presence of such defects may significantly affect the stiffness and integrity of the material. To understand the failure mechanism of materials, analysis of stress and displacement field around the crack vicinities is necessary. The stress field helps to predict the expected crack growth rate, failure assessment, and fracture behavior of materials and the displacement field measures the fracture toughness of the material. Many elastic materials frequently exhibit strong orthotropy, so the study of wave propagation by cracks in an orthotropic medium is of great importance for fracture analysis of the material. Researcher Sneddon [1] discussed various crack problems in the mathematical theory of elasticity. Robertson [2] and

✉ Ujjal Dhabal
udvugm@gmail.com

S. K. Panja
panjasourav706@gmail.com

S. C. Mandal
scmandal.ju@gmail.com

[1] Department of Mathematics, Jadavpur University, Kolkata 700032, India

🌱 Springer

Mal [3] analyzed the diffraction of elastic waves by a circular crack in an infinitely extended elastic medium. Jain and Kanwal [4] derived singular stress for the problem of the dispersion of elastic waves by two Griffith cracks in an infinite isotropic medium. Interaction of antiplane transverse waves by the influence of two collinear finite cracks in an infinite medium has been investigated by Itou [5]. Itou [6] also solved the problem of two co-planar finite cracks in an orthotropic layer sandwich between two elastic half planes. Problems of the interaction of longitudinal waves by Griffith cracks in an orthotropic plate have been made by Mandal et al. ([7, 8]). Mechanics of magneto-elastic solids have gained significant interest in recent years due to the extensive application of magnetic reinforced materials in aerospace engineering, automotive industries, acoustics, optimal design, signal processing, etc. The coupled properties of magnetic field and elastic media offer great opportunities for engineers to create flawless constructions and devices that are capable of answering to internal and (or) external changes. Therefore, the study of magnetoelastic interaction is the focus of many research scholars in the field of fracture mechanics. The basic equations of magnetoelastic deformation theory have been derived by Dunkin and Eringen [9]. The theory of magnetoelasticity was developed by Knopff [10] and Chadwick [11] which was later extended by Kalish and Petykiewicz [12]. P. D. S. Verma [13] has investigated magneto-elastic transverse waves in a self reinforced elastic body. Chattopadhyay and Maugin [14] analyzed the magnetoelastic response of rigid strips in an infinite plate. The propagation of magnetoelastic transverse waves in an infinite self-reinforced lamina has been investigated by Chattophadhyay and Choudhury [15]. Marin ([16, 17]) investigated the influence of the thermoelastic effect on the body with voids. Acharya et al. [18] analyzed the dispersion of interface waves by the impact of magnetic field and initial tension in a transversely isotropic plate. The problems of the interaction of magneto-elastic shear waves by a Griffith crack have been solved by Panja and Mandal [19, 20].

Earth is believed to be surrounded by its own magnetic field dispersing from its center. Therefore, it is very much crucial to consider the effect of magnetic field in a cracked elastic media. To the best of the authors knowledge, no attempt has been made till now to analyse the stress field of an orthotropic elastic material containing two cracks by the impact of magnetic field. Therefore the goal of this paper is to illustrate the shear wave interaction by two collinear finite cracks in an infinite orthotropic plate under the influence of magnetic field. The physical phenomena of wave interaction are formulated as an MBVP. The MBVP has been transformed into a pair of integral equations by introducing Abel's transform, which has further been simplified by using the perturbation method for low frequency. The solution of the simplified integral equations has been derived by Hilbert transformation [21]. The analytic expansions of SIFs and COD have been computed and demonstrated graphically.

Problem Synthesis

Let us consider two Griffith cracks situated at $b \leq |X| \leq a$, $-\infty < Y < \infty$, $Z = 0$ referred to the rectangular frame of reference (X, Y, Z) in a magnetized orthotropic medium. Normalizing all the lengths with respect to a and putting $\frac{X}{a} = X_1$, $\frac{Y}{a} = Y_1$, $\frac{Z}{a} = Z_1$ and $\frac{b}{a} = h$, the new crack location becomes $h \leq |X_1| \leq 1$, $-\infty < Y_1 < \infty$, $Z_1 = 0$ (Fig. 1). Let us assume that there is a time harmonic anti-plane shear wave $h_0 e^{-i\omega t}$ in the positive direction of the Z-axis, where h_o is the antiplane shear traction acting on the crack periphery in the positive direction of the Z-axis. The periodic term $e^{-i\omega t}$ is present in all field variables which is being omitted throughout the analysis.

Fig. 1 Geometry of the problem
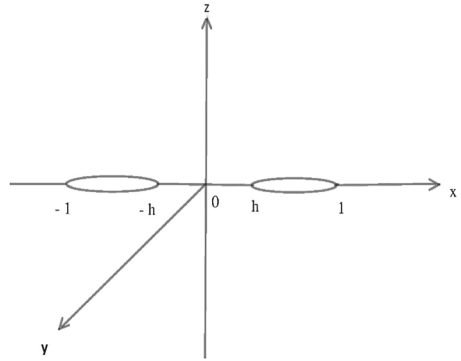
Since shear waves propagate in the Z direction, so the displacement field can be taken as $(0, \ U_y(x, z), \ 0)$. Field equation [22] for perfectly conducting orthotropic elastic media is

$$\frac{\partial \sigma_{xy}}{\partial x} + \frac{\partial \sigma_{yz}}{\partial z} + (\vec{\mathcal{J}} \times \vec{\mathcal{B}})_y + k^2 U_y = 0, \tag{1}$$

where $k^2 = \rho\omega^2$ and $(\vec{\mathcal{J}} \times \vec{\mathcal{B}})_y$ is the Y-component of the Lorentz force ($\vec{\mathcal{J}}$ and $\vec{\mathcal{B}}$ are the electric current density and the magnetic flux density vector).

The non vanishing stresses are given by

$$\begin{aligned} \sigma_{xy} &= 2C_{66}\mathcal{E}_{xy} = C_{66}\frac{\partial U_y}{\partial x} \\ \text{and } \sigma_{yz} &= 2C_{44}\mathcal{E}_{yz} = C_{44}\frac{\partial U_y}{\partial z}, \end{aligned} \tag{2}$$

where C_{66} and C_{44} are orthotropic elastic constants.

The well known Maxwell's equations ([19, 22]) for the governing electromagnetic field are

$$\text{div } \vec{\mathcal{B}} = 0, \ \text{curl } \vec{E} = -\frac{\partial \vec{\mathcal{B}}}{\partial t}, \ \vec{\mathcal{B}} = \mu_e \vec{\mathcal{H}},$$

$$\vec{\mathcal{J}} = \sigma\left(\vec{E} + \frac{\partial \vec{U}}{\partial t} \times \vec{\mathcal{B}}\right) \text{ and curl } \vec{\mathcal{H}} = \vec{\mathcal{J}}, \tag{3}$$

where $\vec{E}$ is the strength of the electric field, $\vec{\mathcal{H}}$ is the intensity of the magnetic field, μ_e is the induced permeability and σ is the conductivity coefficient of electric current.

The expression of Maxwell's stress tensor $\left(\sigma_{ij}^0\right)^{M_x}$ is given by

$$\left(\sigma_{ij}^0\right)^{M_x} = \mu_e(\mathcal{H}^{(1i)}\beta_j + \mathcal{H}^{(1j)}\beta_i - \mathcal{H}^{(1k)}\beta_k\delta_{ij}),$$

where $\vec{\mathcal{H}} = \left(\mathcal{H}^{(1x)}, \ \mathcal{H}^{(1y)}, \ \mathcal{H}^{(1z)}\right)$ and $\vec{\beta} = (\beta_x, \ \beta_y, \ \beta_z)$, β_x, β_y and β_z are the disturbances in the induced magnetic field.

Ignoring the displacement current vector, from Eq. (3) we derive

$$\nabla^2\vec{\mathcal{H}} = \mu_e\sigma\left[\frac{\partial \vec{\mathcal{H}}}{\partial t} - \vec{\nabla} \times \left(\frac{\partial \vec{U}}{\partial t} \times \vec{\mathcal{H}}\right)\right]. \tag{4}$$

From the vector Eq. (4), we get

$$\frac{\partial \mathcal{H}^{(1x)}}{\partial t} = \frac{1}{\mu_e \sigma} \nabla^2 \mathcal{H}^{(1x)},$$

$$\frac{\partial \mathcal{H}^{(1z)}}{\partial t} = \frac{1}{\mu_e \sigma} \nabla^2 \mathcal{H}^{(1z)}, \tag{5}$$

$$\frac{\partial \mathcal{H}^{(1y)}}{\partial t} = \frac{1}{\mu_e \sigma} \nabla^2 \mathcal{H}^{(1y)} + \frac{\partial \left(\mathcal{H}^{(1x)} \frac{\partial U_y}{\partial t} \right)}{\partial x} + \frac{\partial \left(\mathcal{H}^{(1z)} \frac{\partial U_y}{\partial t} \right)}{\partial z}.$$

For perfectly electric conductivity ($\sigma \to \infty$), Eq. (5) reduce to

$$\frac{\partial \mathcal{H}^{(1x)}}{\partial t} = 0 = \frac{\partial \mathcal{H}^{(1z)}}{\partial t} \tag{6}$$

and

$$\frac{\partial \mathcal{H}^{(1y)}}{\partial t} = \frac{\partial \left(\mathcal{H}^{(1x)} \frac{\partial U_y}{\partial t} \right)}{\partial x} + \frac{\partial \left(\mathcal{H}^{(1z)} \frac{\partial U_y}{\partial t} \right)}{\partial z}. \tag{7}$$

According to the Eq. (6), we can conclude that there is no magnetic perturbation in the X-component and Z-component of $\vec{\mathcal{H}}$, nevertheless the Eq. (7) shows that there may exist magnetic perturbation in the Y-component of $\vec{\mathcal{H}}$. Therefore we may consider the magnetic field as $\left(\mathcal{H}^{(0x)}, \ \mathcal{H}^{(0y)} + \beta_0, \ \mathcal{H}^{(0z)} \right)$, where β_0 is the small amount of magnetic perturbation in $\mathcal{H}^{(1y)}$ and $\left(\mathcal{H}^{(0x)}, \ \mathcal{H}^{(0y)}, \ \mathcal{H}^{(0z)} \right)$ are three components of magnetic field $\vec{\mathcal{H}}^0$ in the initial state.

Let ψ be the angle at which the wave crosses the magnetic field and let $\mathcal{H}^{(0)} = | \ \vec{\mathcal{H}}^0 \ |$, therefore the initial state of magnetic field can be expressed as $\vec{\mathcal{H}}^0 = (\mathcal{H}^{(0)} \cos \psi, \ 0, \ \mathcal{H}^{(0)} \sin \psi)$ and finally we have

$$\vec{\mathcal{H}} = \left(\mathcal{H}^{(0)} \cos \psi, \ \beta_0, \ \mathcal{H}^{(0)} \sin \psi \right). \tag{8}$$

Putting the value of $\vec{\mathcal{H}}$ in (7), we derive

$$\frac{\partial \beta_0}{\partial t} = \frac{\partial \left(\mathcal{H}^{(0)} \cos \psi \frac{\partial U_y}{\partial t} \right)}{\partial x} + \frac{\partial \left(\mathcal{H}^{(0)} \sin \psi \frac{\partial U_y}{\partial t} \right)}{\partial z}. \tag{9}$$

Integrating (9) with respect to t, we get

$$\beta_0 = \mathcal{H}^{(0)} \cos \psi \frac{\partial U_y}{\partial x} + \mathcal{H}^{(0)} \sin \psi \frac{\partial U_y}{\partial z}. \tag{10}$$

With the help of $\vec{\nabla}(\frac{\mathcal{H}^2}{2}) = (\vec{\mathcal{H}}.\vec{\nabla})\vec{\mathcal{H}} - (\text{curl } \vec{\mathcal{H}}) \times \vec{\mathcal{H}}$, we obtain

$$(\vec{\mathcal{J}} \times \vec{\mathcal{B}})_y = \mu_e \left[\left(\mathcal{H}^{(0)} \right)^2 \cos^2 \psi \frac{\partial^2 U_y}{\partial x^2} + \left(\mathcal{H}^{(0)} \right)^2 \sin 2\psi \frac{\partial^2 U_y}{\partial x \partial z} + \left(\mathcal{H}^{(0)} \right)^2 \sin^2 \psi \frac{\partial^2 U_y}{\partial z^2} \right]. \tag{11}$$

Utilizing (2) and (9), the Eq. (1) reduces to

$$A \frac{\partial^2 U_y}{\partial x^2} + B \frac{\partial^2 U_y}{\partial z^2} + C \frac{\partial^2 U_y}{\partial x \partial z} + k^2 U_y = 0, \tag{12}$$

where

$$A = C_{66} + \mu_e \left(\mathcal{H}^{(0)}\right)^2 \cos^2 \psi,$$

$$B = C_{44} + \mu_e \left(\mathcal{H}^{(0)}\right)^2 \sin^2 \psi, \tag{13}$$

$$C = \mu_e \left(\mathcal{H}^{(0)}\right)^2 \sin 2\psi.$$

Since the crack geometry is symmetric, we will consider the upper half plane ($Z \geq 0$) only. The Eq. (12) is to be solved subject to the following mixed boundary conditions

$$\sigma_{yz}(x, 0) = -h_0, \ h \leq |x| \leq 1 \tag{14}$$

and

$$U_y(x, 0) = 0, \ |x| > 1, |x| < h. \tag{15}$$

The general solution of the field Eq. (12) can be considered as

$$U_y(x, z) = \int_{-\infty}^{\infty} \mathcal{F}(\zeta) e^{-mz} e^{i\zeta x} d\zeta, \ z > 0, \tag{16}$$

where $m = \frac{i\zeta C}{2B} + \zeta \sqrt{\frac{1}{B}\left(A - \frac{k^2}{\zeta^2}\right) - \left(\frac{C}{2B}\right)^2}$ and $\mathcal{F}(\zeta)$ is an unknown function. The non vanishing stress component is found as

$$\sigma_{yz}(x, z) = -C_{44} \int_{-\infty}^{\infty} m\mathcal{F}(\zeta) e^{-mz} e^{i\zeta x} d\zeta. \tag{17}$$

The expression of $\mathcal{F}(\zeta)$ is to be calculated utilizing the boundary conditions.

Derivation and Solution of Integral Equations

Using the boundary conditions (14) and (15), we derive the following integral equations

$$\int_{-\infty}^{\infty} m\mathcal{F}(\zeta) e^{i\zeta x} d\zeta = \frac{h_0}{C_{44}}, \ h \leq |x| \leq 1 \tag{18}$$

and

$$\int_{-\infty}^{\infty} \mathcal{F}(\zeta) e^{i\zeta x} d\zeta = 0, \ |x| > 1, |x| < h. \tag{19}$$

Equation (18) can be expressed as

$$\int_{-\infty}^{\infty} \zeta \left[1 + R_1(\zeta)\right] \mathcal{F}(\zeta) e^{i\zeta x} d\zeta = \frac{h_0}{\vartheta C_{44}}, \ h \leq |x| \leq 1, \tag{20}$$

where

$$R_1(\zeta) = \frac{R(\zeta)}{\vartheta} - 1, \ R(\zeta) = \frac{iC + \sqrt{4B\left(A - \frac{k^2}{\zeta^2}\right) - C^2}}{2B}, \tag{21}$$

$$\vartheta = \frac{iC + \sqrt{4AB - C^2}}{2B} \text{ and } R_1(\zeta) \to 0 \text{ as } \zeta \to \infty.$$

For the solution of (18) and (19), we consider the following trial solution

$$\mathcal{F}(\zeta) = \frac{1}{\zeta} \int_h^1 \phi(q^2) \sin(\zeta q) dq, \tag{22}$$

where $\phi(q^2)$ is an unknown function which is to be computed with the help of integral transforms.

Using (22) and $\int_0^\infty \dfrac{\sin \zeta q \cos \zeta x}{\zeta} d\zeta = \begin{cases} \frac{\pi}{2}, & q > x \\ 0, & q < x \end{cases}$ in the Eq. (19), it is found that $\phi(q^2)$ satisfy the equation

$$\int_h^1 \phi(q^2) dq = 0. \tag{23}$$

Again using the result $\int_0^\infty \dfrac{\sin \zeta q \sin \zeta x}{\zeta} d\zeta = \dfrac{1}{2} \log \left| \dfrac{q+x}{q-x} \right|$ from [23] and the expression of $\mathcal{F}(\zeta)$ given by the Eq. (22), from the Eq. (20) we get

$$
\begin{aligned}
\frac{d}{dx} \int_h^1 \phi(q^2) \log \left| \frac{q+x}{q-x} \right| dq &= 2 \left[\frac{h_0}{\vartheta C_{44}} - \frac{d}{dx} \int_h^1 \phi(q^2) dq \right. \\
&\quad \left. \int_0^\infty \zeta R_1(\zeta) \frac{\sin \zeta q \sin \zeta x}{\zeta^2} d\zeta \right].
\end{aligned} \tag{24}
$$

Utilizing the result $\dfrac{\sin \zeta q \sin \zeta x}{\zeta^2} = \displaystyle\int_0^x \int_0^q \dfrac{mn J_0(\zeta m) J_0(\zeta n)}{\sqrt{x^2 - m^2}\sqrt{q^2 - n^2}} dm \, dn$, the Eq. (24) becomes

$$
\begin{aligned}
\int_h^1 \frac{q\phi(q^2)}{q^2 - x^2} dq &= \frac{h_0}{\vartheta C_{44}} - \frac{d}{dx} \int_h^1 \phi(q^2) dq \int_0^\infty \zeta R_1(\zeta) \\
&\quad \times \left[\int_0^x \int_0^q \frac{mn J_0(\zeta m) J_0(\zeta n)}{\sqrt{x^2 - m^2}\sqrt{q^2 - n^2}} dm \, dn \right] d\zeta \\
&= \frac{h_0}{\vartheta C_{44}} - \frac{d}{dx} \int_h^1 \phi(q^2) dq \int_0^x \int_0^q \frac{mn}{\sqrt{x^2 - m^2}\sqrt{q^2 - n^2}} dm \, dn \quad (25)\\
&\quad \times \int_0^\infty \zeta R_1(\zeta) J_0(\zeta m) J_0(\zeta n) d\zeta \\
&= \frac{h_0}{\vartheta C_{44}} - \frac{d}{dx} \int_h^1 \phi(q^2) dq \int_0^x \int_0^q \frac{mn\kappa(n,m)}{\sqrt{x^2 - m^2}\sqrt{q^2 - n^2}} dn \, dm,
\end{aligned}
$$

where

$$\kappa(n,m) = \int_0^\infty \zeta R_1(\zeta) J_0(\zeta m) J_0(\zeta n) d\zeta. \tag{26}$$

The integrand of the integration (26) has a branch point at $\zeta = \dfrac{k}{\sqrt{A}}$. Employing the contour integration technique [3], the improper integral (26) has therefore been converted to the following finite integral

$$\kappa(n,m) = -\frac{\iota k^2}{2} \int_0^{\frac{1}{\sqrt{A}}} \zeta \frac{\sqrt{4B\left(\frac{1}{\zeta^2} - A\right) + C^2}}{B\vartheta} J_0(k\zeta m) H_0^{(1)}(k\zeta n) d\zeta, \quad n > m. \tag{27}$$

With the help of the asymptotic series expansion of J_0 and $H_0^{(1)}$, $J_0(k\zeta m) H_0^{(1)}(k\zeta n)$ can be written as

$$J_0(k\zeta m) H_0^{(1)}(k\zeta n) = \frac{2\iota}{\pi} \log k + \left[1 + \frac{2\iota}{\pi}\left(m + \log\left(\frac{\zeta n}{2}\right)\right)\right]. \tag{28}$$

Using (28), (27) becomes

$$\kappa(n, m) = \frac{1}{\pi} k^2 G \log k + \mathcal{O}(k^2), \tag{29}$$

where

$$G = \int_0^{\frac{1}{\sqrt{A}}} \frac{\zeta}{B\vartheta} \sqrt{4B \left(\frac{1}{\zeta^2} - A \right) + C^2} d\zeta. \tag{30}$$

Let us take the iterative form of $\phi(q^2)$ as follows

$$\phi(q^2) = \phi_0(q^2) + k^2 \log k \phi_1(q^2) + \mathcal{O}(k^2). \tag{31}$$

Using the above expression of $\phi(q^2)$ and the expression of $\kappa(n, m)$ given by the Eq. (29) in (25) and equating the coefficients of similar powers of k from both sides of the reduced equation, we derive

$$\int_h^1 \frac{q\phi_0(q^2)}{q^2 - x^2} dq = \frac{h_0}{\vartheta C_{44}}, \ h \leq |x| \leq 1 \tag{32}$$

and

$$\int_h^1 \frac{q\phi_1(q^2)}{q^2 - x^2} dq = -\frac{G}{\pi} \int_h^1 q\phi_0(q^2) dq, \ h \leq |x| \leq 1. \tag{33}$$

Applying Hilbert transformation [21], from (32) we get

$$\phi_0(q^2) = \frac{2h_0}{\pi \vartheta C_{44}} \sqrt{\frac{q^2 - h^2}{1 - q^2}} + \frac{\alpha_1}{\sqrt{(q^2 - h^2)(1 - q^2)}} \tag{34}$$

and from (33) using (34) we have

$$\phi_1(q^2) = -G \left(\frac{h_0(1 - h^2)}{\pi^2 \vartheta C_{44}} + \frac{\alpha_1}{\pi} \right) \sqrt{\frac{q^2 - h^2}{1 - q^2}} + \frac{\alpha_2}{\sqrt{(q^2 - h^2)(1 - q^2)}}, \tag{35}$$

where α_1 and α_2 are constants to be computed with the help of the following conditions

$$\int_h^1 \phi_0(q^2) dq = 0 \tag{36}$$

and

$$\int_h^1 \phi_1(q^2) dq = 0. \tag{37}$$

Using (36) and (37) we found the values of α_1 and α_2 as follows

$$\alpha_1 = \frac{2h_0}{\pi \vartheta C_{44}} \frac{h^2 F_1 - E_1}{F_1} \tag{38}$$

and

$$\alpha_2 = \frac{Gh_0}{\pi^2 \vartheta C_{44}} \frac{(h^2 F_1 - 2E_1 + F_1)(E_1 - h^2 F_1)}{F_1^2}, \tag{39}$$

where $E_1 = E \left(\frac{\pi}{2}, \sqrt{1 - h^2} \right)$ and $F_1 = F \left(\frac{\pi}{2}, \sqrt{1 - h^2} \right)$.

Putting the values of the constants α_1 and α_2 given by the expressions (38) and (39) in (34) and (35), we obtain

$$\phi_0(q^2) = \frac{2h_0}{\pi \vartheta C_{44}} \frac{q^2 F_1 - E_1}{F_1 \sqrt{(q^2 - h^2)(1 - q^2)}} \tag{40}$$

and

$$\phi_1(q^2) = \frac{Gh_0}{\pi^2 \vartheta C_{44}} \frac{(h^2 F_1 - 2E_1 + F_1)(E_1 - h^2 F_1)}{F_1^2 \sqrt{(q^2 - h^2)(1 - q^2)}}. \tag{41}$$

Physical Parameters

Stress Intensity Factors

The non vanishing shear stress outside the crack can be calculated as

$$\sigma_{yz}(x,0) = \begin{cases} -h_0 \left[1 - \frac{G}{2\pi} k^2 \log(k) \left(1 - \frac{2E_1}{F_1} + h^2\right)\right] \left[1 - \frac{x^2 - \frac{E_1}{F_1}}{\sqrt{(1-x^2)(h^2-x^2)}}\right], & 0 \le x \le h \\ -h_0 \left[1 - \frac{G}{2\pi} k^2 \log(k) \left(1 - \frac{2E_1}{F_1} + h^2\right)\right] \left[1 + \frac{x^2 - \frac{E_1}{F_1}}{\sqrt{(x^2-1)(x^2-h^2)}}\right], & x > 1. \end{cases} \tag{42}$$

The SIFs K_h and K_1 at the crack vicinities ($x = h$ and $x = 1$) are computed as

$$K_h = \text{Lt}_{x \to h^-} \frac{(h-x)^{\frac{1}{2}} \sigma_{yz}(x,0)}{h_0}$$

$$= \frac{h^2 - \frac{E_1}{F_1}}{\sqrt{2h(1-h^2)}} \left[1 - \frac{G}{2\pi} k^2 \log k \left(1 - \frac{2E_1}{F_1} + h^2\right)\right] + \mathcal{O}(k^2) \tag{43}$$

and

$$K_1 = \text{Lt}_{x \to 1^+} \frac{(x-1)^{\frac{1}{2}} \sigma_{yz}(x,0)}{h_0}$$

$$= \frac{\frac{E_1}{F_1} - 1}{\sqrt{2(1-h^2)}} \left[1 - \frac{G}{2\pi} k^2 \log k \left(1 - \frac{2E_1}{F_1} + h^2\right)\right] + \mathcal{O}(k^2). \tag{44}$$

Crack Opening Displacement

Another physical quantity COD (Magnitude of the distance between two faces of the crack) is given by

$$\delta W(x) = | U_y(x, 0^+) - U_y(x, 0^-) | = 2 \int_x^1 \phi(q^2) dq$$

$$= \frac{4h_0}{\pi \vartheta C_{44}} \left[1 - \frac{G}{\pi} k^2 \log k \left(1 - \frac{2E_1}{F_1} + h^2\right)\right] \left[E_2 - \frac{E_1 F_2}{F_1}\right], \tag{45}$$

where $E_2 = E\left(\sin^{-1} \sqrt{\frac{1-x^2}{1-h^2}}, \sqrt{1-h^2}\right)$ and $F_2 = F\left(\sin^{-1} \sqrt{\frac{1-x^2}{1-h^2}}, \sqrt{1-h^2}\right)$.

Numerical and Graphical Demonstration

From the expansions of SIFs and COD given by (43), (44), and (45), it is obvious that these physical parameters depend on the values of material parameters and magnetic field. For orthotropic elastic medium, we take the following data [24]:

$$\rho = 2.7g/m^3, C_{44} = 5.3Gpa, C_{66} = 6.47GPa \text{ and } \psi = 10.$$
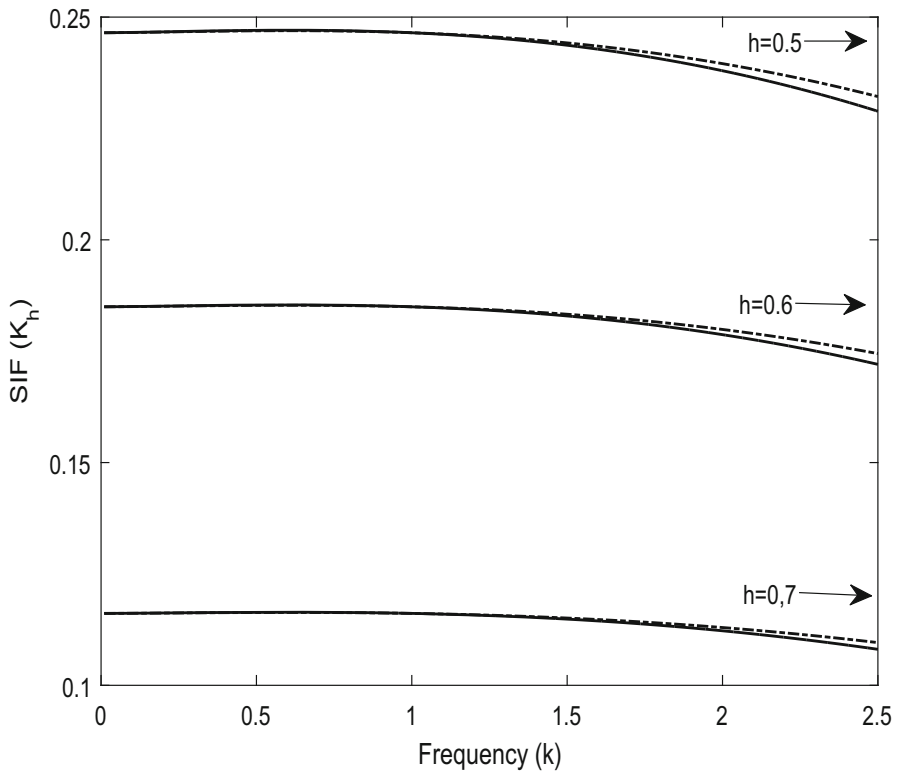
Fig. 2 SIF K_h with respect to frequency (k)

To display the impact of magnetic field, we plot the graphs of SIF versus frequency and COD vs crack width in the presence and absence of magnetic field. For the presence of magnetic field we consider

$$\epsilon_1 = \frac{\mu_e(\mathcal{H}^{(0)})^2}{C_{66}} = 0.30 \text{ and } \epsilon_2 = \frac{\mu_e(\mathcal{H}^{(0)})^2}{C_{44}} = 0.37$$

and the corresponding graph is represented by dash line. In the absence of magnetic field, we assume

$$\epsilon_1 = 0 \text{ and } \epsilon_2 = 0$$

and the graph is represented by solid line.

Firstly the variations of SIF K_h at the inner vicinity of the crack with $h = 0.5, 0.6, 0.7$ are shown in Fig. 2, secondly the variations of SIF at the outer vicinity of the crack are shown in Fig. 3. From both the graphs it is obvious that SIF has a slower decreasing rate up to a certain value of frequency and then the rate of decreasing become high and finally tends to zero. Comparing both the Figs. 2 and 3 it is identified that SIF at the outer tip has a higher rate of decreasing as compared to the SIF at the inner tip and SIFs decrease with the increase of the values of h. It has also been observed that the variations of SIFs are not significant in both the cases for the presence and absence of the magnetic field.

The nature of the Figs. 2 and 3 is quite same as the work discussed by Mandal and Sarkar [8] in the absence of magnetic field. Fig. 4 represents the graph of COD versus crack width
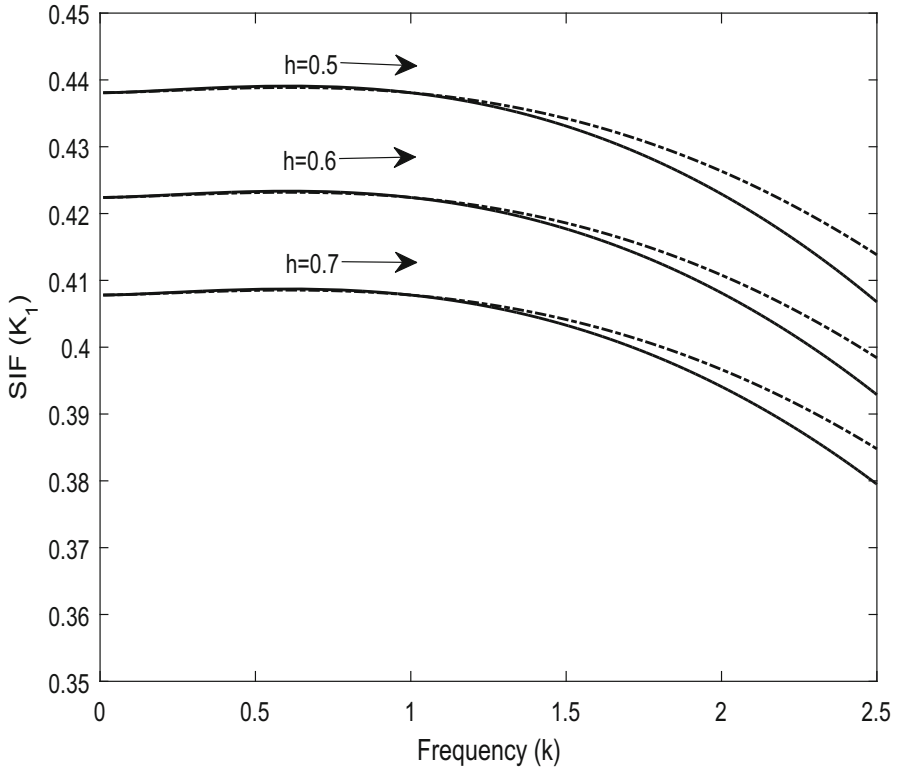
Fig. 3 SIF K_1 with respect to frequency (k)

due to the presence and absence of magnetic field. It is notable that the COD achieves its highest value at the point $x = 0.6$ and reaches zero at the tips of the cracks, so the fracture toughness is high at the point $x = 0.6$. Also, COD increases slightly in the presence of magnetic field as compared to the absence of magnetic field for low frequency k.

Comparison of Results

If we take $h = 0$, then two cracks coincide with a single crack and Fig. 5 represents the graph of SIF for the case of the single crack. If we take $C_{44} = C_{66} \to \mu$, then the medium will tend to be isotropic medium and we have the following expressions

$$A \to \mu + \mu_e (\mathcal{H}^{(0)})^2 \cos^2 \psi,$$
$$B \to \mu + \mu_e (\mathcal{H}^{(0)})^2 \sin^2 \psi,$$
$$C = \mu_e (\mathcal{H}^{(0)})^2 \sin 2\psi.$$

We obtain SIF in the following form

$$K_1 = \frac{\frac{E_1}{F_1} - 1}{\sqrt{2}} \left[1 - \frac{G}{2\pi} k^2 \log k \left(1 - \frac{2E_1}{F_1} \right) \right]. \tag{46}$$
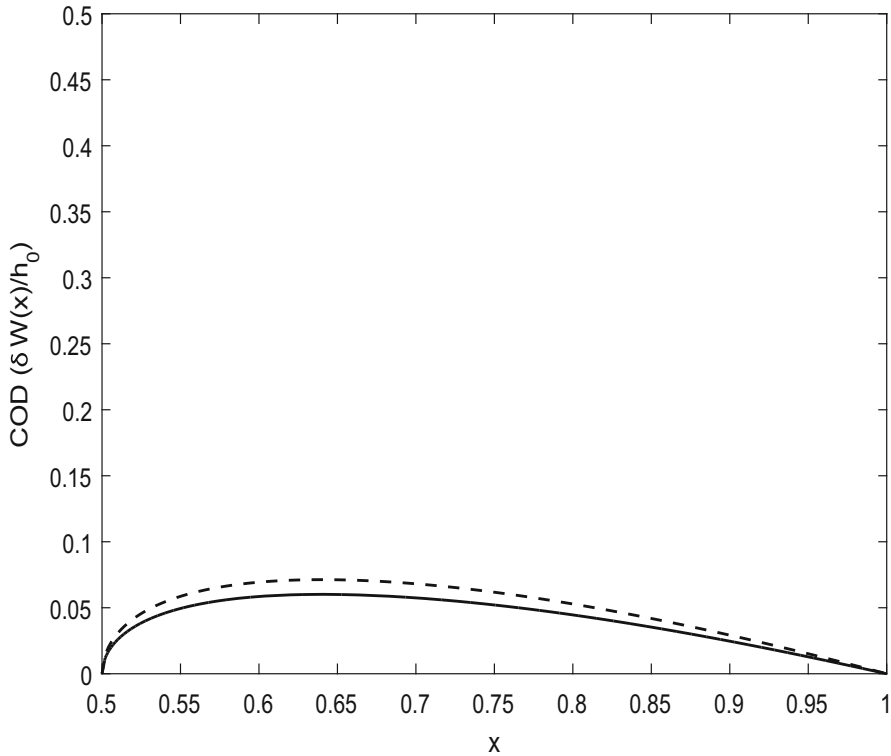
Fig. 4 COD $\frac{\delta W(x)}{h_0}$ against the crack width x

After some numerical manipulation, the approximate expression for SIF given by (46) has been derived from the expression of SIF given by Panja [19] et al. This comparison ensures the validation of the result obtained in this problem.

Conclusion

In the present study, the analytic expressions for SIFs and COD subjected to the magnetic field in an infinite elastic medium have been obtained. The main advantage of the analytical method is that we can plot physical parameters accurately while in the numerical procedure discrete data is used to plot the parameters. The variations of the mechanical parameters SIFs and COD due to the presence and absence of magnetic field have been represented graphically. Graphical results indicate that the propagation of the crack in the magneto-elastic medium is more pronounced compare to the non magneto-elastic medium for small frequency. Around the vicinity of the crack, state of stress is disruptive in nature and loses its toughness far away from the crack. From the figures it is seen that the SIFs and COD decrease as frequency and crack width increases which are physically persistent with the problem. It can be concluded that the material parameters play a major role in the case of fracture. Therefore we can settle the rate of crack growth and fracture toughness by considering a particular range of frequency and manipulating the magneto-elastic parameters. The analysis of the stress field

Fig. 5 SIF with respect to frequency (k)

in the proposed model may help to find the significant applications for the assessment of the toughness of structures containing multiple cracks. Furthermore, the proposed analysis may significantly give an idea to find the implementations of engineering materials which bring some extraordinary impact on the analysis and the design of sustainable materials used in high rising buildings, constructions of bridges, airplane industries, and many more identical types of reinforced constructions.

Appendix A

For large value of ζ, the non vanishing stress component at $z = 0$ is given by

$$
\begin{aligned}
\sigma_{yz}(x, 0) &= -\vartheta C_{44} \int_{-\infty}^{\infty} \zeta \mathcal{F}(\zeta) e^{i\zeta x} d\zeta = -\vartheta C_{44} \int_{h}^{1} \frac{q\phi(q^2)}{q^2 - x^2} dq \text{ [using (22)]} \\
&= -\vartheta C_{44} \int_{h}^{1} \frac{q\phi_0(q^2)}{q^2 - x^2} dq - \vartheta C_{44} k^2 log(k) \int_{h}^{1} \frac{q\phi_1(q^2)}{q^2 - x^2} dq.
\end{aligned}
\tag{47}
$$

Now, $\displaystyle\int_h^1 \frac{q\phi_0(q^2)}{q^2-x^2}dq = \frac{2h_0}{\pi\vartheta C_{44}}\int_h^1 \frac{qdq}{\sqrt{(q^2-h^2)(1-q^2)}} - \frac{2h_0}{\pi\vartheta C_{44}}\left(x^2-\frac{E_1}{F_1}\right)$

$$\times \int_h^1 \frac{qdq}{(q^2-x^2)\sqrt{(q^2-h^2)(1-q^2)}}. \tag{48}$$

For $0 \le x \le h$,

$$\int_h^1 \frac{qdq}{(q^2-x^2)\sqrt{(q^2-h^2)(1-q^2)}} = \frac{1}{\sqrt{(1-x^2)(h^2-x^2)}}\frac{\pi}{2}. \tag{49}$$

For $x > 1$,

$$\int_h^1 \frac{qdq}{(q^2-x^2)\sqrt{(q^2-h^2)(1-q^2)}} = -\frac{1}{\sqrt{(x^2-1)(x^2-h^2)}}\frac{\pi}{2} \tag{50}$$

and

$$\int_h^1 \frac{qdq}{\sqrt{(q^2-h^2)(1-q^2)}} = \frac{\pi}{2}. \tag{51}$$

Finally

$$\int_h^1 \frac{q\phi_0(q^2)}{q^2-x^2}dq = \begin{cases} \dfrac{h_0}{\vartheta C_{44}}\left[1 - \dfrac{x^2-\frac{E_1}{F_1}}{\sqrt{(1-x^2)(h^2-x^2)}}\right], & 0 \le x \le h \\[4mm] \dfrac{h_0}{\vartheta C_{44}}\left[1 + \dfrac{x^2-\frac{E_1}{F_1}}{\sqrt{(x^2-1)(x^2-h^2)}}\right], & x > 1. \end{cases} \tag{52}$$

Similarly we have

$$\int_h^1 \frac{q\phi_1(q^2)}{q^2-x^2}dq = \begin{cases} -\dfrac{Gh_0}{2\pi\vartheta C_{44}}\left(1-\dfrac{2E_1}{F_1}+h^2\right)\left[1 - \dfrac{x^2-\frac{E_1}{F_1}}{\sqrt{(1-x^2)(h^2-x^2)}}\right], & 0 \le x \le h \\[4mm] -\dfrac{Gh_0}{2\pi\vartheta C_{44}}\left(1-\dfrac{2E_1}{F_1}+h^2\right)\left[1 + \dfrac{x^2-\frac{E_1}{F_1}}{\sqrt{(x^2-1)(x^2-h^2)}}\right], & x > 1. \end{cases} \tag{53}$$

From (47) we have

$$\sigma_{yz}(x,0) = \begin{cases} -h_0\left[1-\dfrac{G}{2\pi}k^2\log(k)\left(1-\dfrac{2E_1}{F_1}+h^2\right)\right]\left[1-\dfrac{x^2-\frac{E_1}{F_1}}{\sqrt{(1-x^2)(h^2-x^2)}}\right], & 0 \le x \le h \\[4mm] -h_0\left[1-\dfrac{G}{2\pi}k^2\log(k)\left(1-\dfrac{2E_1}{F_1}+h^2\right)\right]\left[1+\dfrac{x^2-\frac{E_1}{F_1}}{\sqrt{(x^2-1)(x^2-h^2)}}\right], & x > 1. \end{cases} \tag{54}$$

Appendix B

Displacement and the the magnetic field can be written as in the following vector form

$$\vec{U} = U_y(x,z)\hat{j}, \quad \vec{\mathcal{H}} = \mathcal{H}^{(1x)}\hat{i} + \mathcal{H}^{(1y)}\hat{j} + \mathcal{H}^{(1z)}\hat{k}. \tag{55}$$

Then

$$\frac{\partial\vec{U}}{\partial t} \times \vec{\mathcal{H}} = \left(\mathcal{H}^{(1z)}\frac{\partial U_y}{\partial t}\right)\hat{i} - \left(\mathcal{H}^{(1x)}\frac{\partial U_y}{\partial t}\right)\hat{k}. \tag{56}$$

Now,

$$
\begin{aligned}
\vec{\nabla} \times \left(\frac{\partial \vec{U}}{\partial t} \times \vec{\mathcal{H}} \right) &= -\frac{\partial}{\partial y} \left(\mathcal{H}^{(1x)} \frac{\partial U_y}{\partial t} \right) \hat{i} + \frac{\partial}{\partial x} \left(\mathcal{H}^{(1x)} \frac{\partial U_y}{\partial t} \right) \hat{j} + \frac{\partial}{\partial z} \left(\mathcal{H}^{(1z)} \frac{\partial U_y}{\partial t} \right) \hat{j} \\
&\quad - \frac{\partial}{\partial y} \left(\mathcal{H}^{(1z)} \frac{\partial U_y}{\partial t} \right) \hat{k} \\
&= \frac{\partial}{\partial x} \left(\mathcal{H}^{(1x)} \frac{\partial U_y}{\partial t} \right) \hat{j} + \frac{\partial}{\partial z} \left(\mathcal{H}^{(1z)} \frac{\partial U_y}{\partial t} \right) \hat{j}.
\end{aligned}
\tag{57}
$$

We know

$$
\nabla^2 \vec{\mathcal{H}} = \mu_e \sigma \left[\frac{\partial \vec{\mathcal{H}}}{\partial t} - \vec{\nabla} \times \left(\frac{\partial \vec{U}}{\partial t} \times \vec{\mathcal{H}} \right) \right].
\tag{58}
$$

Using (55) (56) and (57), from (58) equating the coefficients of $\hat{i}$ $\hat{j}$ and $\hat{k}$ we have

$$
\begin{aligned}
\frac{\partial \mathcal{H}^{(1x)}}{\partial t} &= \frac{1}{\mu_e \sigma} \nabla^2 \mathcal{H}^{(1x)}, \\
\frac{\partial \mathcal{H}^{(1z)}}{\partial t} &= \frac{1}{\mu_e \sigma} \nabla^2 \mathcal{H}^{(1z)} \\
\text{and } \frac{\partial \mathcal{H}^{(1y)}}{\partial t} &= \frac{1}{\mu_e \sigma} \nabla^2 \mathcal{H}^{(1y)} + \frac{\partial \left(\mathcal{H}^{(1x)} \frac{\partial U_y}{\partial t} \right)}{\partial x} + \frac{\partial \left(\mathcal{H}^{(1z)} \frac{\partial U_y}{\partial t} \right)}{\partial z}.
\end{aligned}
\tag{59}
$$

For $\sigma \to \infty$, $\frac{1}{\sigma} \to 0$. Equations given by (59) reduce to

$$
\frac{\partial \mathcal{H}^{(1x)}}{\partial t} = 0 = \frac{\partial \mathcal{H}^{(1z)}}{\partial t}
\tag{60}
$$

and

$$
\frac{\partial \mathcal{H}^{(1y)}}{\partial t} = \frac{\partial \left(\mathcal{H}^{(1x)} \frac{\partial U_y}{\partial t} \right)}{\partial x} + \frac{\partial \left(\mathcal{H}^{(1z)} \frac{\partial U_y}{\partial t} \right)}{\partial z}.
\tag{61}
$$

Data availability Enquiries about data availability should be directed to the authors.

Declarations

Conflicts of interest The authors declare that they have no conflict of interest.

References

1. Sneddon, I.N.: Crack problems in the mathematical theory of elasticity. Technical report, North carolina state university Raleigh, (1961)

2. Robertson, I.A.: Diffraction of a plane longitudinal wave by a penny-shaped crack. In: Mathematical Proceedings of the Cambridge Philosophical Society, vol. 63, pp. 229–238. Cambridge University Press, Cambridge (1967)
3. Mal, A.K.: Interaction of elastic waves with a griffith crack. Int. J. Eng. Sci. **8**(9), 763–776 (1970)
4. Jain, D.L., Kanwal, R.P.: Diffraction of elastic waves by two coplanar griffith cracks in an infinite elastic medium. Int. J. Solids Struct. **8**(7), 961–975 (1972)
5. Itou, S.: Diffraction of an antiplane shear wave by two coplanar griffith cracks in an infinite elastic medium. Int. J. Solids Struct. **16**(12), 1147–1153 (1980)
6. Itou, S.: Dynamic stress intensity factors around two coplanar griffith cracks in an orthotropic layer sandwiched between two elastic half-planes. Eng. Fract. Mech. **34**(5–6), 1085–1095 (1989)
7. Mandal, S.C., Ghosh, M.L.: Interaction of elastic waves with a periodic array of coplanar griffith cracks in an orthotropic elastic medium. Int. J. Eng. Sci. **32**(1), 167–178 (1994)
8. Sarkar, J., Mandal, S.C., Ghosh, M.L.: Diffraction of elastic waves by three coplanar griffith cracks in an orthotropic medium. Int. J. Eng. Sci. **33**(2), 163–177 (1995)
9. Dunkin, J.W., Eringen, A.C.: On the propagation of waves in an electromagnetic elastic solid. Int. J. Eng. Sci. **1**(4), 461–495 (1963)
10. Knopoff, L.: The interaction between elastic wave motions and a magnetic field in electrical conductors. J. Geophys. Res. **60**(4), 441–456 (1955)
11. Chadwick, P.: Elastic wave propagation in a magnetic field. In: Proceedings of the 9th international congress of applied mechanics, vol. 7, pp. 143–153, (1957)
12. Kaliski, S., Petykiewicz, J.: Equation of motion coupled with the field of temperature in a magnetic field involving mechanical and electrical relaxation for anisotropic bodies. In: Proceedings Vibration Problems, vol. 4, (1959)
13. Verma, P.D.S.: Magnetoelastic shear waves in self-reinforced bodies. Int. J. Eng. Sci. **24**(7), 1067–1073 (1986)
14. Chattopadhyay, A., Maugin, G.A.: Diffraction of magnetoelastic shear waves by a rigid strip. J. Acous. Soc. Am. **78**(1), 217–222 (1985)
15. Chattopadhyay, A., Choudhury, S.: Magnetoelastic shear waves in an infinite self-reinforced plate. Int. J. Numer. Anal. Methods Geomech. **19**(4), 289–304 (1995)
16. Marin, Marin: On the domain of influence in thermoelasticity of bodies with voids. Archivum Mathematicum **33**(3), 301–308 (1997)
17. Marin, Marin: An uniqueness result for body with voids in linear thermoelasticity. Rendiconti di Matematica **17**(7), 103–113 (1997)
18. Acharya, D.P., Roy, I., Sengupta, S.: Effect of magnetic field and initial stress on the propagation of interface waves in transversely isotropic perfectly conducting media. Acta mechanica **202**(1), 35–45 (2009)
19. Panja, S.K., Mandal, S.C.: Interaction of a finite crack with shear waves in an infinite magnetoelastic medium. Appl. Comput. Mech. **15**(1), 45–56 (2021)
20. Panja, Sourav Kumar, Mandal, S.C.: Interaction of magnetoelastic shear waves with a griffith crack in an infinite strip. J. Eng. Math. **126**(1), 1–11 (2021)
21. Srivastava, K.N., Lowengrub, M.: Finite Hilbert transform technique for triple integral equations with trigonometric kernels. Proc. R. Soc. Edinburgh Sect. A: Math. **68**(4), 309–321 (1970)
22. Chattopadhyay, A., Singh, A.K.: Propagation of a crack due to magnetoelastic shear waves in a self-reinforced medium. J. Vib. Control **20**(3), 406–420 (2014)
23. Abramowitz, M., Stegun, I.A.: Handbook of mathematical functions with formulas, graphs, and mathematical table. US Department of Commerce; National Bureau of Standards Applied Mathematics Series, 55, (1965)
24. Panja, Sourav Kumar, Mandal, S.C.: Propagation of love wave in multilayered viscoelastic orthotropic medium with initial stress. Waves Random Complex Media **32**(2), 1000–1017 (2022)